Abstract

The purpose of this work is to detect the faults that lead to decrease the level of the signal of the single mode fiber (SMF) for a length of (20km) for two wavelengths (1310nm & 1550nm) with attenuation of (0.34dB/km & 0.2dB/km) respectively .

Splice, connector and bend which are in different distances from the fiber are assumed to be existent in optical fiber. The losses of these splices, connectors, bends and the levels of the reflected signals along the single mode fiber have been calculated by the methods of the optical time domain reflectometer OTDR and optical frequency domain reflectometer OFDR.

The fusion splice is assumed to be existent about (5km), the connector about (10km) and the bend about (15km). The losses of these splices, bends, connectors and the levels of the reflected signals from the beginning of the fiber to its end have been calculated. A mathematical models of OFDR system were obtained to calculate the losses and reflected power of defected and undefected single mode fiber .

The calculation of the reflected signals by OFDR system has shown high resolution by magnitude of (1.7cm) which is higher than OTDR system, and the level of the reflected signals in the wavelength (1310nm) has an attenuation more than of the wavelength (1550nm) especially in the long distances ($Z \geq 15$km), It has been shown that the bends inside the optical fiber lead to big losses in the level of the reflected signals for the longer wavelength as in the wavelength (1550nm) where the level of the reflected signals at the bend for this wavelength was (-87.852dBm) and (-80.2dBm) for the wavelength (1310nm).

In this research novel technique has been employed to measure losses and faults inside the optical fiber. This technique is the (phase detection method)that uses OFDR system. The degree of the phase is changing suddenly for the signals in the places where the faults are happening. The phase degree increases with the increase of the fiber length.

Also, in this research another novel technique has been used, It is the Artificial Neural Networks (ANNS) . ANNS was merged with the OFDR system for the purpose of detecting, Defining and locating the faults locations inside the optical fiber with high speed. Thus the ANNS has been designed with two layers, in the hidden layer there are (20) neuron node and in the output layer there is (1) neuron node, and different data have been given about kinds of faults, the losses, their values and their own shapes to this networks. These networks will save all the data and training itself on this information. When this system is implemented effectively over any optical fiber the system of ANNS-OFDR will detect any fault early inside the fiber thus by comparison with the information that it owns.

Acknowledgements

First, I thank Allah for his guidance and for blessing me with the special people who helped and supported me so much .

I wish to extend my most sincere thanks and great gratitude to my supervisor Assist. Professor Dr. **Hussain Joma Abbas** for his never-ending support, guidance and encouragement throughout this work .

A great thank to the head of the Department of Laser and Optoelectronics Engineering, Assist. Prof. Dr. **Mohammed Hussain Ali.**

I would like to introduce a great thank to Dr. **Hassan A. Hassan**, Dr. **Amjad Jalel** and Mr. **Abdullah Khudiar Abass** for their appreciable help.

I am deeply indebted to my friends and colleagues for their encouragement and help .

My appreciation should finally be extended to the memory of my **Father** , to my **Mother** , my **Wife** , and my **Family** .

1)SMA (sub-miniature assembly)

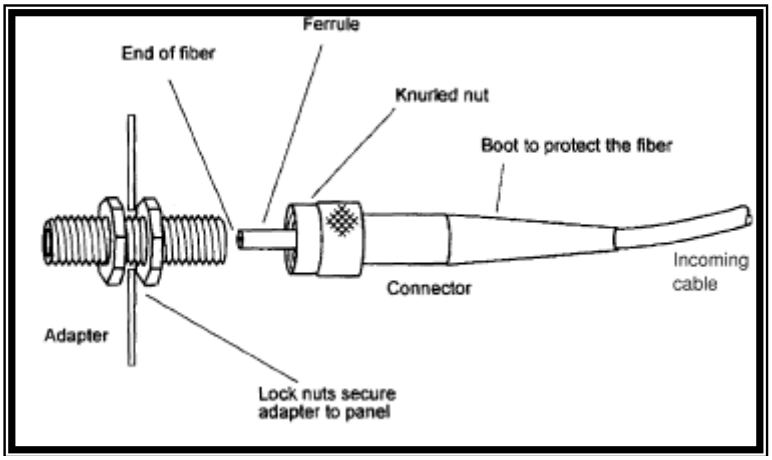

Figure (1) SMA connector [21]

2)ST (straight tip)

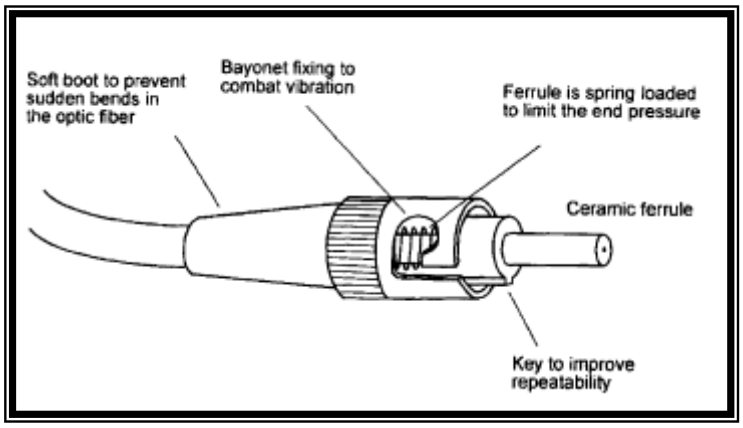

Figure (2) ST connector [21]

3)Physical Contact (FCPC)

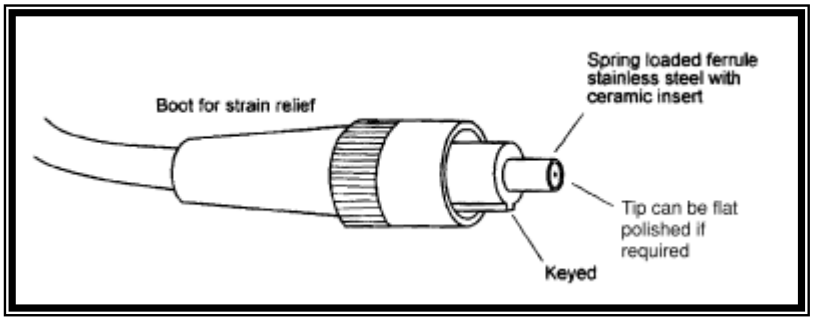

Figure (3)The FCPC connector[22]

4)Mini-BNC Figure

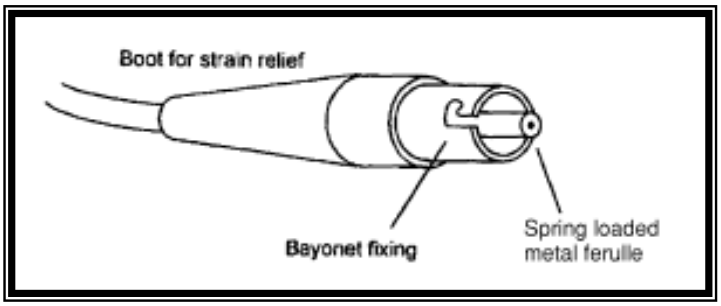

Figure (4) Mini-BNC connector [21]

5)Biconic Connector

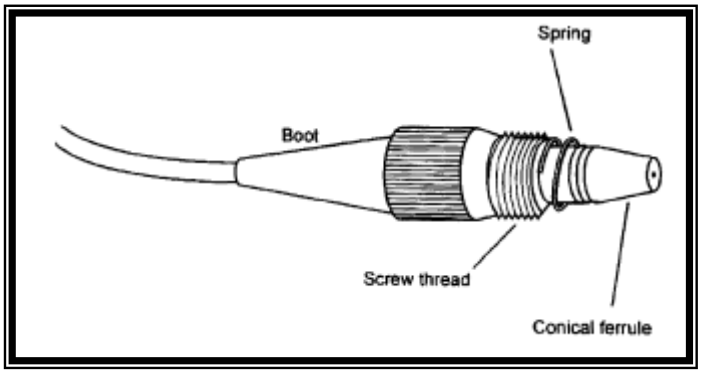

Figure (5) Biconic connector[21]

6) Fiber End-Face Preparation

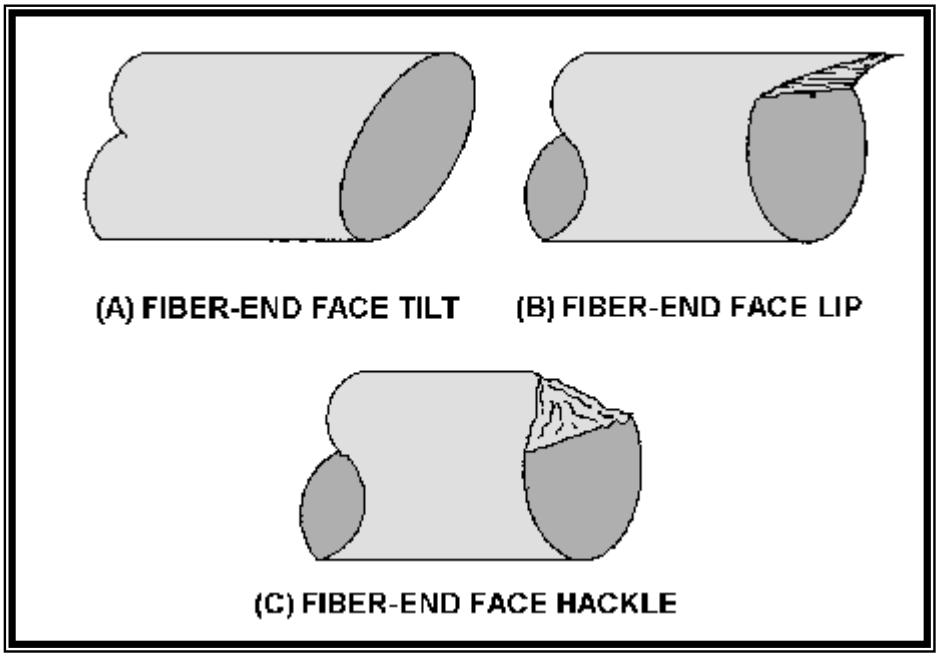

Figure(6) [23]

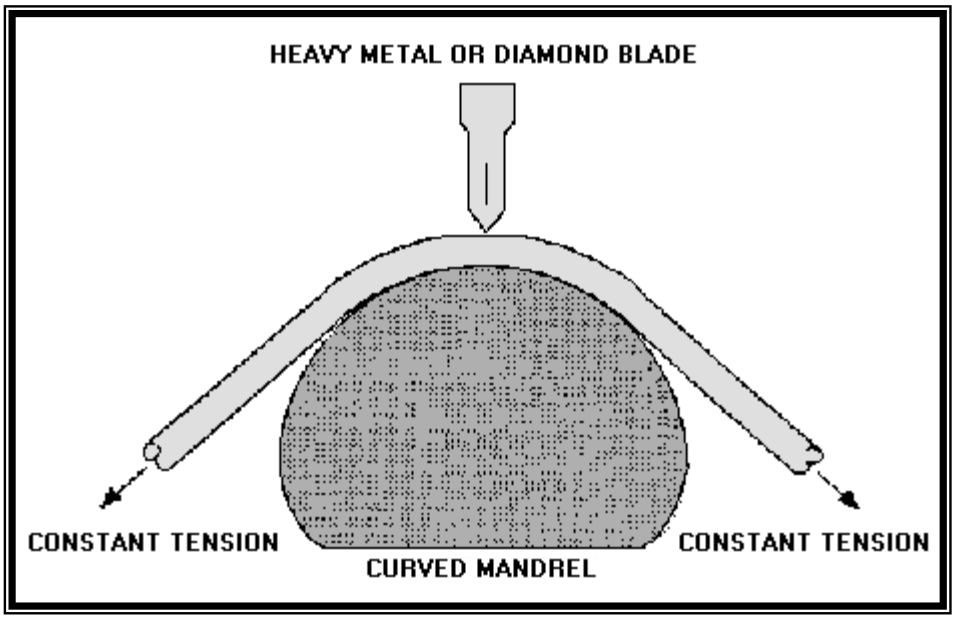

Figure (7) [23]

7)Fusion splices:

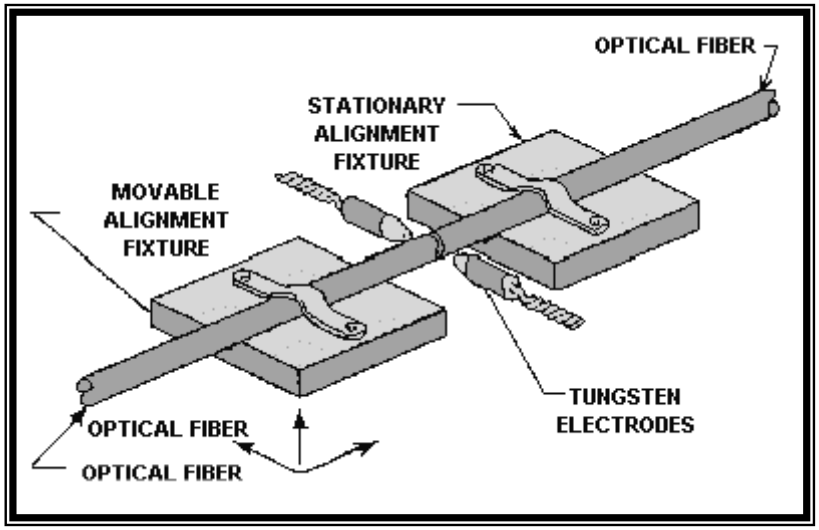

Figure (8) A basic fusion splicing apparatus[25]

8)Mechanical Splices:

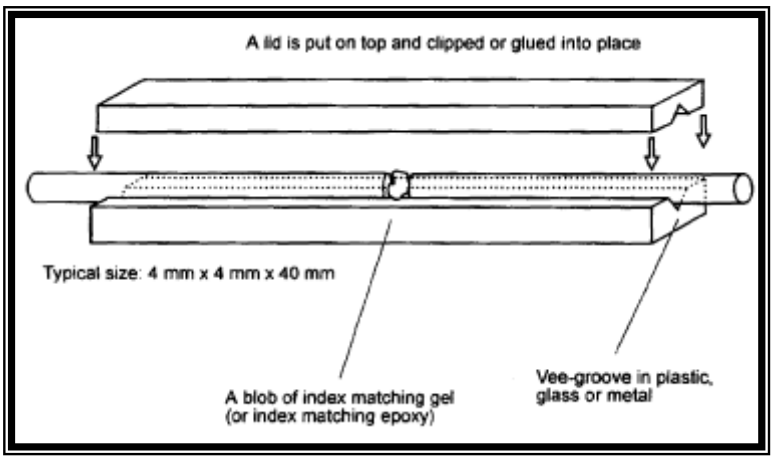

Figure (9) The principle of most mechanical splices[21]

Coupling ratio (primary/secondary)	Insertion loss (PP/SP), dB
50/50	3.4/3.4
60/40	2.5/4.4
70/30	1.8/5.6
80/20	1.2/7.6
90/10	0.6/10.8
95/05	0.4/14.6

1) Laser Diode Material Mixtures and Their Characteristics

Material	Wavelength range nm	Bandgap energies eV
GaAs	900	1.4
GaAlAs	800-900	1.4-1.55
InGaAs	1000-1300	0.95-1.24
InGaP	900-1700	0.73-1.35

2) list the performance values for avalanche photodiodes .

Parameter	Symbol	Unit	Si	Ge	InGaAs
Wavelength range	λ	nm	400–1100	800–1650	1100–1700
Avalanche gain	M	—	20–400	10–200	10–40
Dark current	I_D	nA	0.1–1	50–500	10–50 @ M = 10
Rise time	τ_r	ns	0.1–2	0.5–0.8	0.1–0.5
Gain × bandwidth	$M \cdot B$	GHz	100–400	2–10	20–250
Bias voltage	V_B	V	150–400	20–40	20–30

3) Indium Gallium Arsenide Avalanche Photodiodes-Fiber- Optic &Window Packages-900nm to 1700 nm InGaAs APDs

InGaAs APDs

Typical Characteristics @ T = 22° C

Part #	Standard Package	Photo Sens. Diam. (µm)	Resp. (A/W) 1300 nm	Resp. (A/W) 1550 nm	Dark Curr. Id (nA)	Spect. Noise Curr. Dens. In (pA/√Hz)	Cap @ 100 kHz Cd (pF)	Bandwidth (GHz) [into 50 Ω]	NEP @ 1550 nm (pW/√Hz)	Bias Volt (V)
C30644E CER	D1 ceramic	50	8.4	9.4	6	0.15	0.8	2	0.03	40 to 70
C30644E	D2 window	50	8.4	9.4	6	0.15	1.0	2	0.03	40 to 70
C30645E CER	D1 ceramic	80	8.4	9.4	10	0.25	1.0	1.0	0.13	40 to 70
C30645E	D2 window	80	8.4	9.4	10	0.25	1.2	1.0	0.13	40 to 70
C30662E CER	D1 ceramic	200	8.4	9.4	50	1	2.5	0.2	0.15	40 to 70
C30662E	D2 window	200	8.4	9.4	50	1	2.5	0.2	0.15	40 to 70

4) Window Properties

Window	Peak Sidelobe (dB)	Rolloff Rate (dB/oct)	3 dB Bandwidth
Rectangle	-13	-6	0.86/T
Hamming	-42	-6	1.3/T
Hanning (cosine4)	-47	-30	1.86/T
Kaiser ($\beta = 11$)	-82	-6	1.83/T
Minimum 4-term Blackman-Harris	-92	-6	1.9/T

Chapter Five

Results and Discussion

5.1 Introduction

In this chapter the calculations of the different fault in SM optical fiber were presented. These measurements and calculations include first, the design of single mode fiber, where the core diameter, fractional change in the index of refraction Δ, refractive index (n_2) of the cladding, were described with another parameters of optical fiber.

The coherence length of the source (I_C) and resolution were designed in order to calculate the optical fiber length, and select the optical power of the source. The insertion losses of the coupler was described in order to calculate the reflected power from oscillator (R_{LO}) round-trip.

The power reflected from optical fiber (DUT) at different lengths were calculated by using OFDR and OTDR systems. The faults along the optical fiber due to different losses were described and different faults were compared with the wavelengths of 1550 nm and 1310 nm, and between OTDR, OFDR system for the same wavelength. A new design for detecting faults in SMF by using the phase of reflected signal was presented.

A new method to detect the amplitude of the fault along the optical fiber by processing the information with artificial neural networks (ANNS) was designed. All the above parameters were calculated by using mathematical model of simulink matlab.

5.2 The calculations of SMF

As it was explained in theoretical part the attenuation due to scattering and absorption was chosen as in table below for wavelengths 1310 nm and 1550 nm. From Table (2-1) the fractional change in the index of refraction (Δ) was selected. From figure(2-7) and equation(2.11) the refractive index of cladding was chosen. From equations(2.5 and 2.6) numerical aperture (NA) and normalize frequency (V) were calculated. A summarized list for these parameters were given to the Table (5-1).

Table 5-1 SMF calculations

	n_1	n_2	NA	V	a (μm)	α (dB/km)
λ_1 = 1310 nm	1.4524	1.4468	0.1274	2.404	4	0.34
λ_2 = 1550 nm	1.4516	1.44402	0.1482	2.40	4	0.2

5.3 Fiber Joint Calculation

The fraction of light (r) reflected at a single interface (Fresnel reflection) was obtained from equation(2-12). For fusion splice the lateral displacement misalignment (round-trip) was calculated for wavelength 1310 nm and 1550 nm from equation (2-14) and equation (2-15). These parameter were given to the Table (5-2).

Table 5-2 Insertion Losses for Splice (round-trip)

	d (μm)	$\overline{\omega_o}$ (μm)	L_{Lat} (dB)	r
λ_1 = 1310 nm	1	4.35	0.459	0.034
λ_2 = 1550 nm	1	4.4	0.466	0.034

For connector the insertion losses (round-trip) or fault due to difference in core radius of two fibers was calculated from equation (2-16), where the numerical aperture and core index for emitting and receiving fiber are equal. The return losses from connector pair were calculated from

equations 2.19 to 2.23. All these parameters of connector were summarized in the Tables (5-3) and (5-4).

Table 5-3 Insertion Losses of Connector

	a_R (μm)	a_E (μm)	L_F (d)(dB)
λ_1 = 1310 nm	3.0	4.0	5
λ_2 = 1550 nm	3.0	4.0	5

Table 5-4 Return Losses From Connector

	$\bar{n}_0 = n_1$	r_1	r_2	$\bar{n}_1$	$\bar{n}_2$	$\bar{d}$ (μm)	h (μm)	δ	R	RL_{IM}(dB)	$r_c = P_{ref}/P_{inc.}$
λ_1 = 1310nm	1.4524	0.091	0.095	1	1.21	0.22	0.12	1.393	0.034	-43.3608	4.612×10^{-5}
λ_2 = 1550nm	1.4516	0.091	0.095	1	1.21	0.22	0.12	1.1772	0.034	-44.822	3.295×10^{-5}

5-4 Bending Losses

Insertion losses for the bending for single mode fiber SMF was calculated from the figure(2-21), and all parameter of bending losses were given to the Table (5-5).

Table 5-5 Bending Losses

	Critical Radius (cm)	Bending Radius (cm)	Losses (dB)
λ_1 = 1310 nm	1.5	1.35	0.2
λ_2 = 1550 nm	2.5	1.35	8.3

5-5 2×2 Coupler Losses

All the equations of the coupler losses were taken from section (2.21). The power of (20 mw) for optical source was assumed from section(3.3-4). The losses were calculated by using equations 2.28 to 2.31 and given in the Table (5-6) .

Table 5-6 Coupler Insertion Losses

	Excess Losses (dB)	Split Ratio	P_o(mW)	$P_1=P_2$	Insertion Losses(dB)
λ_1 = 1310 nm	0.2	50%	20	9.6 mW	6.2
λ_2 = 1550 nm	0.2	50%	20	9.6 mW	6.2

5-6 The Faults Calculation By Using OFDR For Defected SMF

5-6-1 Scattering Coefficient (α_s)

This parameter was calculated from equation(3.6), see Table (5-7).

Table 5-7 Scattering Coefficient

	T_F (K)	β_C (m^2N^{-1})	k ($J.K^{-1}$)	P	α_S (1/km)
λ_1 = 1310 nm	1400	$7x10^{-11}$	$1.381x10^{-23}$	0.286	0.0615
λ_2 = 1550 nm	1400	$7x10^{-11}$	$1.381x10^{-23}$	0.286	0.0313

The reflected power from oscillator was taken from equation(2.12)and (3.7), the distance from connector of oscillator source and coupler is 40cm[33] .

Table 5-8 Reflected Oscillator Power (r.t.)

	R_{Lo} (mW)	L (cm)
λ_1 = 1310 nm	0.157	40
λ_2 = 1550 nm	0.157	40

5-6-2 Coherence Range

The line-width of the source was tuned, so that the line-width of (5.14 kHz) was assumed[48]. The coherence range was calculated from equation (3.9). The total frequency linear sweep $\Delta\nu$ of the laser source signal is (6 GHz) and its time ΔT is (22 ms) considering the period of triangular waveform FFT triggering[3]. The spatial resolution $\Delta\ell$ was taken from equation (3.10).

The coherence time of the source was chosen from equation (3.12), the linear sweep rate β of the laser source signal was taken from equation (3.16). All the above parameters were given to the Table (5-9) below.

Table 5-9 Characteristic of the Laser Source using in OFDR system

	Δf (kHz)	I_C (km)	$\Delta\nu$ (GHz)	$\Delta\ell$ (cm)	t_c (μs)	ΔT (ms)	β(Hz/s)
λ_1 = 1310 nm	5.14	20.09	6	1.72	61.93	22	$2.7x10^{11}$
λ_2 = 1550 nm	5.14	20.104	6	1.7	61.9	22	$2.7x10^{11}$

5-6-3 Coherence Reflected Power I_A (t, τ) at (Z = 0 km)

The losses (α_A) due to Fresnel reflection and coupler losses at Z=0km taken from equations 2.13, table 5-6 respectively were added to get total attenuation from the source until this point. Reflected power (R_A) from (DUT) at this point was calculated from equation (2.23). The round trip-time of flight of light until this point was evaluated from equation (3.13). The liner beat frequency at this point in the (DUT) was taken from equation (3.17). The linear condition was taken in equation(3.14) and the non-linearity (γ) becomes (zero)[3] .

So, the coherence reflected power I_A(t, τ) at this point was calculated from equation (3.14) under the above condition, and all the parameters were given in the Table(5-10) for wavelengths 1310 nm and 1550 nm.

Table 5-10 Reflected Power at Z = 0 km (r.t.)

	Z (km)	τ (μs)	r (dB)	α_A (dB)	R_A (mW)	f_b (MHz)	I_A(t, τ) (dBm)
λ_1 =1310 nm	0	0	-14.68	-20.88	0.163	0	-27.986
λ_2 =1550 nm	0	0	-14.68	-20.88	0.163	0	-27.986

5.6.4 Coherence Reflected Power I_B (t, τ) at (Z = 960 m)

From equation(3.5) reflected power (R_B) from (DUT) at Z = 960 m was calculated. In this equation the signal duration is ($w = \frac{1}{\Delta \nu}$) [3][26]. The coherence reflected power I_B (t, τ) was calculated from equation (3.14) under linear condition, see Table (5-11).

Table 5-11 Reflected Power at Z = 960 m (r.t.)

	Z (km)	S	ΔZ(cm)	R_B (W)	τ (μs)	f_b(MHz)	I_B(t, τ)(dBm)
λ_1=1310 nm	0.96	2.4561×10^{-3}	3.45	2.153×10^{-11}	9.29	0.4	-63.01
λ_2=1550 nm	0.96	2.3×10^{-3}	3.45	1.202×10^{-11}	9.29	0.4	-63.665

5.6.5 Coherence Reflected Power I_C (t, τ) at (Z = 5 km), Splice Fault

From equation (3.5) the first reflected power (R_{C1}) at Z = 5 km was calculated and added to all losses before it. The second reflected power (R_{C2}) at Z = 5km was taken from adding the total power to the insertion losses of splice. Coherence reflected powers I_{C1} and I_{C2} were taken from equation (3.14) under linear condition. The above parameters were tabulated in (5-12).

Table 5-12 Reflected Power at Z = 5 km

	Z (km)	τ (s)	f_b(MHz)	R_{C1} (pW)	R_{C2}(pW)	I_{C1} (dBm)	I_{C2} (dBm)
λ_1=1310 nm	5	4.84×10^{-5}	2.08	11.428	10.28	-67.126	-68.3
λ_2=1550 nm	5	4.84×10^{-5}	2.08	7.52	6.75	-68.013	-69.5

5.6.6 Coherence Reflected Power I_D(t, τ) at Z =10 km, Connector Fault

The Fresnel reflected power (R_{D1}) was taken from equation (3.7) with using (r_c) from table(5-4)after adding (R_{D1}) to all losses before it. The second reflected power (R_{D2}) was taken from equation (3.5) and adding it to all losses before it. The third reflected power (R_{D3}) was obtained from adding the second reflected power (R_{D2}) to the insertion losses of the connector. The beat signals ($I_{D1,2,3}$) were evaluated from equation (3.14), all results were tabulated in Table (5-13).

Table 5-13 Reflected Power at Z = 10 km

	Z(km)	τ (s)	f_b(MHz)	R_{D1} (W)	R_{D2}(pW)	R_{D3}(pW)	I_{D1}(dBm)	I_{D2}(dBm)	I_{D3}(dBm)
λ_1=1310 nm	10	$9.683x10^{-5}$	4.16	$3.82x10^{-8}$	5.01	1.6	-52.9	-72.3	-74
λ_2=1550 nm	10	$9.68x10^{-5}$	4.16	$5.65x10^{-8}$	4.26	1.346	-52.038	-72.65	-75.153

5.6.7 Coherence Reflected Power $I_E(t,\tau)$ at Z =15 km, Bending Fault

The first reflected power (R_{E1}) at Z = 15 km was obtained from equation (3.5),and adding it to all losses before it. The second reflected power (R_{E2}) was taken from adding the first reflected power to the insertion losses of bending (table5-5). The beat signal($I_{E1,2}$)were taken from equation (3.14). The results above are given below in the table (5-14).

Table 5-14 Reflected Power at Z = 15 km

	Z (km)	τ (s)	f_b(MHz)	R_{E1} (W)	R_{E2}(W)	I_{E1} (dBm)	I_{E2} (dBm)
λ_1=1310 nm	15	$1.4524x10^{-4}$	6.24	$6.761x10^{-13}$	$6.166x10^{-13}$	-80.04	-80.2
λ_2=1550 nm	15	$1.4516x10^{-4}$	6.24	$8.5x10^{-13}$	$1.85x10^{-14}$	-79.547	-87.852

5.6.8 Coherence Reflected Power $I_F(t,\tau)$ at Z =20 km, Fresnel Reflection

In the end of optical fiber the Fresnel reflected power (R_{F1}) was taken from equation (3.7) with using (r) from table (5-2) and adding (R_{F1}) to all the losses before it. The second reflected power (R_{F2}) was obtained from equation (3.5) and adding it to all the losses before it. The beat signals ($I_{F1,2}$) were taken from equation (3.14).The results above are given below in Table(5-15).

Table 5-15 Reflected Power at Z = 20 km

	Z (km)	τ (s)	f_b(MHz)	R_{F1} (W)	R_{F2}(W)	I_{F1} (dBm)	I_{F2} (dBm)
λ_1=1310 nm	20	$1.94x10^{-4}$	8. 34	$1.847x10^{-6}$	$2.83x10^{-13}$	-51.25	-85.325
λ_2=1550 nm	20	$1.94x10^{-4}$	8. 34	$1.622x10^{-6}$	$1.17x10^{-14}$	-56.533	-92.248

A summarized list for these beat signals and their corresponding frequencies and distances values are given below in the Table (5-16a,b) for wavelength 1310nm and 1550nm respectively, by using mathematical model (4-1) and table (5-16a). fig.(5-1) show these relevant relations.

Table 5-16a Beat Signal at 1310 nm

1. λ_1=1310 nm			
No.	**Z (km)**	**f_b (MHz)**	**I(t, τ)(dBm)**
1	**0**	**0**	**I_A = – 27.986**
2	**0.96**	**0.4**	**I_B = – 63.01**
3	**5**	**2.08**	**I_{C1} = – 67.126** **I_{C2} = – 68.3**
4	**10**	**4.16**	**I_{D1} = – 52.9** **I_{D2} = –72.3** **I_{D3} = –74.76**
5	**15**	**6.24**	**I_{E1} = – 80.04** **I_{E2} = – 81.2**
6	**20**	**8.34**	**I_{F1} = – 51.25** **I_{F2} = – 85.325** **I_{F3} = – 116.99**

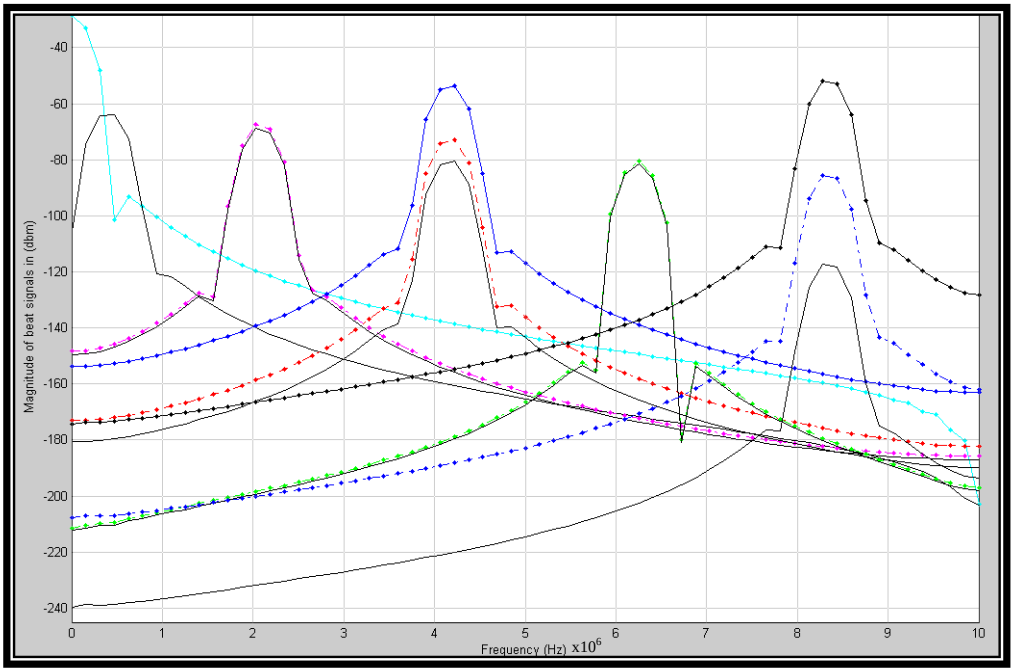

Figure (5-1) : Beat signals of defect optical fiber by using (OFDR) at wavelength (1310nm) by (DFT-FFT)) :1) Fresnel reflection fault.2)splice fault. 3) connector fault.4) bending fault .

By using mathematical model (4-2) and Table (5-16b), fig.(5-2) show these relevant relations.

Table 5-16b Beat Signal at 1550 nm

2. λ_2=1550 nm			
No.	**Z (km)**	**f_b (MHz)**	**I(t, τ)(dBm)**
1	**0**	**0**	**I_A = – 27.986**
2	**0.96**	**0.4**	**I_B = – 63.01**
3	**5**	**2.08**	**I_{C1} = – 68.013** **I_{C2} = – 69.5**
4	**10**	**2.08**	**I_{D1} = – 52.038** **I_{D2} = –72.65** **I_{D3} = –75.153**
5	**15**	**6.24**	**I_{E1} = –79.547** **I_{E2} = – 87.852**
6	**20**	**8.34**	**I_{F1} = – 56.533** **I_{F2} = – 92.248** **I_{F3} = – 116.99**

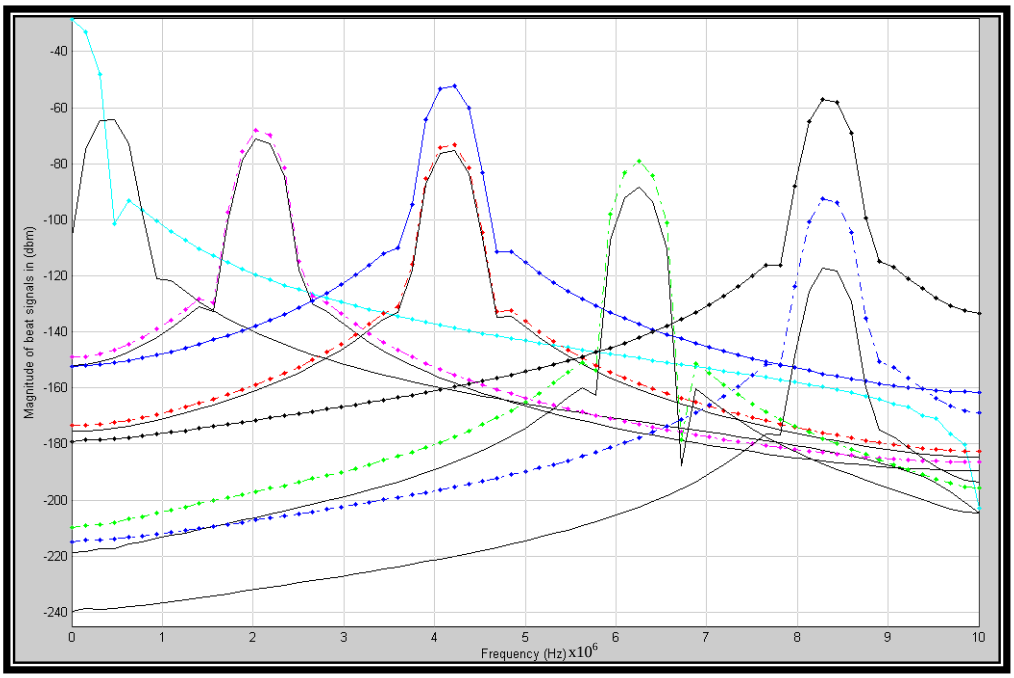

Fig(5-2) : Beat signals of defect optical fiber by using (OFDR) at wavelength (1550nm) by (DFT-FFT)) :1)Fresnel reflection fault.2)splice fault. 3)

figure (5-3, 5-4) show the relation between (λ_1 and λ_2).

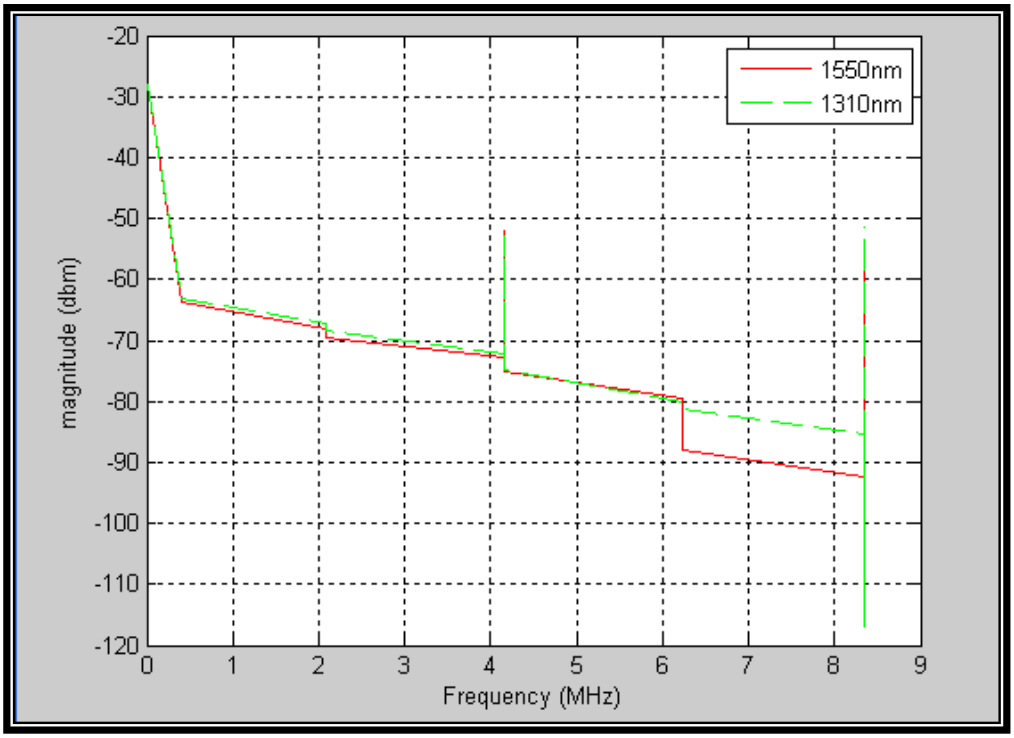

Figure (5-3) Beat signals of defect optical fiber by using (OFDR) at Wavelength (1310nm,1550nm) :1)Fresnel reflection fault.2)splice fault. 3) connector fault.4) bending fault .

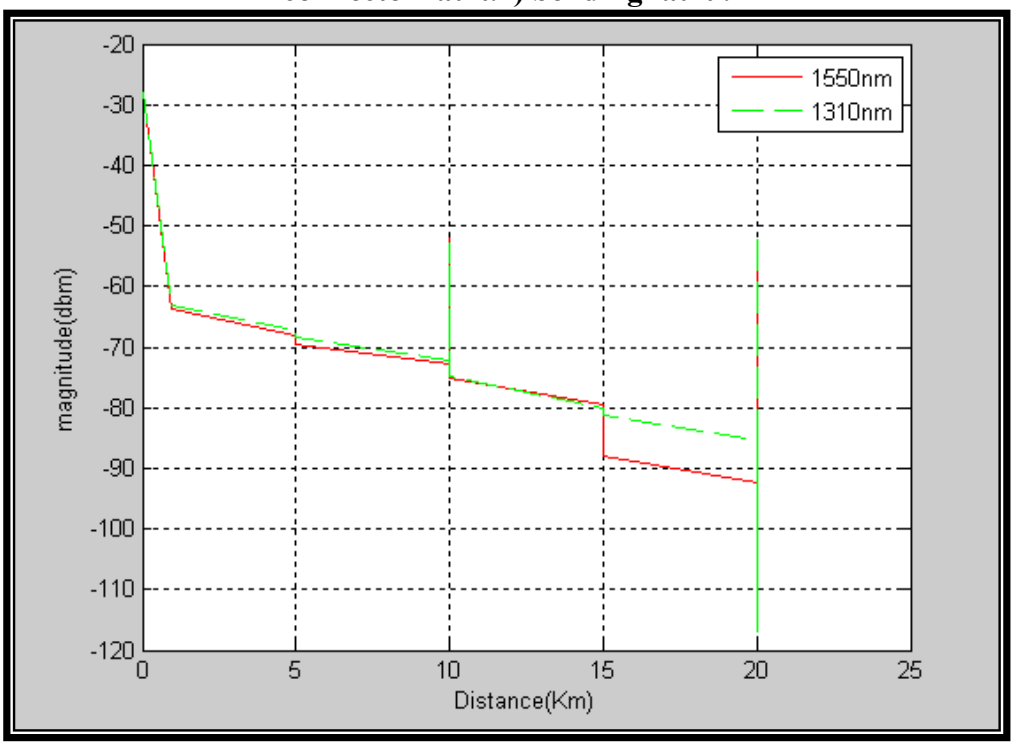

Fig.(5-4) Beat signals of defect optical fiber by using (OFDR) at Wavelength (1310nm,1550nm) :1)Fresnel reflection fault.2)splice fault. 3) connector fault.4) bending fault

Fig.(5-1) shows OFDR signal trace of SMF with wavelength 1310nm by using mathematical modeling of simulink matlab package fig.(4-1).The individual sharp spikes results from using FFT of different reflection faults. At Z=0 one spike is appear results from Fresnel reflection with frequency of 0MHz .

At Z = 0.96km of fiber optic length, One sharp spike appears is resulted from the back reflection (I_B) at beat frequency 0.4 MHz .

At Z=5km, Two sharp spikes are appeared at looking closely ,the second spike (Ic_2) is seen short after the first spike (Ic_1) because the insertion losses of the splices is (0.459dB,Table 5-2).

At Z=10km, three sharp spikes are appeared ,first spike (I_{D2})was result from reflection, second spike (I_{D1}) was result from Fresnel reflection, third spike (I_{D3}) was result from insertion losses of connector.

At Z=15km, first sharp spike was result from reflection at this point with beat frequency 6.24MHz ,Second spike was result from bending losses at this point (0.2dB ,table 5-5) .

At Z= 20km, first spike (I_{F2}) was result from reflection at this point ,Second large spike was result from Fresnel reflection at the end of fiber optic.

From fig.(5-3),(5-4), at short distances it appears that the reflected power at 1310nm is larger than that for 1550nm because the scattering coefficient (α_s) and backscattering factor (S) of 1310nm is larger than it in 1550nm, [Table (5-7), and Table(5-11), eq.3-5] .

At long distances the reflected power at 1550nm become larger than it at 1310nm until the bending fault at distance 15km where the reflected power of the wavelength 1550nm become more attenuated than 1310nm , table(5-5) .

5.7 The Faults Calculation By Using OFDR For Undefected SMF

The same equations and methods which were used in section (5.6), The results of undefected SMF are given below in the Table (5-17,a,b).

Table 5-17a Beat Signal at 1310 nm

1- λ_1=1310 nm			
No.	**Z (km)**	**f_b (MHz)**	**I(t, τ)(dBm)**
1	**0**	**0**	**I_A = -27.986**
2	**0.96**	**0.4**	**I_B = -63.01**
3	**20**	**8.34**	**I_{F2} = -82.4** **I_{F1} = -48.33** **I_{F3} = -116.99**

Figure (5-5) shows the relation between beat signal amplitude(dBm) and frequency(MHz) by FFT(taken from Table 5-17a) By using mathematical model fig.(4-3) .

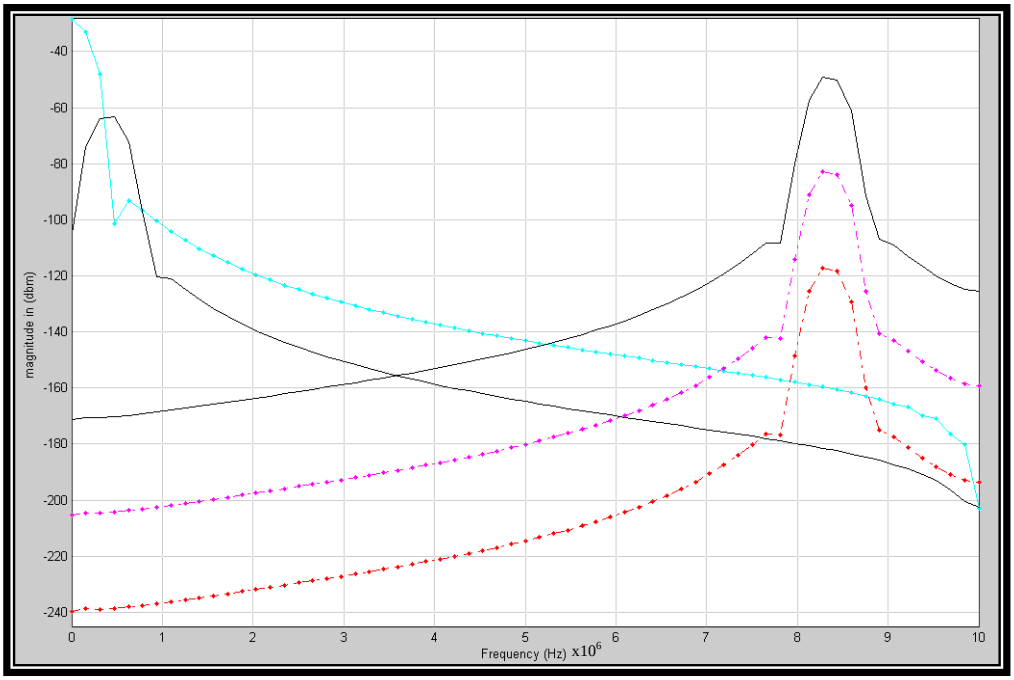

Figure(5-5)Reflected (beat) signals of (undefected optical fiber) by using (OFDR) and wavelength of (1310nm) with (DFT-FFT)

Table 5-17b Beat Signal at 1550 nm

2- λ_2=1550 nm			
No.	**Z (km)**	**f_b (MHz)**	**I(t, τ)(dBm)**
1	**0**	**0**	**I_A = -27.986**
2	**0.96**	**0.4**	**I_B = -63.665**
3	**20**	**8.34**	**I_{F2} = -81.2** **I_{F1} = -45.513** **I_{F3} = -116.99**

Figure (5-6) shows the relation between beat signal amplitude(dBm) and frequency (MHz) by FFT (taken from Table 5-17b) with using mathematical model fig.(4-4). Figures (5-7),(5-8) shows the relation between beat signal amplitude and frequency, distance respectively for two wavelengths (taken from Table 5-17a , 5-17b) .

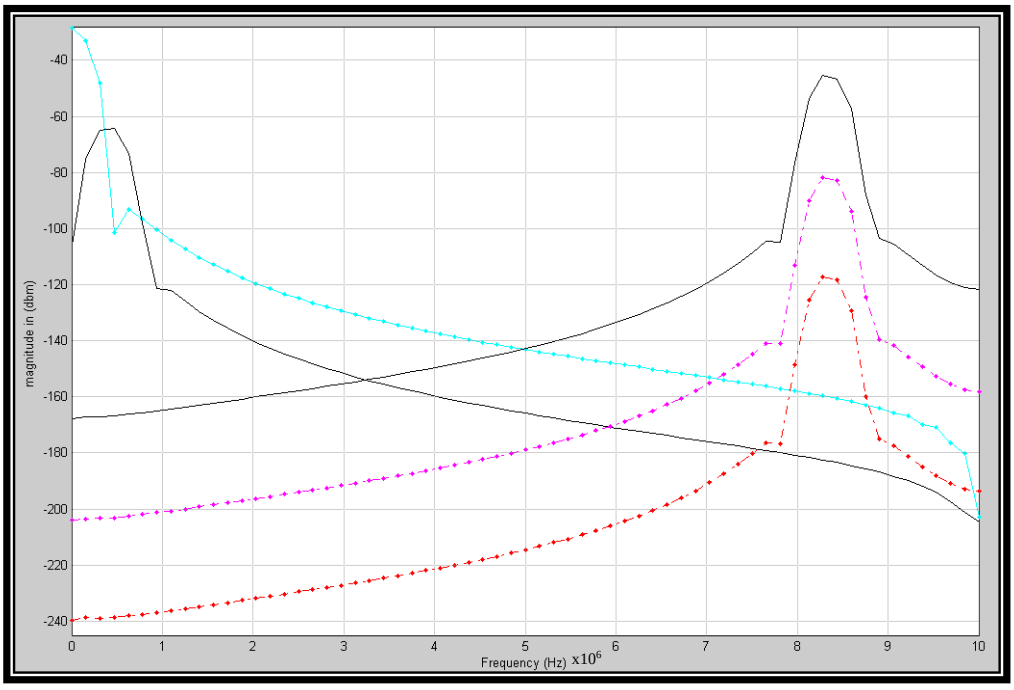

Figure (5-6) Reflected (beat) signals of (undefected optical fiber) by using (OFDR) and wavelength of (1550nm) with (DFT-FFT) .

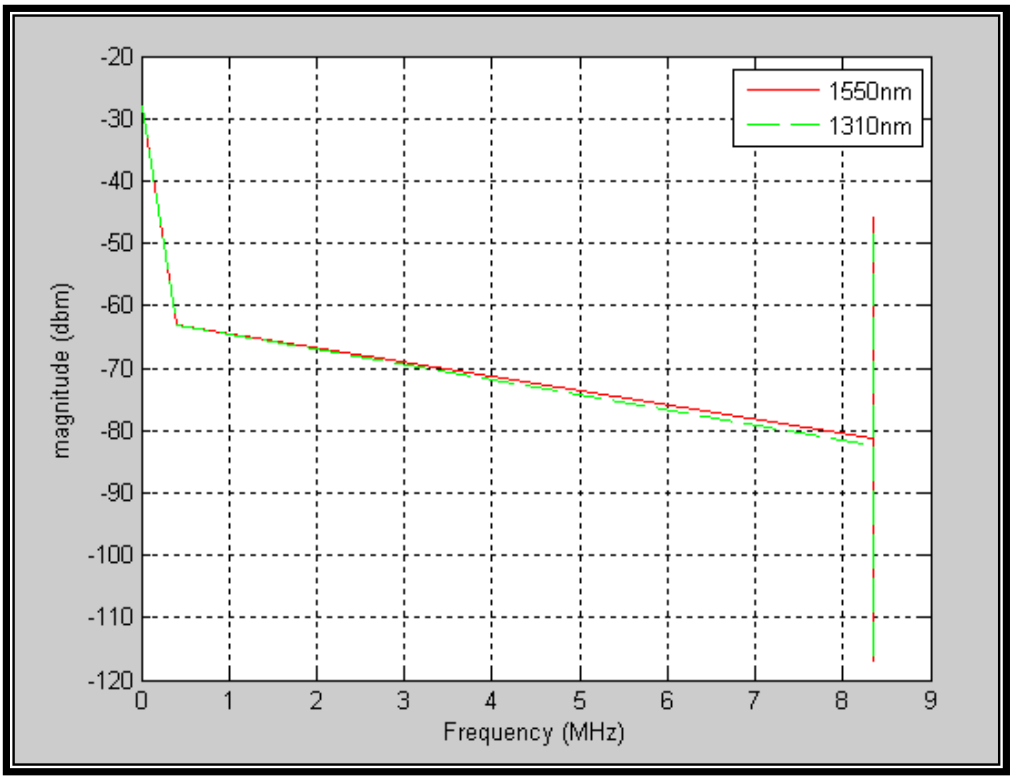

Figure (5-7) Beat signals of undefected optical fiber by using (OFDR) at Wavelength (1310nm,1550nm) .

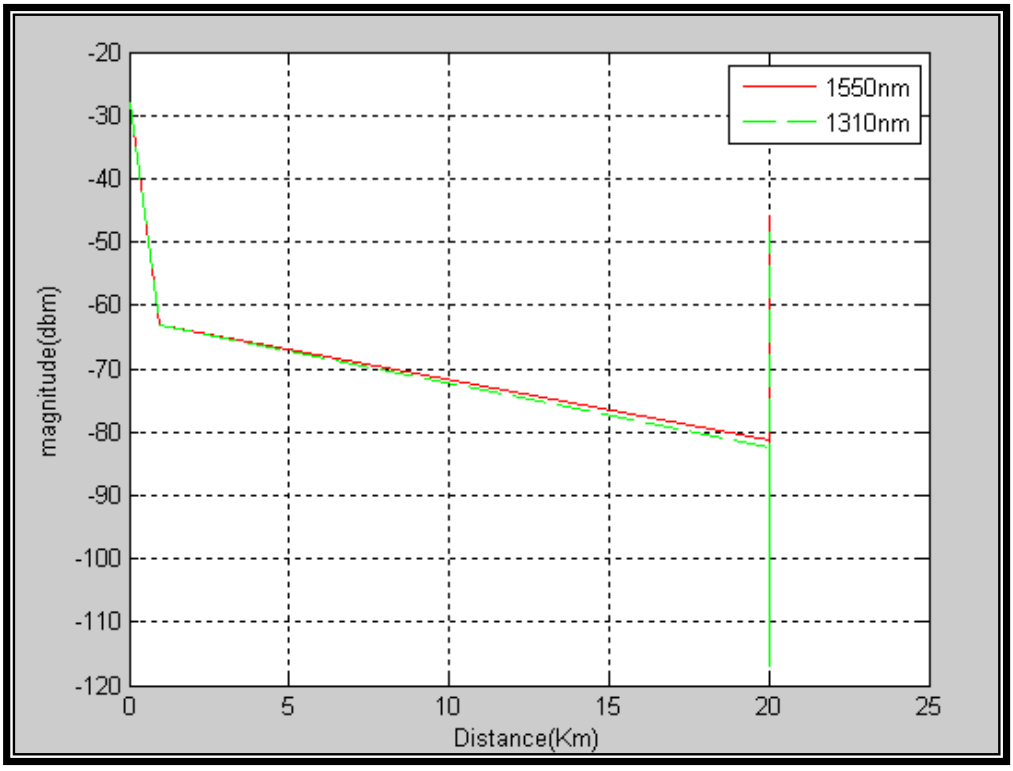

Figure (5-8)) Beat signals of undefected optical fiber by using (OFDR) at Wavelength (1310nm,1550nm) .

Fig (5-7),(5-8) shows optical fiber without fault. At z=0km , One spike (IA) was result from Fresnel reflection .

At Z=20km ,One sharp spike (I_{F1}) was result from Fresnel reflection at end of optical fiber .It is appeared that at closed distances the reflected power of 1310nm is larger than it at 1550nm because the scattering coefficient (α_s) and backscattering factor (S) of 1310nm is larger than it in 1550nm, from table (5-7),table(5-11),and eq.3-5 .

At long distances the reflected power at 1550nm become larger than it at 1310nm because the attenuation (α) [table(5-1)] of 1310nm is larger than 1550nm and the parameter (10–2 α Z / 10 dB) of equation (3-5) becomes more larger at 1550nm than it at 1310nm .

5.8 Resolution Comparing between the System of OFDR and OTDR

5.8.1 OFDR Resolution System

The characteristics of laser source used in OFDR system was taken from Table (5-9), In this section the same calculations and equations which were used in the above section, But the distance between the splice fault and bending fault is very small as in table (5-18a) in order to calculate the resolution of OFDR . The resolution of OFDR system is tabulated in Tables (5-18a) and (5-18b).

Table 5-18a Beat Signal at 1310 nm

1- λ_1=1310 nm				
No.	**$\Delta\ell$ (cm)**	**Z (km)**	**f_b (MHz)**	**I(t, τ)(dBm)**
1	**1.72**	**0**	**0**	**I_A = -27.986**
2	**1.72**	**0.96**	**0.4**	**I_B = -63.01**
3	**1.72**	**5**	**2.08**	**I_{C1} = -67.126** **I_{C2} = -67.976**
4	**1.72**	**5.03**	**2.09**	**I_{E1} = -68.069** **I_{E2} = -68.6**
5	**1.72**	**20**	**8.34**	**I_{F2} = -82.84** **I_{F1} = -48.76** **I_{F3} = -116.99**

Table 5-18b Beat Signal at 1550 nm

2- λ_2=1550 nm				
No.	**$\Delta\ell$ (cm)**	**Z (km)**	**f_b (MHz)**	**I(t, τ)(dBm)**
1	**1.7**	**0**	**0**	**I_A = -27.986**
2	**1.7**	**0.96**	**0.4**	**I_B = -63.665**
3	**1.7**	**5**	**2.08**	**I_{C1} = -68.013** **I_{C2} = -69.268**
4	**1.7**	**5.03**	**2.09**	**I_{E1} = -69.3** **I_{E2} = -76.6**
5	**1.7**	**20**	**8.34**	**I_{F2} = -89.7** **I_{F1} = -54.07** **I_{F3} = -116.99**

Figures (5-9, 5-10) shows the relation between beat signal amplitude and frequency, distance respectively for two wavelengths (taken from Table 5-18a , 5-18b) . From fig.(5-9), (5-10), the first sharp spike was result from splice fault at distance 5km or 2.08MHz .

the second is sharp sloping near the first at distance 5.03km was caused by bending fault ,

the two spikes are appear clearly because the resolution ($\Delta\ell$)of OFDR system is 1.72cm ,so the OFDR system has high resolution .

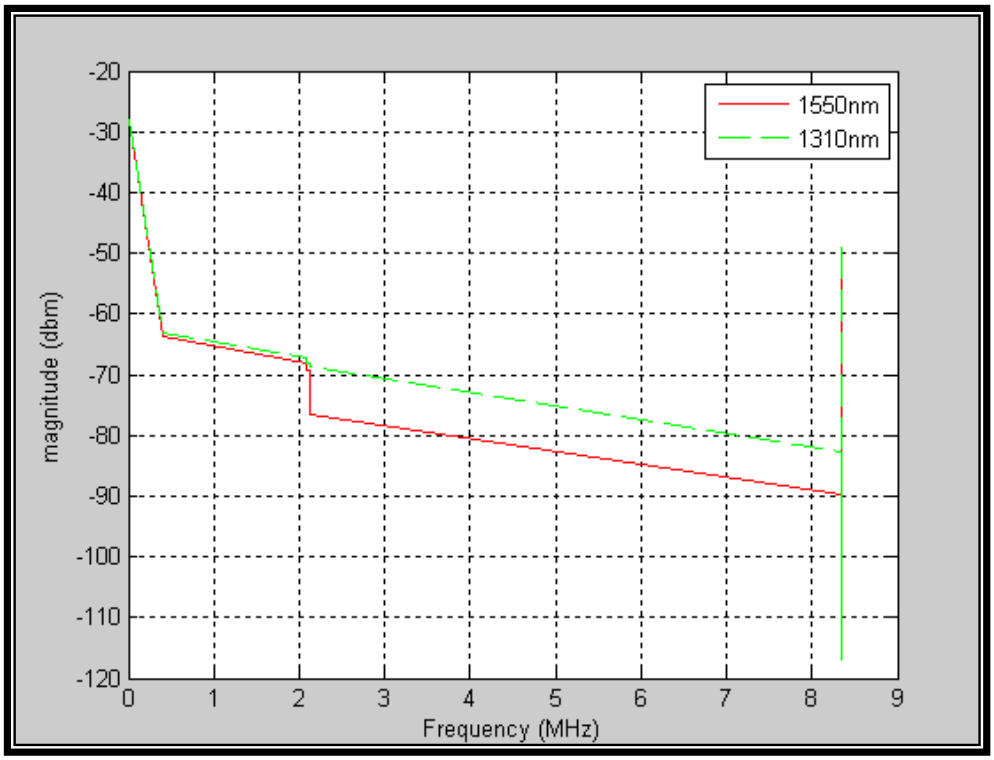

Figure (5-9) Beat signals of defected optical fiber by using (OFDR) at Wavelength (1310nm,1550nm) with resolution of (1.7cm)

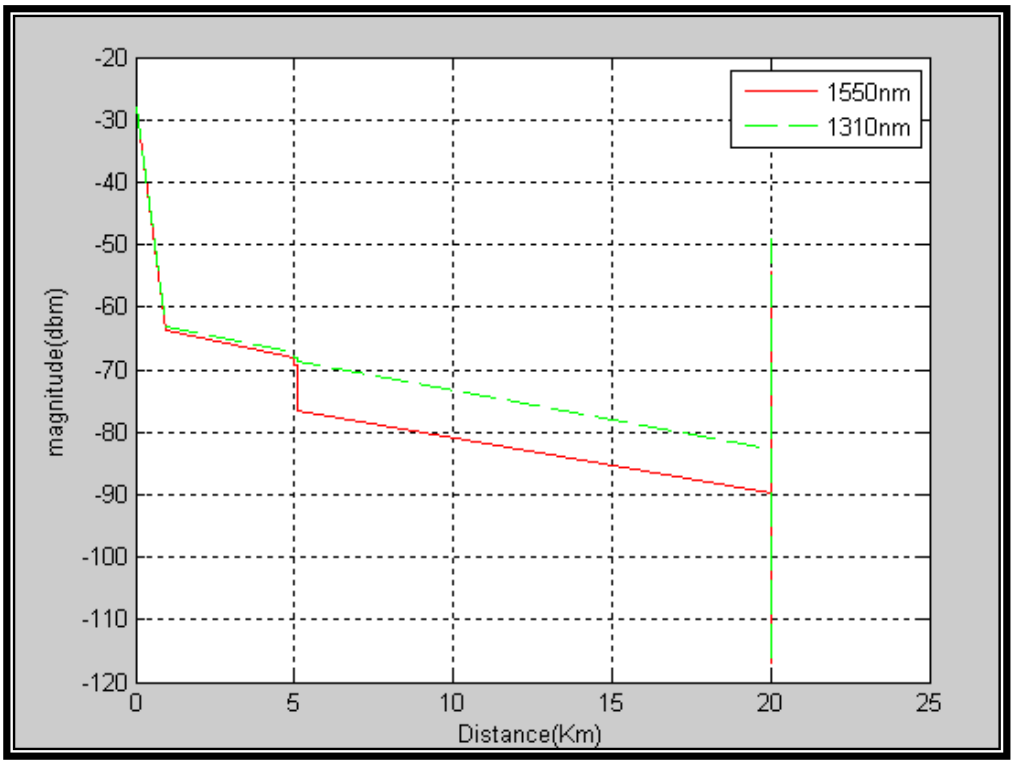

Fig.(5-10) Beat signals of defected optical fiber by using (OFDR) at Wavelength (1310nm,1550nm) with resolution of (1.7cm) .

5.8.2 OTDR Resolution System

All the characteristics of SM optical fiber were used in this system. The source is a laser diode with O/P power of (20 mW) and pulse width of (0.5 μs) [26].From equation (3.5), the pulse length (resolution) of this source was taken, the resolution (ΔZ) of OTDR system was obtained from equation (3.5). In this comparison the fault of splice and bending were calculated at distance 5km and 5.03km respectively . All the above parameters are given in Tables (5-19a, 5-19b,5-19c) below .

Table 5-19a characteristics of pulses laser diode

	P (mw)	W (μs)	ΔZ (m)
λ_1 =1310 nm	20	0.5	52
λ_2 =1550 nm	20	0.5	52

Table 5-19b Reflected Power at 1310 nm

No.	Z (km)	R(dBm)
1	0	R_A = -7.875
2	0.96	R_B = -41.53
3	5	R_{C1} = -44.46 R_{C2} = -45
4	5.03	R_{E1} = -45 R_{E2} = -45
5	20	R_{F2} = -55.126 R_{F1} = -21.741 R_{F3} = -80

Table 5-19c Reflected Power at 1550 nm

No.	Z (km)	R(dBm)
1	0	R_A = -7.875
2	0.96	R_B = -45
3	5	R_{C1} = -46.5 R_{C2} = -47.0
4	5.03	R_{E1} = -47.0 R_{E2} = -47.0
5	20	R_{F2} = -53.0 R_{F1} = -16.34 R_{F3} = -80

Figure (5-11, 5-12)shows the relation between beat signals amplitude and distance for two wavelengths for OFDR and OTDR system (taken from table 5-18 a, b) and (table 5-19 b, c) respectively .

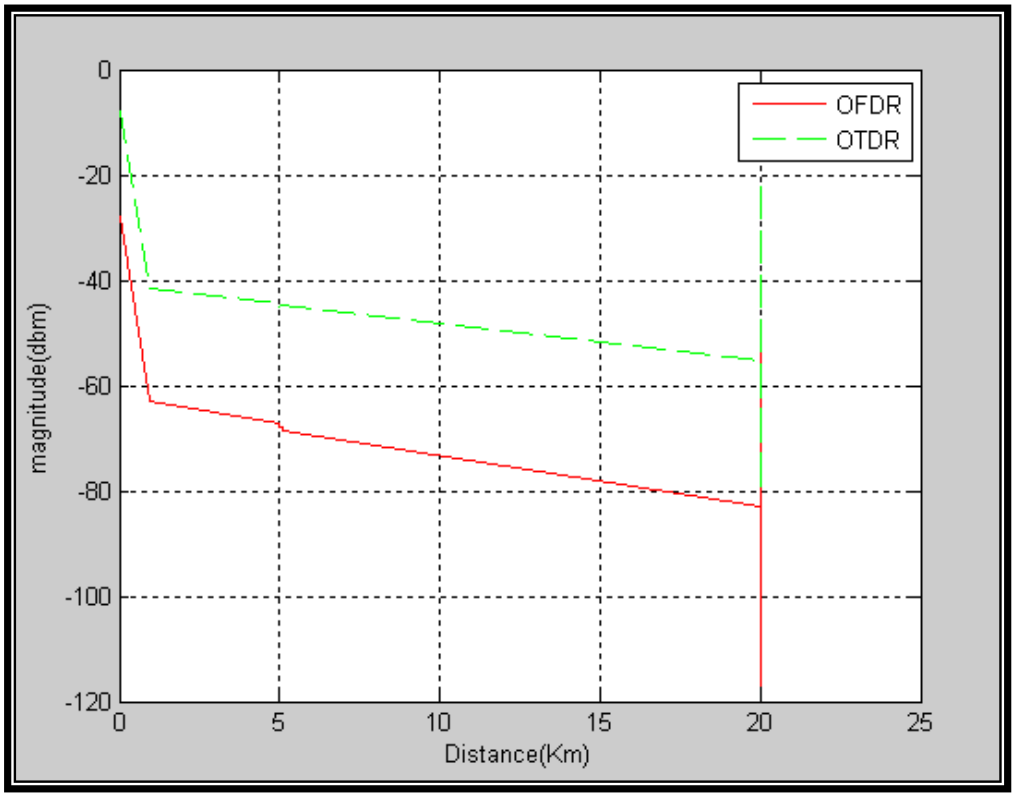

Fig.5-11 : Reflected signals from optical fiber(SMF) by using (OFDR)and(OTDR) respectively at (1310nm) for resolution measuring .

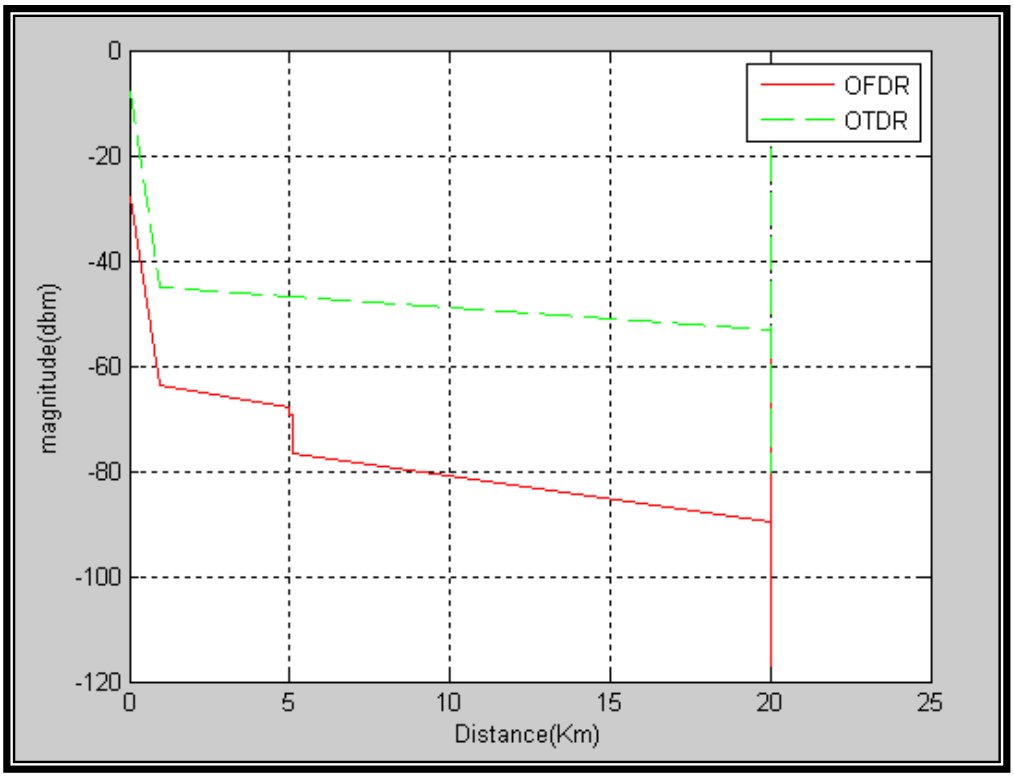

Fig.5-12 : reflected signals from optical fiber(SMF) by using (OFDR)and(OTDR) respectively at (1550nm) for resolution measuring .

From figure(5-11,5-12) the first fault is appeared at distance (5km) for OTDR system , the second fault is not appear at distance(5.03km) because the distance between the two faults (30m) are less than the resolution of OTDR system ($\Delta z = 52m$).

At the same time the two faults are appear at OFDR system because the distance between the two faults (30m) are larger than the resolution of OFDR system ($\Delta \ell = 1.72cm$) . In addition to that it is appear that OFDR system is operated with low amplitude of reflected power so OFDR system has larger sensitivity than OTDR system .

5.9 Single Fault Calculation By Using OFDR For Defected SMF

5.9.1 Splice Fault

In this section the analysis and design is calculated by the same method and equations that used in the section (5-6-5) and by using mathematical model fig.(4-5) .All the results of this section were tabulated in Table (5-20,a, b) by using two wavelength (1310nm,1550nm) .

Table 5-20a Beat Frequency for Splice Fault

1- λ_1=1310 nm			
No.	**Z (km)**	**f_b (MHz)**	**I(t, τ)(dBm)**
1	**0**	**0**	**I_A = -27.986**
2	**0.96**	**0.4**	**I_B = -63.01**
3	**5**	**2.08**	**I_{C1} = -67.126** **I_{C2} = -67.357**
4	**20**	**8.34**	**I_{F2} = -82.63** **I_{F1} = -48.54** **I_{F3} = -116.99**

Figure (5-13) shows this relation of Table (5-20a).

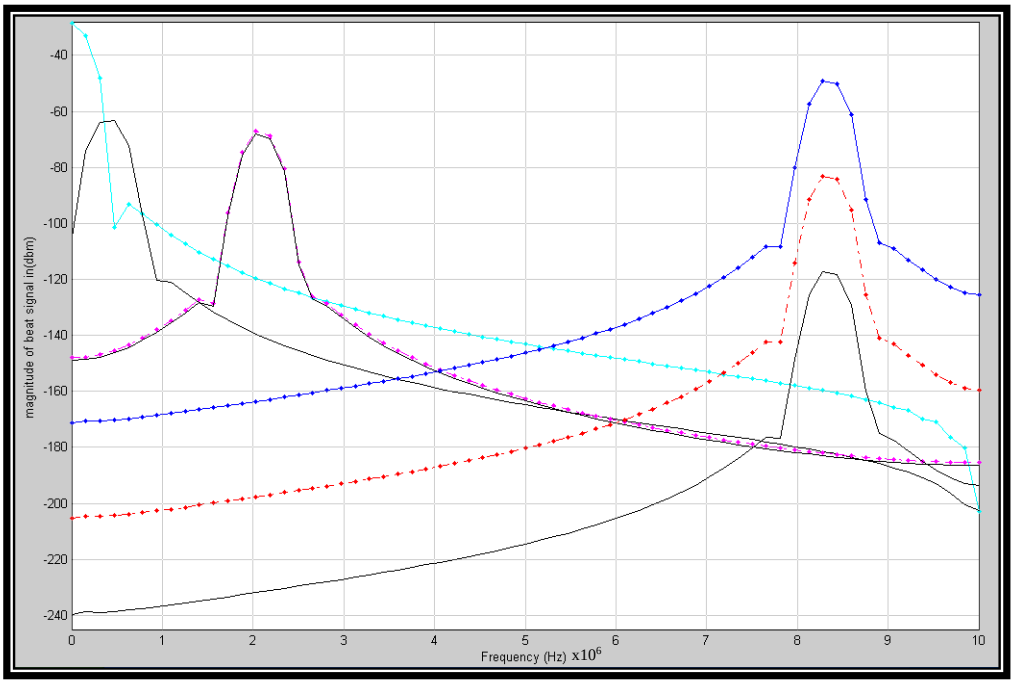

FIG.5-13) Beat signals of defected SM optical fiber by using (OFDR) at wavelength (1310nm) by (DFT-FFT)) for splice fault .

Table 5-20b Beat Frequency for Splice Fault

2- λ_2=1550 nm			
No.	**Z (km)**	**f_b (MHz)**	**I(t, τ)(dBm)**
1	**0**	**0**	**I_A = -27.986**
2	**0.96**	**0.4**	**I_B = -63.665**
3	**5**	**2.08**	**I_{C1} = -68.013** **I_{C2} = -68.268**
4	**20**	**8.34**	**I_{F2} = -81.45** **I_{F1} = -45.75** **I_{F3} = -116.99**

Figure (5-14, 5-15, 5-16) shows these relation .

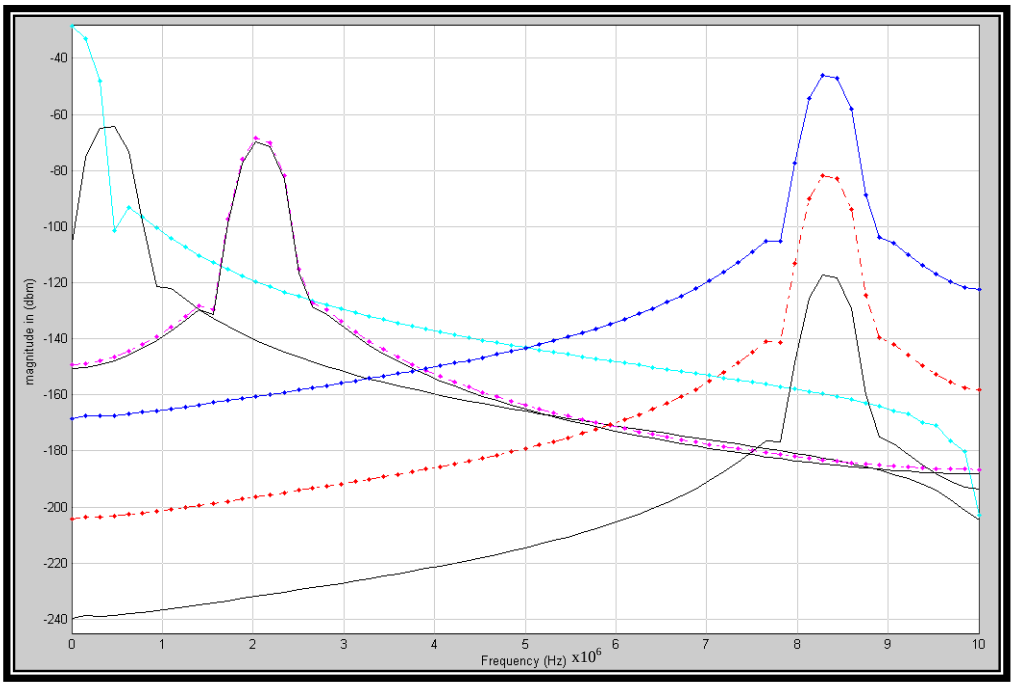

Figure (5-14) Beat signals of defected SM optical fiber by using (OFDR) at wavelength (1550nm) by (DFT-FFT)) for splice fault .

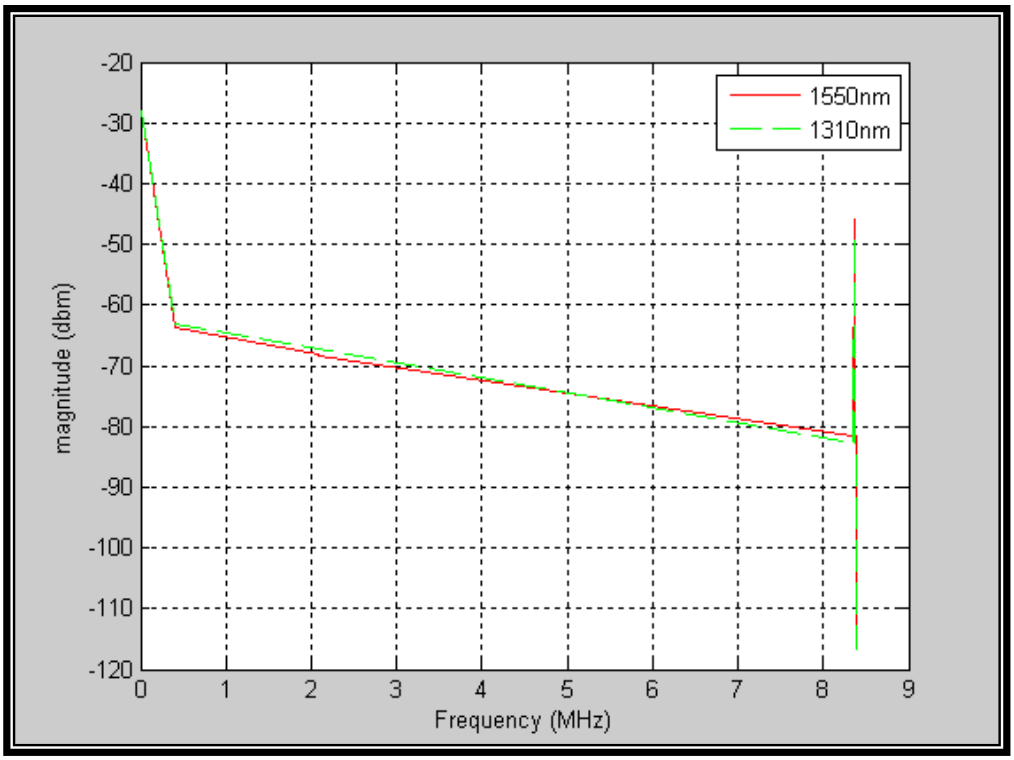

Figure (5-15) Beat signals of defected SM optical fiber by using (OFDR) at wavelength (1550nm and 1310nm) for splice fault .

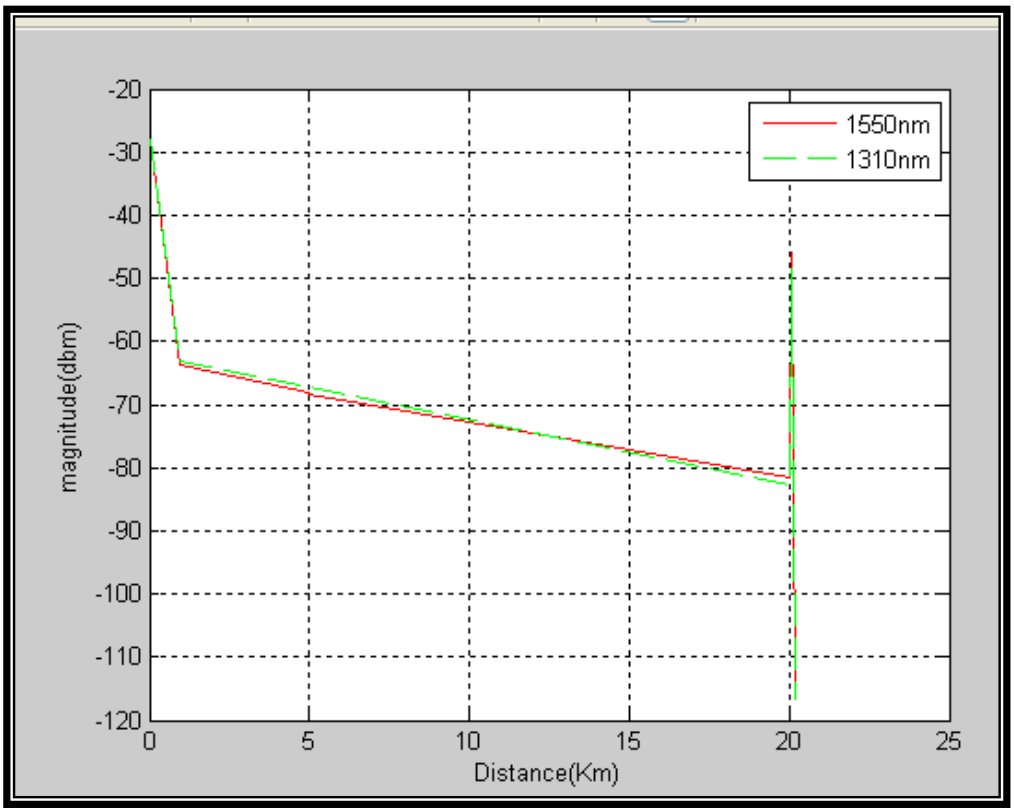

Figure (5-16) Beat signals of defected SM optical fiber by using (OFDR) at wavelength (1550nm and 1310nm) for splice fault .

Fig.(5-15,5-16),show small sloping of wavelength 1550nm larger than wavelength 1310nm at the distance 5km because the insertion losses at 1550nm is larger than 1310nm as in table (5-2) .

5.9.2 Bending Fault

In this section the analysis and design of the bending fault only was calculated by the same method and equations that used in section (5.6.7) . The results of this section were given below in Table (5-21a, b).

Table 5-21a Bending Fault

1- λ_1=1310 nm			
No.	**Z (km)**	**f_b (MHz)**	**I(t, τ)(dBm)**
1	**0**	**0**	**I_A = -27.986**
2	**0.96**	**0.4**	**I_B = -63.01**
3	**15**	**6.24**	**I_{E1} = -77.036** **I_{E2} = -77.5**
4	**20**	**8.34**	**I_{F2} = -82.6** **I_{F1} = -48.5** **I_{F3} = -116.99**

Table 5-21b Bending Fault

2- λ_2=1550 nm			
No.	**Z (km)**	**f_b (MHz)**	**I(t, τ)(dBm)**
1	**0**	**0**	**I_A = -27.986**
2	**0.96**	**0.4**	**I_B = -63.665**
3	**5**	**6.24**	**I_{E1} = -76.8** **I_{E2} = -85.1**
4	**20**	**8.34**	**I_{F2} = -89.51** **I_{F1} = -53.84** **I_{F3} = -116.99**

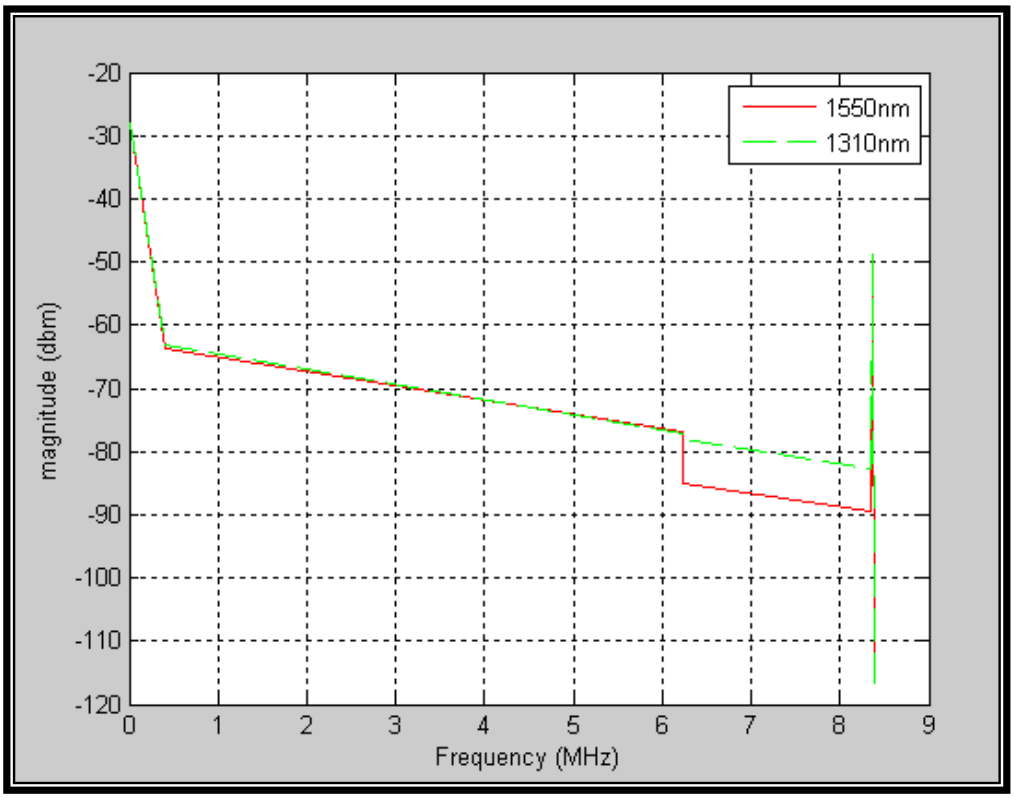

Figure (5-17) Beat signals of defected SM optical fiber by using (OFDR) at wavelength (1550nm and 1310nm) for bending fault .

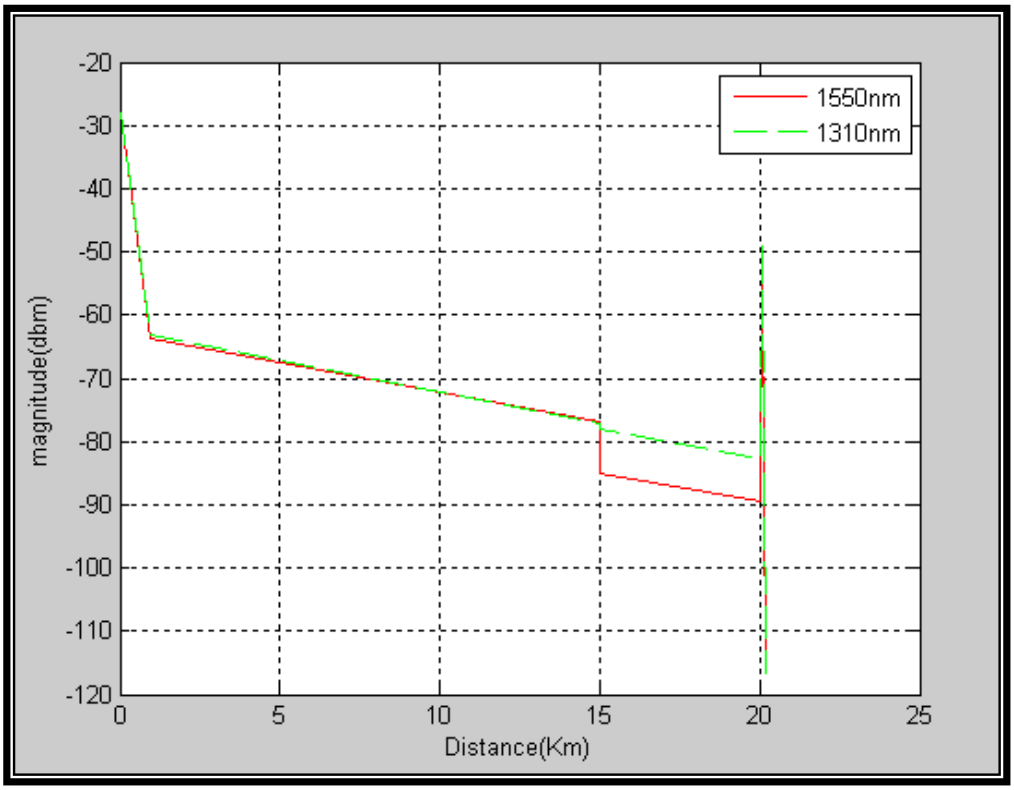

Figure (5-18) Beat signals of defected SM optical fiber by using (OFDR) at wavelength (1550nm and 1310nm) for bending fault .

Fig.(5-17),(5-18) shows the relations of table (5-21 a,b),the sharp sloping in the wavelength 1550nm is because the bending losses at long wavelength is more larger than the short wavelength 1310nm as in table (5-5) ,so the reflected power at long wavelength is attenuated more larger than short wavelength .

5.9.3 Connector Fault

In this section the analysis and design of connector fault only was calculated by the same method and equations that used in section (5.6.6) , The calculation of this section was given in Table (5-22a, b).

Table 5-22a Connector Fault

1- λ_1=1310 nm			
No.	**Z (km)**	**f_b (MHz)**	**I(t, τ)(dBm)**
1	**0**	**0**	**I_A = -27.986**
2	**0.96**	**0.4**	**I_B = -63.01**
3	**10**	**4.16**	**I_{D2} = -71.2** **I_{D1} = -52.3** **I_{D3} = -74**
4	**20**	**8.34**	**I_{F2} = -84** **I_{F1} = -50.825** **I_{F3} = -116.99**

Table 5-22b Connector Fault

2- λ_2=1550 nm			
No.	**Z (km)**	**f_b (MHz)**	**I(t, τ)(dBm)**
1	**0**	**0**	**I_A = -27.986**
2	**0.96**	**0.4**	**I_B = -63.665**
3	**10**	**4.16**	**I_{D2} = -72.42** **I_{D1} = -51.8** **I_{D3} = -74.92**
4	**20**	**8.34**	**I_{F2} = -83.711** **I_{F1} = -48.02** **I_{F3} = -116.99**

Figures (5-19, 5-20) show these relations .

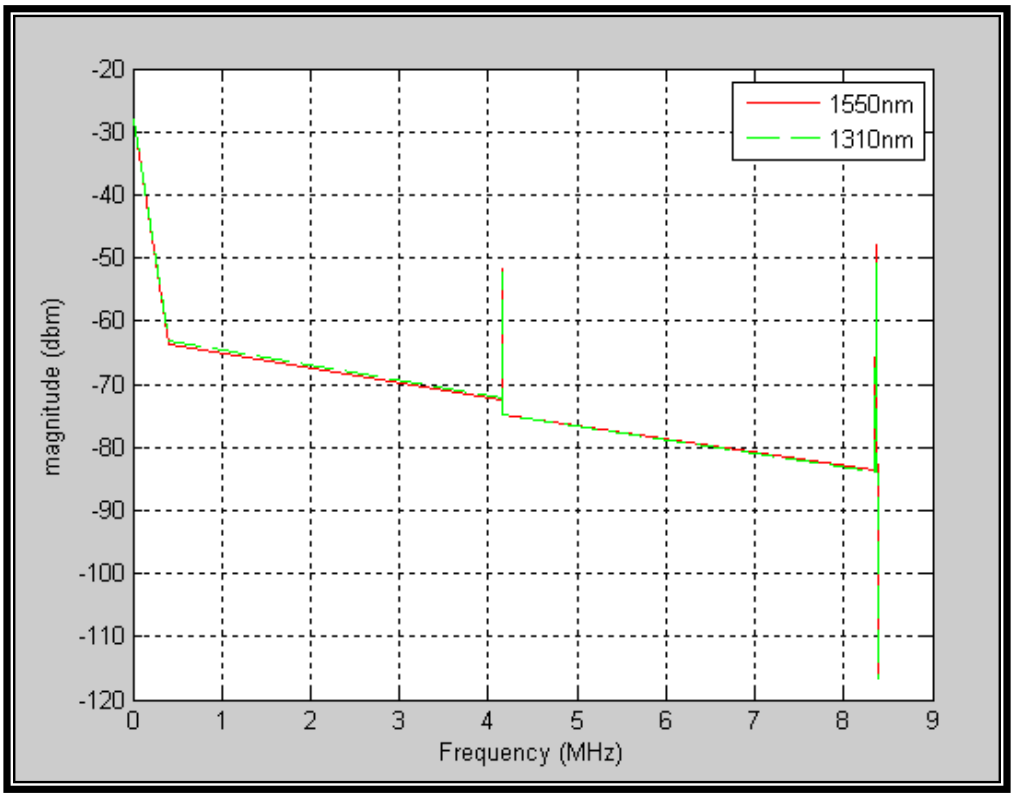

Fig.5-19 : Beat signals of defected SM optical fiber by using (OFDR) at wavelength (1550nm and 1310nm) for connector fault .

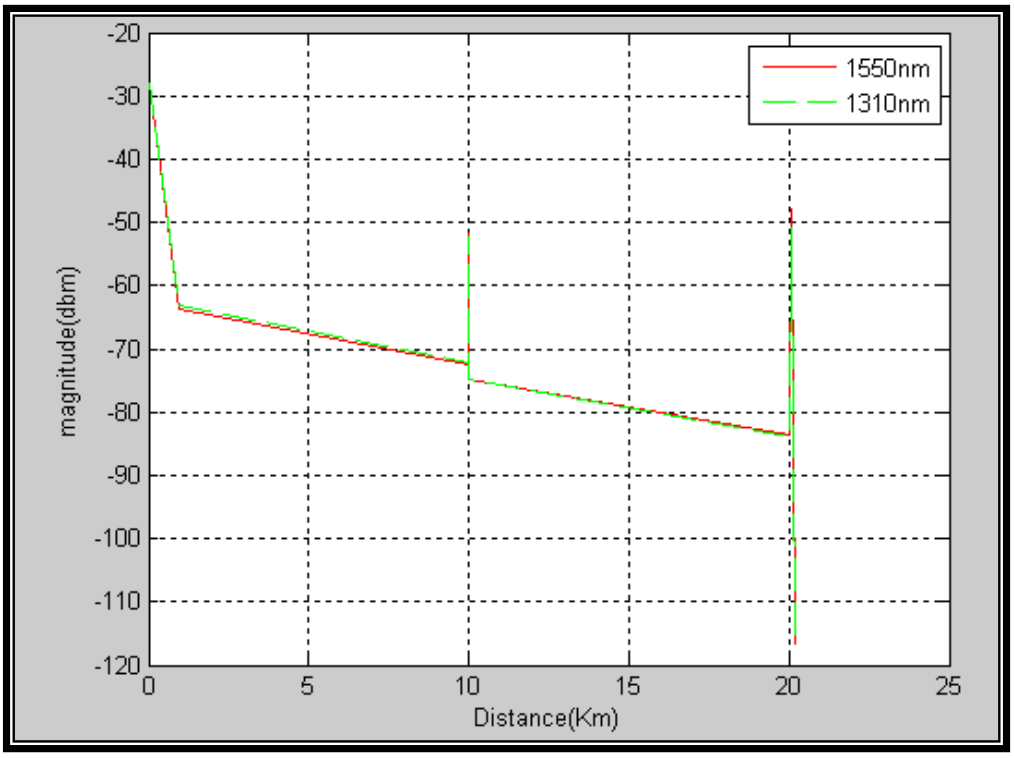

Fig.5-20 : Beat signals of defected SM optical fiber by using (OFDR) at wavelength (1550nm and 1310nm) for connector fault .

The same sharp sloping at distance 10km for the long and short wavelength (1550nm-1310nm)caused by insertion losses of connector as in table (5-3), So the same reflected power at the long-short distances for two wavelengths . At the same distance, the sharp spike of the two wavelengths is result from Fresnel reflection of connector as in table (5-22a) .

5.10 The Fault Detection by using Phase of the Signal

A novel technique was built to detect the fault by using the phase of the reflected signals. Model of phase detection was built as illustrated in figure (4-7). The faults were assumed as in table (5-16a, b). The reflected beat signal (magnitude Vs frequency) was shown in figure (5-21). The same reflected beat signal but between (phase Vs frequency) was illustrated in figure (5-22),(5-23) .

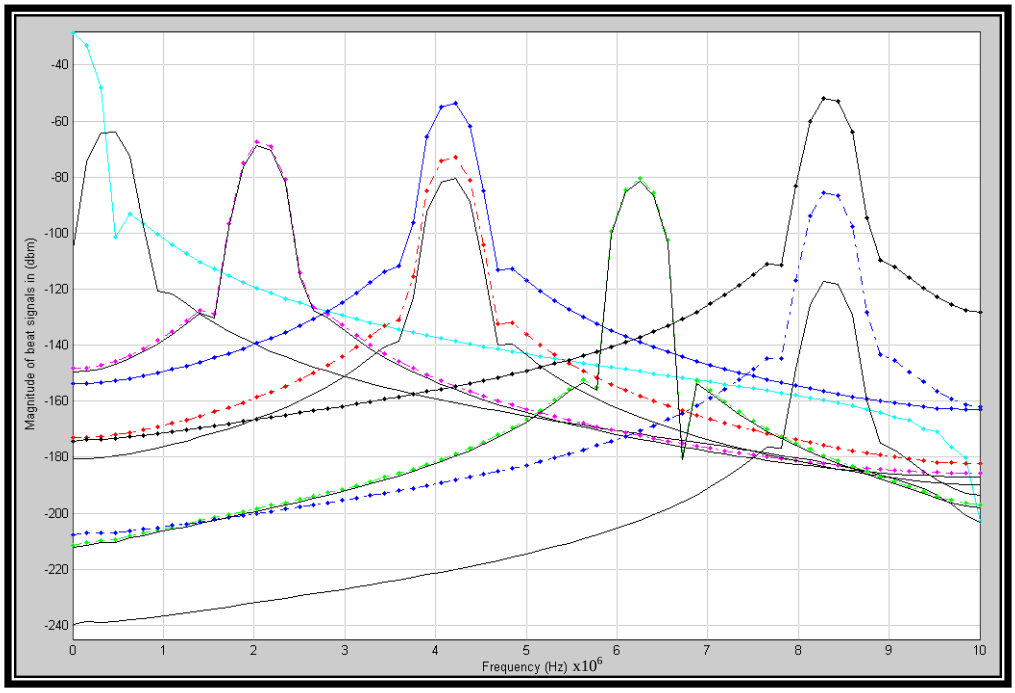

Figure (5-21) Reflected beat signals from SM defect optical fiber at (1310nm) for different faults

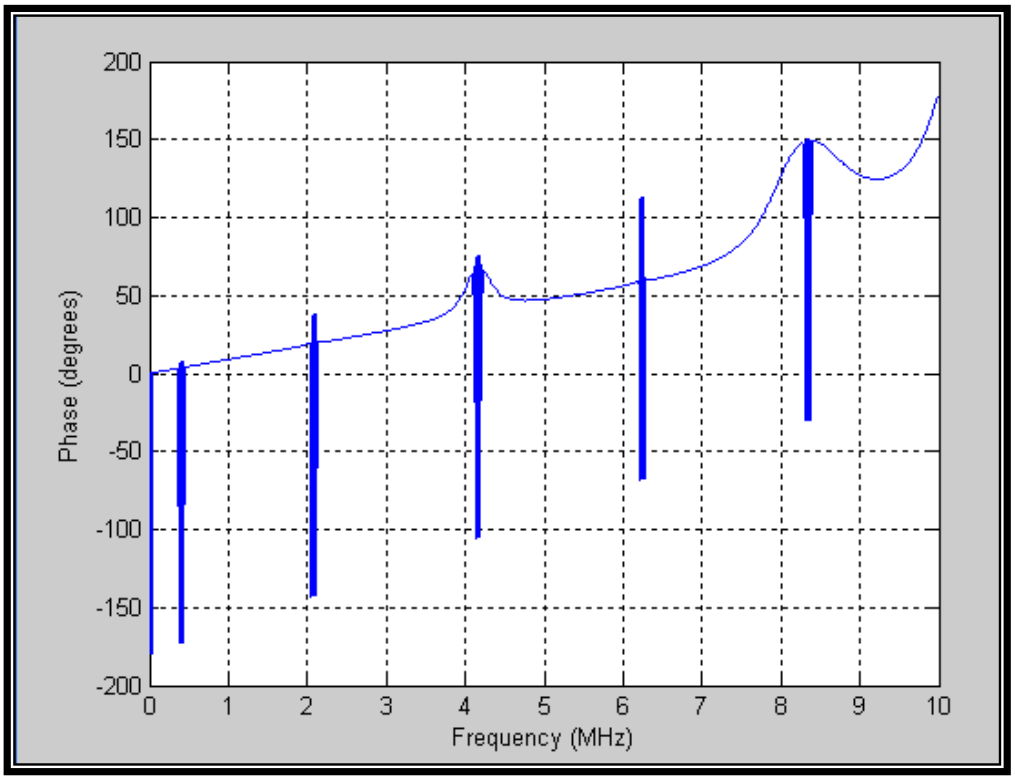

Figure (5-22)Faults detection by (PHASE) for defected SM optical fiber by using (OFDR) with (DFT-FFT) .

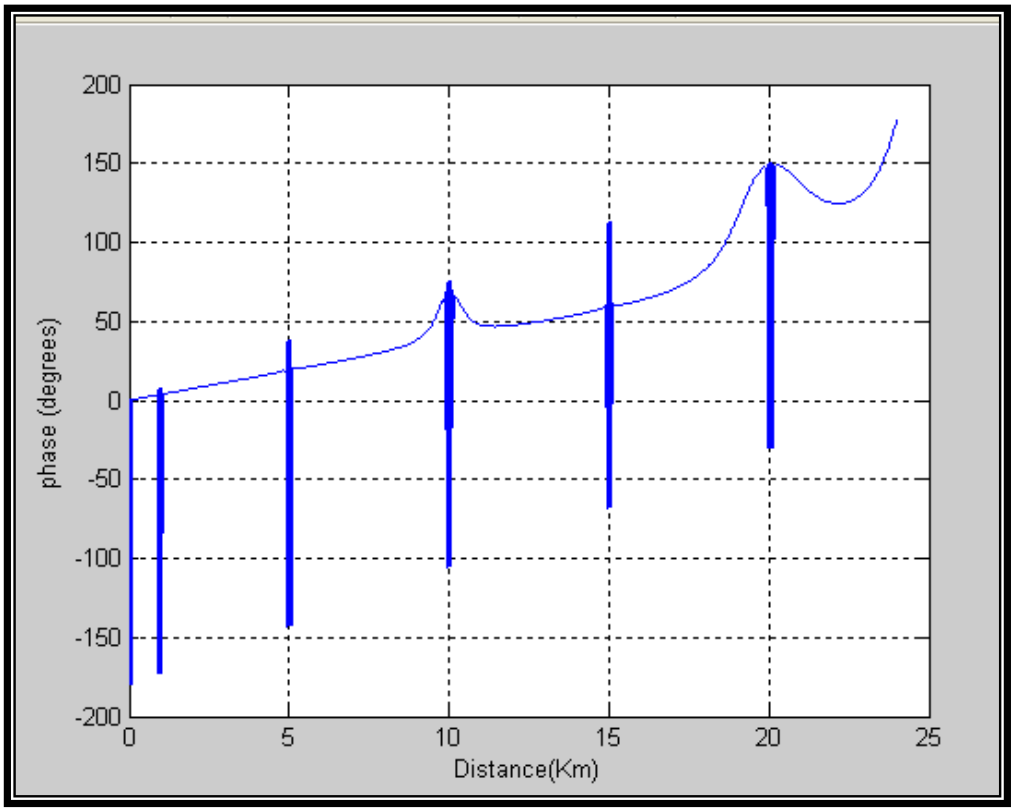

Figure (5-23) :Faults detection by (PHASE) for defected SM optical fiber by using (OFDR) with (DFT-FFT) .

fig.(5-22),(5-23) shows the degree of phases for reflected signals are changed suddenly in the places where the faults are happening .

5.11 The Fault Detection By Using Artificial Neural Networks (ANNS)

A novel technique was used to detect the amplitude of the fault along the optical fiber by using (Neural-Network) . The most useful neural networks in function approximation are the method of Multilayer Perceptron (MLP).

5.11-1 The Bending Fault Calculation by ANNS-OFDR for 1550nm .

Analysis and design of the bending fault of SMF was calculated by the same method as in table (5-21b) with mathematical model fig.(4-8). The reflected power was shown in fig.(5-24),the sharp spike was shown at beginning (0MHz) caused by the Fresnel losses ,the bending fault at (6.24MHz) . This waveform was entered to the neural network software fig.(4-9) as discussed in section (4-8-2) called neural input, the output of ANNS was shown in fig. (5-25)

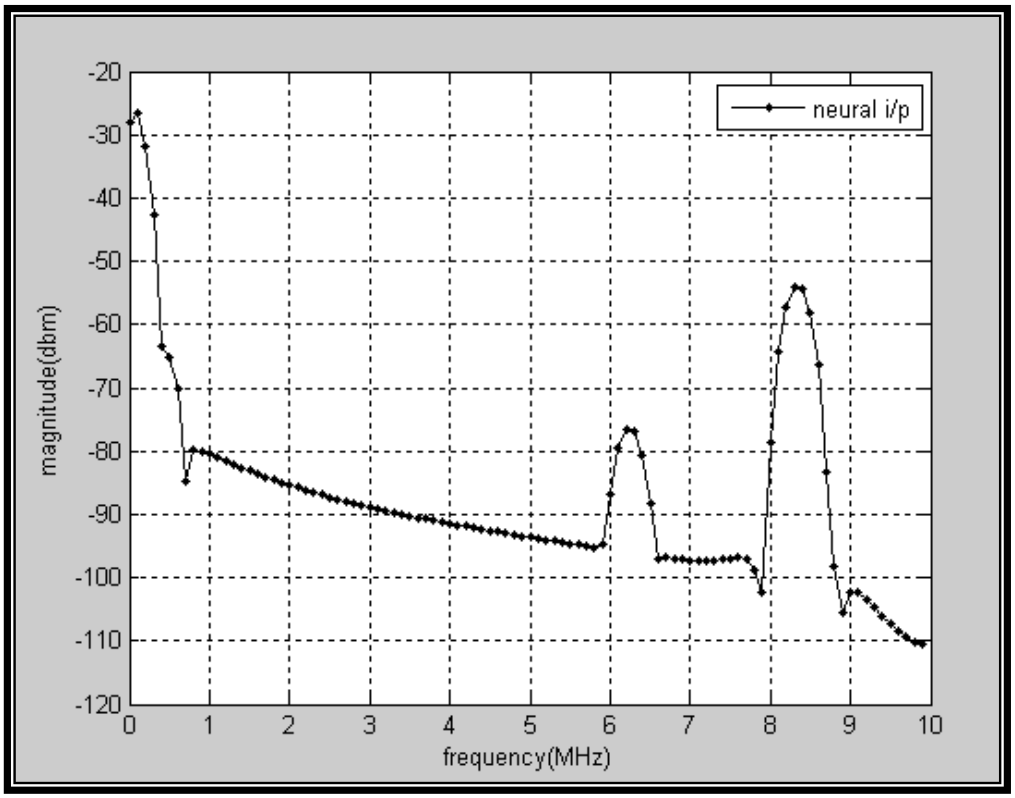

Figure (5-24) Reflected beat signal of defected SM optical fiber (bending fault) by (OFDR) and before using (MLP) neural network at 1550nm.

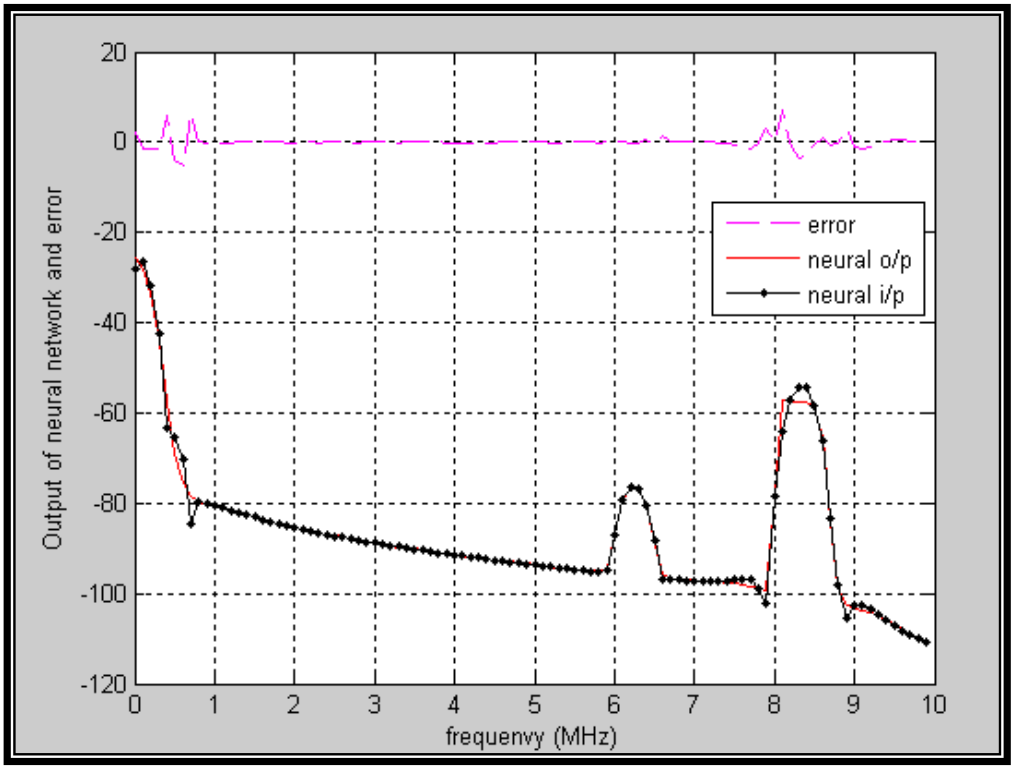

Fig.5-25:Reflected beat signal of defected SM optical fiber (bending fault) by (ANNS-OFDR) with (MLP) method at 1550nm.

It is clear that the error figure(5-25,red color) between the input neural fig.(5-25,black color) and the o/p of the neural network fig.(5-25, red color) was small so it means that the neural network was save the signal . when this ANN was implemented on the fiber optics practically, this system will detect any fault early inside the fiber by comparison with the information that it owns. small error is seen from fig.(5-25) in the beginning and end of fig.(5-25) between input and output waveform of neural network ,The error can be decreased by increase of neural nodes and number of epochs of software .

Chapter Four

Mathematical-Modeling of the Detecting System using Simulink Matlab Package

4.1 Introduction

Simulink is a software package for modeling, simulating, and analyzing dynamical systems. It supports linear and nonlinear systems, modeled in continuous time, sampled time, or a hybrid of the two. Systems can also be multirate, i.e., have different parts that are sampled or updated at different rates. For modeling, Simulink provides a graphical user interface (GUI) for building models as block diagrams, using click-and-drag mouse operations. Simulink includes a comprehensive block library of sources, linear and nonlinear components, and connectors. Simuling matlab customize and create our blocks. Models are hierarchical, so anyone can build models using both top-down and bottom-up approaches. Simuling matlab can view the system at a high level, then double-click on blocks to go down through the levels to see increasing levels of model detail. This approach provides insight into how a model is organized and how its parts interact[56] . In this chapter the elements of the design of faults detection Model are described ,different models are designed for different fault detection and then processed by artificial neural networks (ANNS) programming .

4.2 Fault detection design model:

4.2-1 Fault detection design model for 1310nm

Fault detection model was built by using OFDR system to detect any reflected signal along the single mode fiber SMF. Figure(4-1) was built to detect all faults of optical fiber by using OFDR at wavelength (1310 nm) by (DFT-FFT), the faults are :

1. Fresnel reflection fault.
2. Splice fault.
3. Connector fault.
4. Bending fault

To create the model, first simulink in the matlab command window was chosen On Microsoft Windows, the Simulink Library Browser was seen. From fig.4-1, the twelve blocks to the left were built from sources library (the Sine Wave block) . The Sine Wave blocks were sent from the Library Browser blocks to the model window by copying. Figure (4-1) was built from many blocks :

1. The Sine Wave block

The Sine Wave block generates a multi-channel real or complex sinusoidal signal, with independent amplitude, frequency, and phase in each output channel.

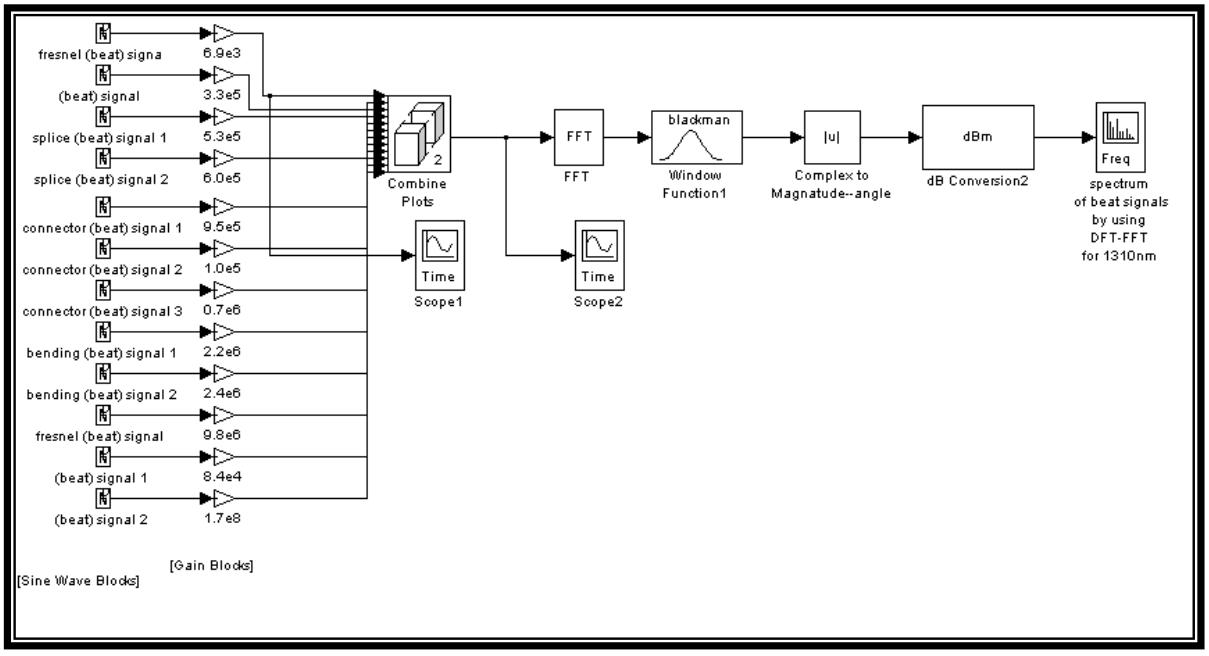

Fig.(4-1) Design model for all Faults detection(1310nm)

A real sinusoidal signal is generated when the output complexity parameter is set to real, and is defined by an expression of the type[57]

$$y = A\sin\left(2.\pi.f.t + \phi\right) \qquad \ldots\ldots\ldots\ldots (4.1)$$

Where :

A : the amplitude of beat signal reflected from SM optical fiber in watt .
f : the frequency of the beat signal in Hz .
ϕ : the phase of the beat signal.

A complex exponential signal is generated when the Output complexity parameter is set to complex, and is defined by an expression of the type[57] :

$$y = Ae^{j(2\pi ft+\phi)} = A\left\{\cos\left(2\pi ft + \phi\right) + j\sin\left(2\pi ft + \phi\right)\right\} \ldots\ldots(4.2)$$

2. Gain

The Gain block multiplies the input by a constant value (gain). The input and the gain can each be a scalar, vector, or matrix. Each element of the input is multiplied by each element of the gain. The block performs expansions, if necessary, so that the input and gain have the same dimensions.

3. Combine plots

Concatenate input signals of same data type to create contiguous output signal. Accepts signals of any data type supported by Simulink software. All inputs must be of the same data type. The Outputs are the same data type as the input.

4. Fast Fourier Transform (FFT)

Fourier Transform is one of the widely used mathematical tools by the engineers. It reduces the complex problems, such as spectrum analysis, in a more understandable form. It is almost impossible to analyze spectrum of any signal without using Fourier transform. Therefore, it is an essential tool during computer aided design of circuits and systems. However, computer can not use real numbers; it has to use finite precision numbers due to its digital nature. It is also not possible to process continuous signals in a computer; all the signals must be discrete. These requirements can be solved by discrete Fourier transform (DFT). Using the discrete version of

Fourier transform, computer can easily calculate the Fourier transform of any signal. The calculation speed of DFT is also reduced by Fast Fourier Transform (FFT). This powerful tool comes with almost all the circuit and system design tools[58]. FFT of reflected signal was Computed by this block .

5. Window function

The DFT results can be significantly different than what might be viewed on an analog spectrum analyzer if the input signal is non-integer multiple of frequency resolution. In this case the signal can be recovered by applying appropriate window to the data. The well-known window functions are summarized in Appendix C-4 .

6. Complex to Magnitude-Angle

The magnitude and/or phase angle of complex signal was computed by this block ,the phase angle was selected in calculation of (phase detection).

7. dB-Conversion

The dB Conversion block converts a linearly scaled power or amplitude input to dB or dBm. The reference power is 1W for conversions to dB and 1mW for conversions to dBm. The Input signal parameter specifies whether the input is a power signal or a voltage signal.

8. Scope

The Scope block is a comprehensive display tool similar to a digital oscilloscope. The block can display time-domain, frequency-domain, or user-defined signals. The Vector Scope block was used to plot consecutive time samples, or to plot vectors containing data such as spectral magnitudes.

4.2-2 Fault Detection Design Model for 1550 nm

Fault detection model was built by using OFDR system to detect any reflected signal along the SM optical fiber. Fig.(4-2) was built to detect all faults of optical fiber by using OFDR at wavelength (1550nm) by (DFT-FFT) .The same blocks were used as in fig.(4-1) to find all reflected signals but with different amount of reflected power.

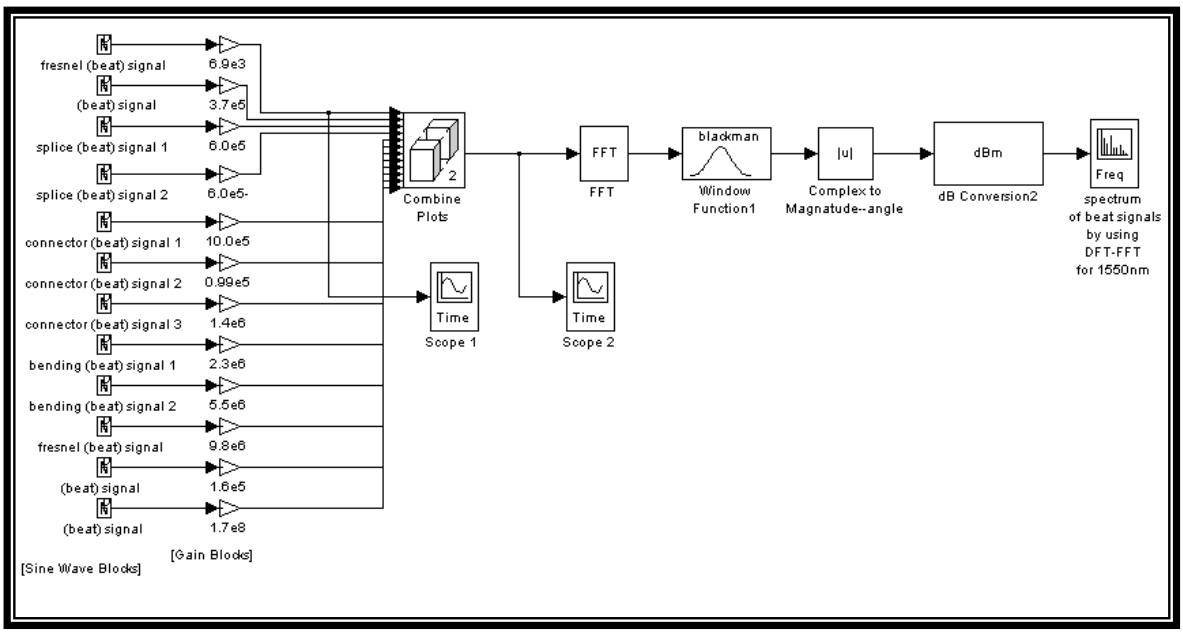

Fig.4-2 design model for all Faults detection(1550nm)

4.3 Undefected Optical Fiber Design Model for 1310 nm

Fault detection model was built by using OFDR system to detect any reflected signal along the Undefected SMF . Fig.(4-3) was built to detect all faults of Undefected optical fiber by using OFDR at wavelength (1310nm) with (DFT-FFT) ,the same blocks were used as above.

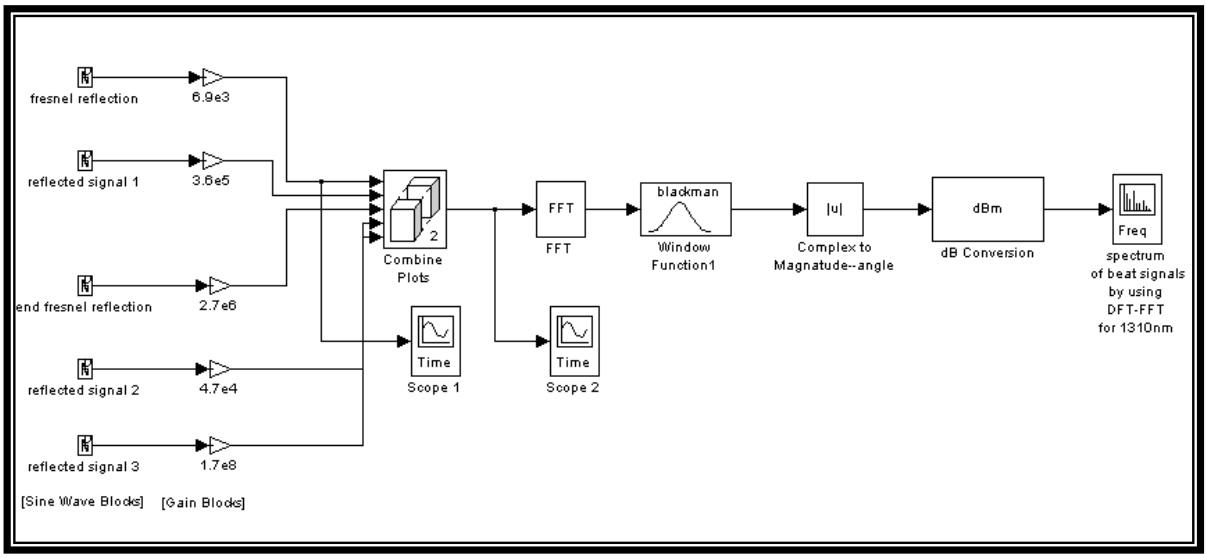

Fig.(4-3) design model for fault detection for undefected optical fiber

4.4 Undefected Optical Fiber Design Model 1550 nm

Fault detection model was built by using OFDR system to detect any reflected signal along the (SM undefected optical fiber). Figure(4-4) was built to detect all faults of undefected optical fiber by using OFDR at wavelength (1550 nm) with (DFT-FFT) ,the same blocks were used as above.

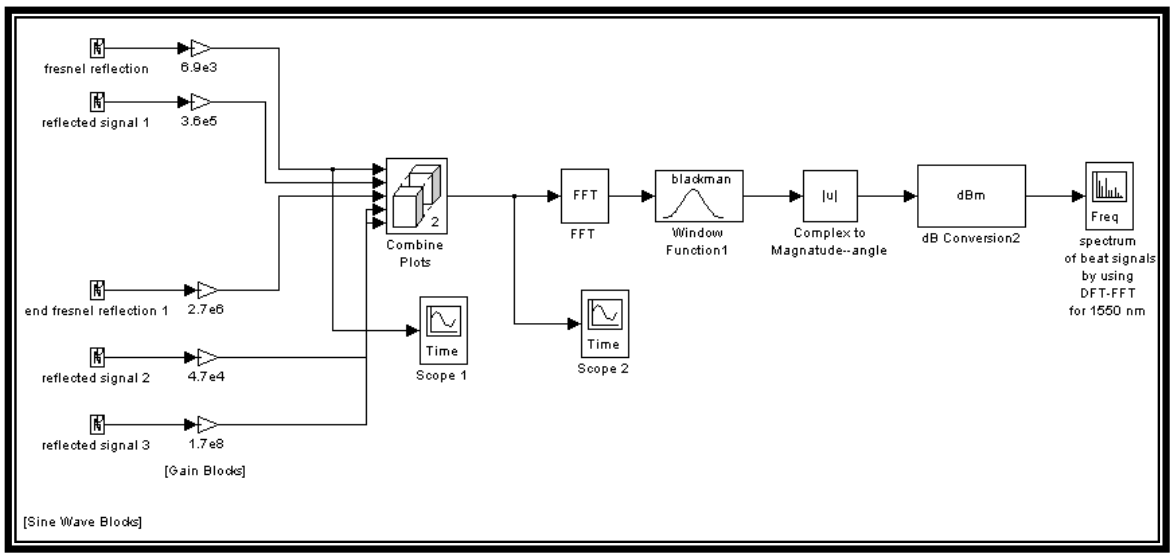

Fig.(4-4) design model for fault detection for undefected optical fiber (1550nm)

4.5 Single Fault Detection Design Model for 1310 nm

Single Fault detection model was built by using OFDR system to detect any reflected signal along the SM optical fiber. Figure(4-5) was built to detect single fault (splice fault) of optical fiber by using OFDR at wavelength (1310nm) by (DFT-FFT).All blocks were built as the same as above.

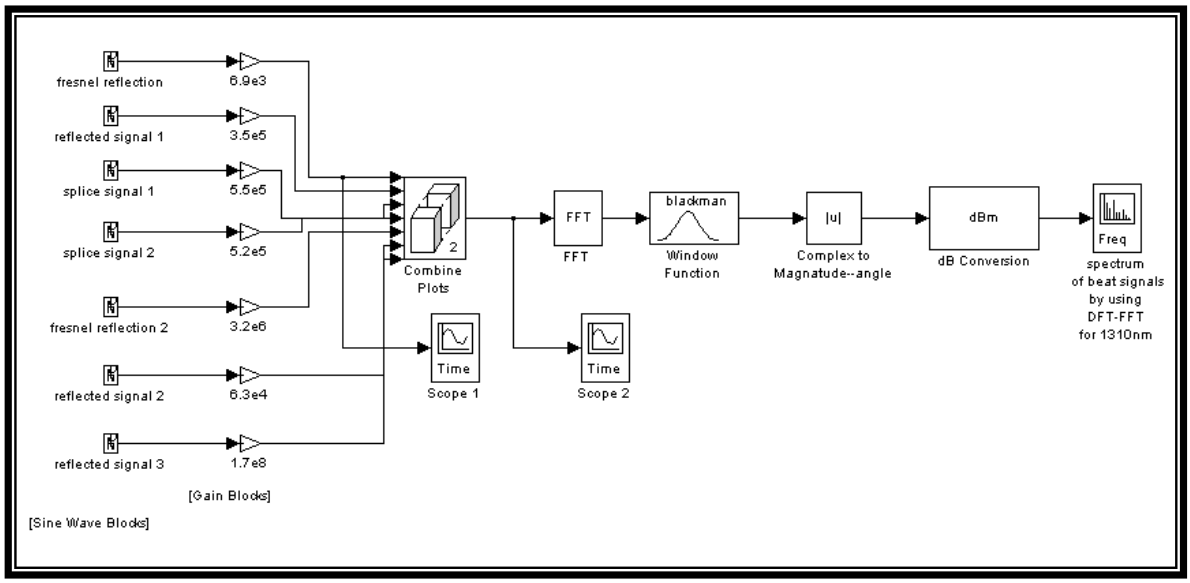

Fig.(4-5) Design of (faults Detection)of splice fault for (defected SM fiber) by using (OFDR)and wavelength of (1310nm) by (DFT-FFT)

4.6 Single Fault Detection Design Model for 1550 nm

Single Fault detection model was built by using OFDR system to detect any reflected signal along the SM optical fiber. Fig.(4-6) was built to detect single fault(splice fault) of optical fiber by using OFDR at wavelength (1550nm) by (DFT-FFT).All blocks were built as the same as above.

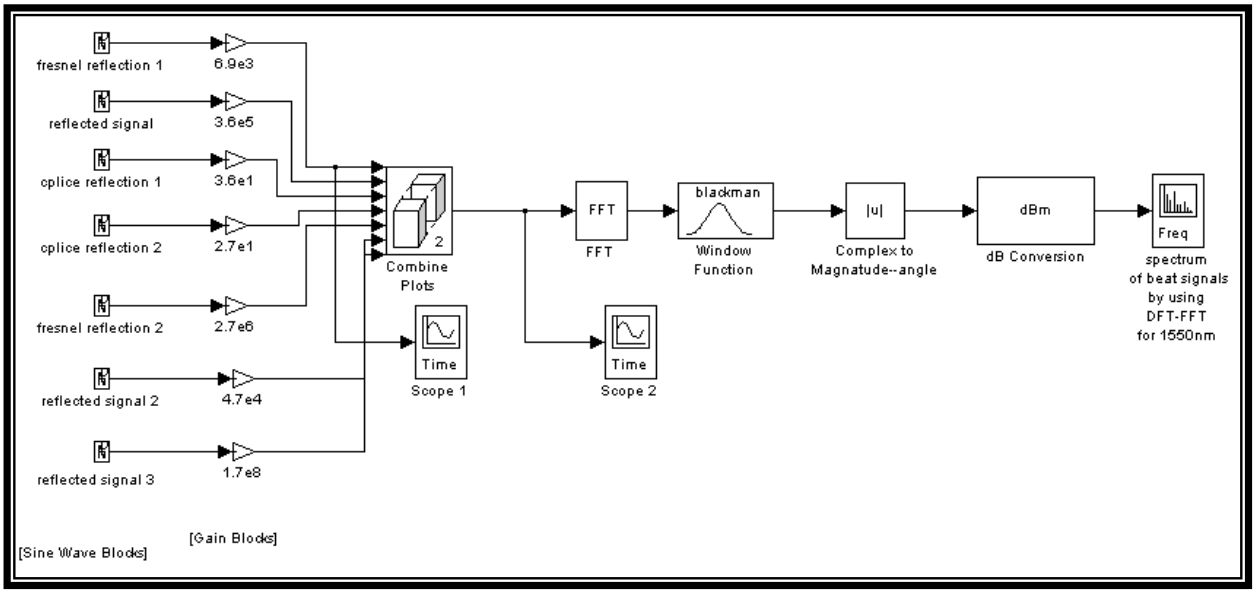

Fig.4-6 : Design of (faults Detection)of splice fault for (defected SM fiber) by using (OFDR) and wavelength of (1550nm) by (DFT-FFT).

4.7 Phase Detection Design Model for 1310 nm

Novel technique has been employed to measure losses and faults inside the optical fiber. This technique is the (phase detection method). Phase detection model was built by using OFDR system to detect any reflected signal along the SM optical fiber by using the phase. Figure(4-7) was built to detect fault from the phase of reflected signal at wavelength (1310 nm) .All blocks were built as the same above .The (Angle) was chosen from magnitude - angle block .

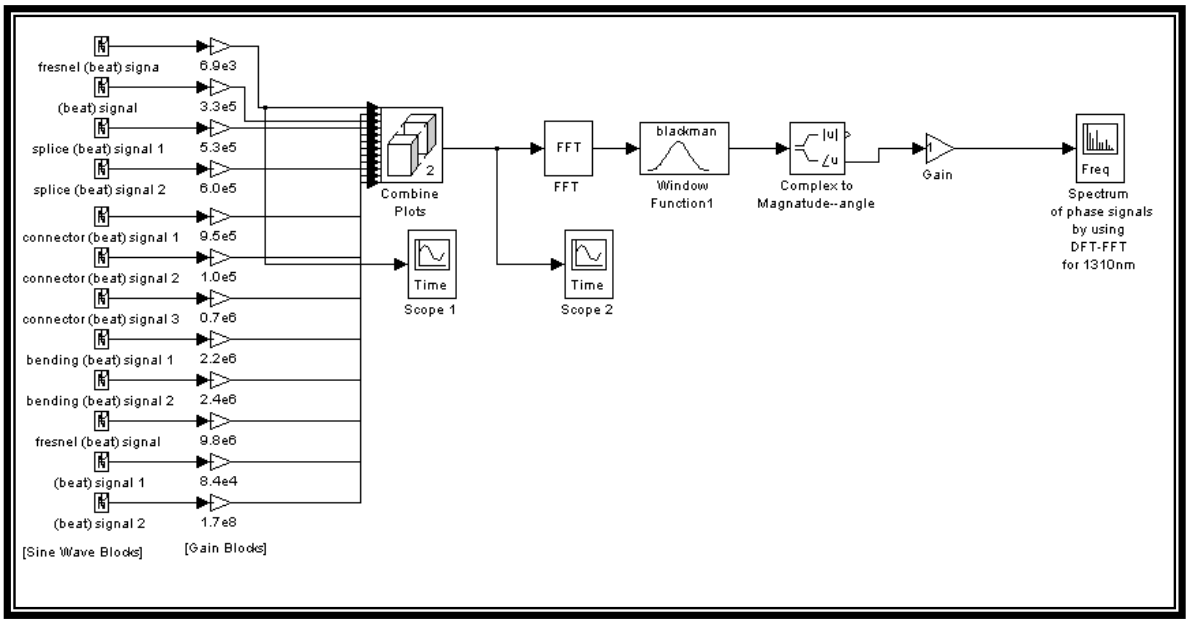

Fig.4-7 Design of (Phase Detection)of fault for (defected SM fiber) by using (OFDR) and wavelength of (1310nm) by (DFT-FFT)

4.8 Fault Detection Design Model by Artificial Neural Networks(ANNS) .

A novel technique was used to detect the amplitude of the fault along the optical fiber by using the Artificial Neural Network ANN .

4.8-1 Bending Fault Amplitude Design for 1550nm

The Bending Fault detection model was built by using OFDR system to detect bending signal along the single mode fiber SMF. Figure(4-8) was built to detect the bending fault of optical fiber at wavelength (1550 nm).The model consist of :

1) Fresnel reflection signal at Z = 0 km .

2) Reflected signal at Z = 0.96 km .

2) Bending reflection signal at Z = 15 km .

3) Fresnel reflection signal at Z = 20 km .

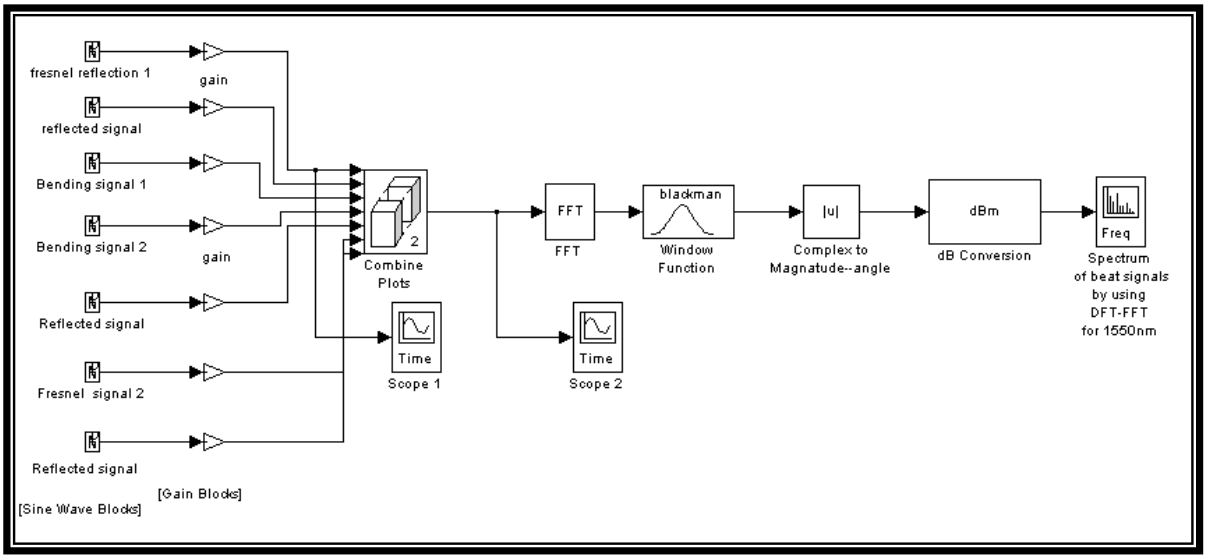

Fig.(4-8) Design of the bending fault detection for (defected SM fiber) by using (OFDR)and wavelength of (1550nm).

All the components of the fig.(4-8) were created by the same method as above from the simulink matlab package **.**

4.8-2 Single Fault Detection Design by ANNS and OFDR for 1550nm

All the parameters of the fig.(4-8) were implemented in the neural software of fig.(4-9) .

This parameters are :

1) The equations of the reflected signals along the fiber optic are included the amplitude and the frequency .

2) FFT equations .

3) Window function .Where the Blackman-Harris windows function was chosen . The resolution of this window, i.e., the ability to distinguish two closely spaced sinusoids from a single sinusoid is better than other windows .

5) dBm conversion .

The software of the neural network was operated by the matlab Package . The Neural Network software fig.(4-9) ANN has been designed with two layers, in the hidden layer there are (20) neuron node and in the output layer there is (1) neuron node, and different data have been given about kinds of faults, the losses, their values and their own shapes to this networks as above. The Matlab commands used in the procedure are (*newff* , *train,* and *sim*) .

The Matlab command (*newff*) generates a (MLPN) neural network, which is called (*net*) .The network training is originated using (*train*) command[54]. These networks will save all the data and training itself on this information. When this system is implemented effectively over any optical fiber the system of ANNS-OFDR will detect any fault early inside the fiber thus by comparison with the information that it owns .The software of the Artificial neural network (ANN) was shown in flowchart form below .

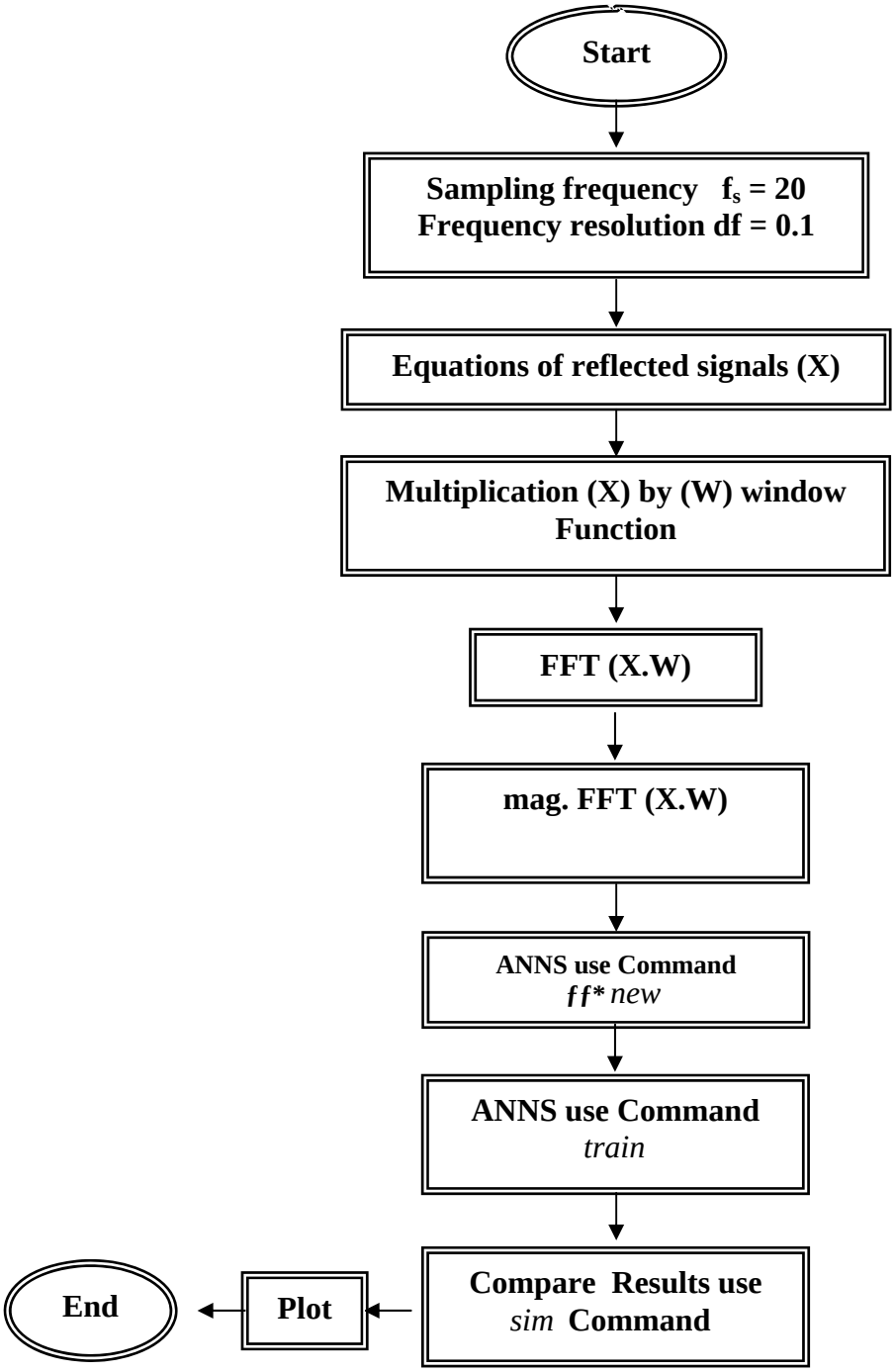

Figure (4-9) Flow Chart ANNS-OFDR

Chapter One

General Introduction

1.1 Introduction

The Fiber optic technician's today have high performance test equipment available to evaluate and test fiber optic cable and links. OTDR and OFDR allows the technician to evaluate connectors and splices measure loss per unit length and locate fault[1]. Optical reflectometry is critical diagnostic tool for light wave systems and components, there are basically three reflectometric techniques suitable for fiber-based applications: optical time domain reflectometry OTDR, low coherence frequency domain reflectometry (OLCR) and coherent optical frequency domain reflectometry OFDR, the different methods have tradeoffs in range, resolution, speed, sensitivity and accuracy. Typically the low coherence technique is used for sub-millimeter resolution measurements with very high sensitivity but only over limited range(5m). OTDR is used for longer range (several kilometers), low- resolution system-level applications[2]. OFDR falls between OTDR and OLCR in that its range capabilities are on the order of tens to hundreds of meters with millimeter-range resolution[3,4]. Optical fiber is the medium in which communication signal are transmitted from one location to another in the form of light guided through thin fibers of glass or plastic. These signals are digital pulses or continuously modulated analog streams of light representing information. These can be voice information , data information , computer information, video information ,or any other type of information, so the test of the fiber by (OFDR,OLCR,OTDR) is very important [5] .

1.2 Literature Survey

Barnoski M.K. and Jensen S.M. (1976)[6] have demonstrated a new method for the measurement of attenuation along an optical fiber. The method consisted of transmitting a short pulse of light through the fiber and measuring the time dependence of the Rayleigh backscattered light. This nondestructive technique, called optical time-domain reflectometry (OTDR), has become an indispensable tool for fiber characterization. It is applied from one end of the fiber and allows location and loss measurements of splices, defects, and other anomalies.

Michael K. Barnoski et al (1978)[7] have determined the insertion loss for a given fiber length, but give no information concerning the length-dependence of the loss. If the loss varies with length, then quoting attenuation as determined by insertion loss measurements in dB/km is meaningless. A new measurement technique in which an optical time domain reflectometer (OTDR) allows the length-dependence of the fiber attenuation to be displayed. The technique, based on the analysis of backscattered light in the fiber, requires neither cutting the fiber nor access to both ends of the fiber.

Gilgen H.H. et al(1989)[8] have developed optical reflectometer with a spatial resolution in the submillimeter range, optical time-domain reflectometer (OTDR) used mode-locked laser sources emitting subpicosecond pulses and a correlation detection or heterodyne receivers. Optical low coherence reflectometer (OLCR) are equipped with continuous wave broad-band light sources and coherent correlation detectors.

Ripamonti G. et al(1990)[9] have developed a new design of an optical time-domain reflectometer (OTDR) operating at room temperature with the single-photon counting technique. It features subcentimeters resolution without data deconvolution .The key component for the instrument is a single-photon avalanche diode (SPAD) .

Glombitza U. and Brinkmeyers E.(1993)[10] have developed a new system based on the principles of optical frequency domain reflectometry (OFDR) with highly resolving and sensitive technique suitable for detecting, localizing, and quantifying weakly reflecting irregularities in single-mode optical fiber. A DFB-laser diode at $\lambda o \cong 1.3\,\mu m$ tuned within a range of $\Delta\lambda \cong 6\,nm$ and $\Delta\nu \cong 1\,THz$, respectively, was used as a source in the experimental arrangement employing an auxiliary interferometer. The tuning need not be linear in time, in contrast to early implementations. They were got spatial resolution of 50μm and a dynamic range of about 60dB. These data surpass OFDR-results published at that time. Prospects of closing the gap to coherence-domain reflectometric results and specific advantages make OFDR to be a promising technique.

Passy R. et al (1994)[11] have investigated of coherent optical-frequency domain reflectometry using semiconductor laser sources. Good agreement was found between the analysis of the signal-to-noise ratio due to the phase noise and the experimental results. Limitations due to the nonlinearity in the optical frequency sweep produced by the thermal-response time of the laser and mode hopping are investigated and compared with experimental results. Two interferometer methods to characterize the thermal-response time of the laser and their implementations are described. The effects of mode hopping in the optical-frequency sweep are compared to numerical simulations.

A simple formula to predict the position of spurious peaks due to mode hopping are presented. A spatial resolution of 400μm over 10cm was obtained by correcting the nonlinearity in the optical-frequency sweep by using an auxiliary interferometer. The Rayleigh backscattering was observed for the first time over more than 400m of fiber using a DFB laser coupled to an external cavity.

Mussi G. et al (1996)[12] have evaluated polarization effects in coherent optical frequency domain reflectometry(OFDR). The use of a polarization average procedure completely eliminated these effects, giving rise to a measurement accuracy of 0.27dB for an arbitrary polarization vector of the detected signal, without making use of polarization diversity receivers, which are not suitable to this case.

Von Der J.P. et al (1997)[13] have proved the reflectivity measurements of wavelength-division multiplexed (WDM) filters were performed with polarization independent coherent optical frequency domain reflectometry OFDR. The spectral resolution of 0.012 nm allowed to characterize side lobe spacing and reflectivity with 90-dB dynamic range. The off-channel reflectivity was also measured for estimating the interchannel crosstalk in WDM systems and the experimental results were fitted to a theoretical equation, extracting the physical parameters of the filter.

Huttner B. et al (1997)[14] have performed the measurements of the intrinsic birefringence of optical fibers at 1550nm using the optical frequency domain Reflectometry technique OFDR. Polarization mode coupling length was obtained from local birefringence and polarization mode dispersion measurements.

Yoshihko T. et al (1999)[15] have developed the primary invention of OFDR system, an optical-fiber inspection device which detects the distance to a reflection point within the DUT light by dividing into two laser beam which is possible to be frequency-swept. The final reference light was obtained by providing an optical coupler in the reference light path and after taking out a part of the reference light and making it pass through an optical frequency shifter, combining this again with the original reference light with the optical coupler.

Jihong Geng et al (2005)[16] have used diode-pumped single-frequency piezoelectrically tuned fiber laser with narrow spectral line width as a light source in applications for long-range coherent frequency-domain reflectometry OFDR. Frequency-modulated continuous-wave (FMCW) measurements of Rayleigh back-scattering and Fresnel reflection from a 95-km-long fiber have been demonstrated without the use of an optical amplifier. This is the longest distance measurement with FMCW. The high sensitivity and dynamic range of the long-range backscattering measurements benefit from the extremely long coherence length of the narrow linewidth fiber laser, which has been estimated to be 210 km in air.

1.3 Aim of the Work

1. Analyzing and designing of optical frequency domain reflectometer OFDR and calculating the Rayleigh backscattered signal of defected and undefected single mode optical fiber (SMF) by using Fast Fourier Transformer (FFT) with different optical wavelengths of 1310nm,1550nm.

2. Comparing the resolution between the Rayleigh backscattered signal of defected single mode fiber SMF produced by optical frequency domain reflectometer OFDR and the Rayleigh backscattered signal of defected single mode optical fiber SMF produced by optical time domain reflectometer OTDR.

3. Detecting , locating , and classifying the faults or losses of single mode optical fiber SMF. The types of faults selected are : Fresnel reflection , splices losses, connector Fresnel reflection and losses, microbending and macrobending losses, scattering coefficient losses and total attenuation.

4. Presenting a computer simulation by using Matlab program for the signals reflected from the optical fiber with different faults by optical frequency domain reflectometer OFDR using FFT, and then implementing to the design model and comparing the artificial neural networks (ANNS) results of defected cables with non-defected ones.

1.4 Thesis Layout

Chapter one provides an introduction and literature survey about design of faults detection systems of OTDR, And OFDR .

Chapter two presents the analysis of single mode optical fiber, radius of the core, numerical aperture, normalized frequency, fiber attenuation and windows, Rayleigh scattering, bandwidth, birefringence, Fresnel reflection, losses of fiber joint, bending losses and coupler operation and it's losses.

In chapter three different faults detection system are described, first the equations of the OTDR and OFDR are derived . The equation of the Fresnel reflection is presented, and finally Fast Fourier Transform (FFT) and Neural Networks (ANNS) were implemented .

Chapter four presents the designs of faults detection model by using Matlab simulating Modeling Software for two wavelengths (1310, 1550 nm), for OFDR system. And a novel technique for faults by phase detection is designed.

In chapter five all the calculations and results of the designs introduced in chapter four will be discussed under the light of theoretical meaning that presented in chapter three.

Chapter six presents the summary and conclusions of the work in addition to a suggested future work.

Chapter Six

Conclusions & Future Work

6.1 Conclusion

OFDR and OTDR systems and related investigation by the fault of the SMOF lead us to conclude the following:

1. OFDR system has a better resolution than OTDR system.
2. OFDR system is more sensitive than OTDR system in SMF.
3. At fusion splice point, the losses are the same at short/long wavelength.
4. At bending point, the losses are more large for long wavelength.
5. At connector point, the losses are the same at short / long wavelength.
6. Novel technique of (phase detection) is used .The degree of the phase is changing suddenly for the signals in the places where the faults are happening. The phase degree increases with the increase of the fiber length which means that this new method is very useful in the optical fiber and for very long distances.
7. Novel technique of ANNS was used to detect the fault of SMF with high resolution and small error .

6.2 Future Work

The basic of this work can be developed toward further investigations for future work. The following research points may be suggest :

1. Developing the design of phase detection in relation to splice fault, the connector fault, and the bend fault practically .
2. Studying the effect of reduction of splice fault ,the bend fault , and the connector fault against the amplitude of the signal .
3. Studying the fault in the optical fiber by using (3) wavelengths instead of (2) wavelengths .
4. Developing the design of fault detection by Artificial Neural Network (ANNS) practically .
5. Studying the dispersion in SMF by using OFDR system .
6. Studying the polarization in SMF by using OFDR system .

Chapter Three

Theoretical Analysis of Optical Time Domain Reflectometer OTDR, Optical Frequency Domain Reflectometer OFDR and Artificial Neural Networks ANNS

3.1 Introduction

In this chapter different faults equations are described, first the equations of the OTDR are derived. The equation of the Fresnel reflection is presented. Some equations are explained for calculating the backscattering power signal at distance equal zero, and the backscattering power signal for different distances of the optical fiber. The equation of the Fresnel reflection in the end distance of the optical fiber is presented. The type of the laser source and its power and the type of the detector are discussed. The equation that describes the scattering coefficient is presented, and the equation that calculates the total attenuation is described. In the optical frequency domain reflectometer OFDR the same equations of the different faults at all distances of the optical fiber are presented however in frequency domain. The type of the source and its line width are described, the coherence time and the coherence length of the source are presented. OFDR system is operating by coherence detection hence the equations of coherence detection are presented. Artificial neural network(ANN) was used for the purpose of detecting the faults in fiber optic. Theoretical analysis of ANNS are described .

3.2 Fundamentals of OTDR Operation

Clearly, OTDR's are versatile instruments for testing optical fiber. Figure (3-1) illustrates the principal optical components. In a simple standard OTDR a laser is pigtailed to a connector on the OTDR (commonly called the front panel) through a 3dB optical coupler or beam splitter.

This coupler is typically a fused bidirectional device but may also be made of bulk optics. The laser fires short, intense bursts of light that are directed through the coupler and then out through the front-panel connector and into the fiber under test. As the pulse travels along the fiber, some of the light is lost via absorption and Rayleigh scattering. The pulse is also attenuated at discrete locations, such as splices, connectors, and bends, where local abrupt changes in the waveguide geometry couples light out of the core and into the cladding. When the pulse encounters discontinuities in the index of refraction (such as those found in connectors or the cleaved end of a fiber), part of the pulse's optical energy is reflected back toward the OTDR[27].

It is seen in chapter 2 that scattered light radiates in all directions, and some of it is scattered in the direction opposite the pulse and returns to the OTDR. Connectors, and un terminated fiber ends are all causes of Fresnel reflections that return light back to the OTDR. When this backscattered and back-reflected light reaches the OTDR, the coupler or beam splitter directs it to the optical receiver. This receiver typically is an avalanche photodiode (APD), but in some designs it may be a p-type-intrinsic-n-type (PIN) detector or even a photomultiplier tube. Whatever device is used in the optical receiver, the receiver's function is to convert the optical power into an electric current, which is then amplified, sampled, digitized, and displayed to the operator.

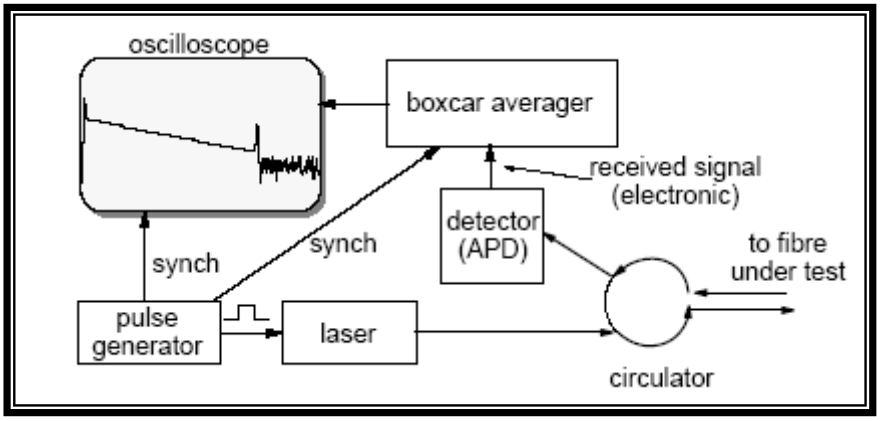

Figure(3-1)OTDR Instrument Principle[31]

3.2-1 Laser Diode (Pulse Type)

Pulse lasers are normally used in high-power pulse applications such as OTDR. The most common pulse laser is of the single-heterostructure type, which is somewhat simpler than the double-heterostructure laser, only one Indium Gallium Phosophide (InGaP) layer is used for optical guiding for wavelength 1310 nm and 1550 nm, Appendix C-1.

Signal pulses can not used with high power for many reasons and so pulses of (10-20) mW are typically sent. The problem of low return power is addressed in two ways:

1. A very sensitive APD detector is used. As noted elsewhere detectors double in sensitivity every time you halve the digital bit rate. Thus an APD becomes very sensitive indeed at the very low pulse rates used. The penalty for using APDs is additional noise but this is mitigated by the averaging process.
2. A “boxcar averager” circuit is used to average many thousands of returning pulses. The averaging process removes a large amount of noise. (Most of the noise comes from the APD and its associated circuitry.) In some (very sensitive, long distance) OTDRs the averaging time can be of the order of several minutes.

The averager provides logarithmic scaling of its output so that the vertical scale on the display can be displayed in dBm. The pulse rates used are quite slow, Since the optical signal propagates at approximately 5 microseconds per kilometer so it means 10 microseconds per kilometer of fiber length(r.t), for 20 km of fiber the propagation time is 200 microseconds between pulses and so a pulse rate (repetition rate) of 5000 pulses per second would be the maximum possible[31] .

3.2-2 Typical OTDR Waveform

Figure(3-2) shows a typical OTDR signal trace, commonly referred to as a waveform. The broad, sloping regions of the waveform result from Rayleigh backscattering, and the sharp spikes result from discrete points of reflection on the fiber. The spike near the beginning of the waveform, on the left side, is a reflection from the OTDR's front-panel connector. At the looking closely, the second spike is seen short after the first. This second spike was caused by the connector .

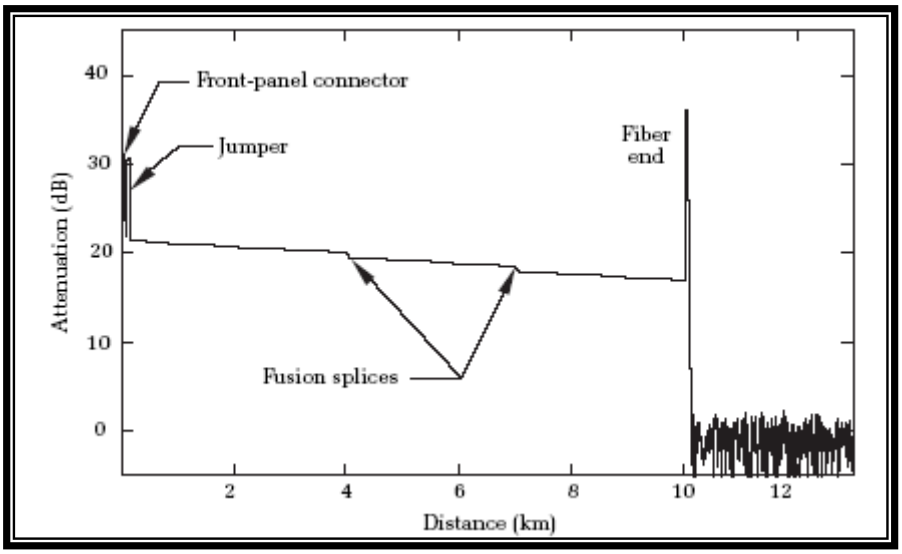

Figure(3-2) A typical OTDR waveform[19].

Along the broad, sloping portion of the waveform two points are seen where the Rayleigh scattering level drops abruptly. These two drops in the backscatter result from a pair of non reflective fusion splices. The large spike at the end of the waveform is caused by reflected light off the patch panel's connector located at the opposite end. These connections tend to be highly reflective due to the glass-to-air surface when not cross connected to a patch cord or when connected to the optical receiver[19].

3.2.3 Measurable Parameters

From an OTDR one can quickly determine the following characteristics of the fiber link under test:

a. The length of the fiber .

b. The attenuation in dB of the whole fiber link and the attenuation of separate sections of fiber

c. The attenuation characteristics of the basic fiber itself.

d. The locations of connectors, joints and faults in the cable.

These locations are measured from the beginning of the fiber and can be as accurate as a few meters[39].

3.2.4 Backscattering in Single Mode Fiber

Rayleigh scattering is caused by the microscopic non uniformity of the refractive index of glass. A ray of light is partially scattered into many directions, thus some light energy is lost. An important precondition for this phenomena is the scattering coefficient (α_s) decreases as the wavelength increases, (α_s) is proportional to 1/ λ^4. Rayleigh scattering represents by far the strongest attenuation mechanism in modern silica fibers, it may be responsible for 90% of the total attenuation.

The second effect is the absorption caused by unwanted material in the fiber. Water (OH-ions) is the dominant absorber in most fibers, causing the peaks in optical loss at 1.25 and 1.39 μm. Above 1.7μm, glass starts absorbing light energy due to the molecular resonance of $Si0_2$. Modern manufacturing methods are capable of reducing these effects to almost zero. The attenuation curve clearly shows in Figure(2-5) why communication link designers prefer the 1.31μm and the 1.55μm wavelengths[33]. Attenuation causes an exponential decay of the optical power along the fiber[26]:

$$P(Z) = P_o \exp(-\bar{\alpha} Z) \qquad \text{..... (3.1)}$$

P(z) - optical power at distance Z from input

P_0 - optical power at fiber input

$\bar{\alpha}$ - attenuation coefficient. [1/km]

$\alpha = 4.35\ \bar{\alpha}$ dB/km

Engineers are used to thinking in dB, therefore the equation(3.1) may be rewritten by conversion base (e) to base (10), the attenuation coefficient of a fiber can be as[26]

$$\alpha = \alpha_a(absorption) + \alpha_s(scattering) \qquad \text{..... (3.2)}$$

A pulse with power (P_o) and pulse duration (w) shall be launched into the fiber. From attenuation of fibers, at a distance (z) from the fiber input the transmitted pulse power $P_t(z)$ is attenuated to[26]:

$$P_t(Z) = P_o.10^{-\alpha Z/10dB} \qquad \text{..... (3.3)}$$

The pulse duration (w) corresponds to a geometrical pulse length Δz. The total scattered power P_s (z) at the distance z is [26] :

$$P_s(Z) = \alpha_s \Delta Z P_t(Z) \qquad \text{..... (3.4)}$$

Due to the limited numerical aperture of the fiber, only the fraction (S) of the scattered power travels back to the source. While traveling back the same distance, the backscattered power is attenuated again. At the input, the backscattered power P_{bs} (z) which was generated at a distance Z is[40][41] :

$$P_{bs}(Z) = S \alpha_s \Delta Z T_s P_o 10^{-2\alpha Z / 10\, dB} \qquad \text{..... (3.5)}$$

with $Z = t V_{gr} / 2$

and $\Delta z = w.V_{gr} = w\, c / n_{gr}$

and $S = (NA / n_1)^2 / 4.55$

α - total attenuation coefficient, [dB/km]

S - backscattering factor

P_0 - power launched into the fiber, [Watt]

T_s - round-trip transmission rate of the beam splitter in OTDR.

z - one-way length parameter

t - round trip time from fiber input to location z

Δz - pulse length on the fiber, [m]

V_{gr} - group velocity

c - speed of light. 3×10^5 km/s

n_1 - refractive index of the fiber core center

n_{gr} - group index, $n_{gr} = c / v_{gr} \approx n$

w - pulse duration

NA - the fiber's numerical aperture.

The subsequent scattering due to the density fluctuations ,which is in almost all directions, produces an attenuation proportional to $1/\lambda^4$ for a single component glass this is given by[32]:

$$\alpha_s = \frac{8\pi}{3\lambda^4} n_1^8 P^2 \beta_c k T_F \qquad \text{..... (3.6)}$$

α_s - scattering coefficient. [1/km], In the case that α_s is given in [dB/km] multiply by 0.23 to get α_s in[1/km] .
λ - optical wavelength
n_1 - refractive index of the core
P - average photoelastic coefficient
β_c - isothermal compressibility
T_F - fictive temperature
k - Boltzmanns constant

The backscattered signal clearly decays exponentially with length or time. Averaging techniques (boxcar averaging) are necessary to resolve such small signals. The Fresnel reflection from the fiber input and output is usually the largest signal ,its magnitude may be up to 4% or –14dB of the launched optical power .If the laser emits polarized light ,then the front reflex can be suppressed by using polarizing beam splitter .

Fresnel reflection from input and output optical fiber dose not depend on the backscattering factor (S). this power can be calculated from input power (P_o) ,the round-trip loss ($2\alpha L$),and the reflection coefficient (r) of (eq.2.15) at the input and end of the fiber[40] :

$$P_p = rP_oT_s10^{-2\alpha L/10\,dB} \qquad \text{..... (3.7)}$$

3.2-5 Laser Source Coupling

Laser sources, have asymmetric beam patterns (although the patterns are much narrower than the LED patterns). An additional difficulty is incurred when trying to couple the light into a small-core single-mode fiber. (Core diameters can range from 5 to 9 μm.) The small size of the core increases the sensitivity of the coupling efficiency to misalignment. Lens elements are frequently used to match the small active source area to the size of the fiber core.

Both microlenses and graded-index lenses (also called "GRIN lenses") have been used , as well as cylindrical lenses. While the use of lenses helps to match the source and fiber core areas, it also has the effect of increasing the sensitivity of the coupling coefficient to lateral misalignment errors. In addition, the presence of reflections from the lens elements and the fiber back into the laser can upset the frequency stability of single-frequency single-mode fiber[42] .

3.2-6 Lens-Coupled Fiber

As indicated in the coupling efficiency results for the butt-coupled fiber, mismatching of the source area and the area of the fiber core wastes power. The obvious solution is to physically match the size of the source and the size of the fiber. If the size of the source is smaller than the size of the fiber (a case that typically exists with a laser), a lens can be used to optically match the apparent size while increasing the directivity of the source by the magnification factor. (Unfortunately, no remedy exists if the size of the source exceeds the size of the fiber).

Since the source and fiber sizes are so small and one does not want to have to use a lens much bigger than this size, there arises a need for small microlenses to perform this coupling task. Several lens geometries have been attempted some are illustrated in Figure(3-3). The goal of each of these schemes is to magnify the effective emitter area to match the area of the fiber core. The "bulb-end" fiber is easily made by heating the end of the fiber and letting it cool[43] .

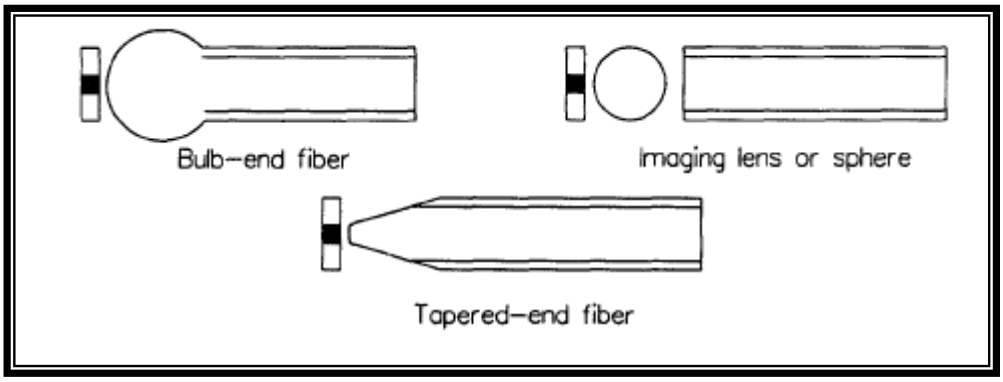

Figure(3-3) Source-fiber coupling using lenses[43].

3.2-7 Avalanch Photodiodes (APD)

An avalanche photodiode APD internally multiplies the primary signal photocurrent before it enters the input circuitry of the following amplifier. The multiplication effect is achieved by applying a very high electric field across the photodiode. When a photon-generated electron encounters this high electric field, it can acquire sufficient energy to kick more electrons from the valence to the conduction band, thereby creating secondary electron-hole pairs.

These secondary pairs also get accelerated to higher energies and therefore can generate even more electron-hole pairs. This increases receiver sensitivity since the photocurrent is multiplied prior to encountering the electrical noise associated with the receiver circuitry. The process is called avalanche multiplication, and hence the device is called an avalanche photodiode.

Since the avalanche process is random, the mean number of electron-hole pairs created is a measure of the carrier multiplication. This is called the gain and is designated by M (or sometimes by G or Gm). The value of M can be made quite large, but larger gains increase the noise currents of the device because of larger variations in the photocurrent. the performance of an ***APD*** is characterized by its responsivity $\boldsymbol{R_{APD}}$. Thus in an ***APD*** the multiplied photocurrent IM is given by[25]:

$$I_M = R_{APD}\, P_o = M\, \bar{R}\, P_o \qquad \text{..... (3.8)}$$

Where:

$\bar{R}$ - is the unity-gain responsivity[25] . Appendixes C-3 .

3.3 Optical Frequency Domain Reflectometer OFDR

Optical reflectometry is a critical diagnostic tool for light wave systems and components. There are basically three reflectometric techniques suitable for fiber-based applications: optical time domain reflectometry (OTDR), low coherence frequency domain reflectometry (OLCR) and coherent optical frequency domain reflectometry OFDR. The different methods have tradeoffs in range, resolution, speed, sensitivity and accuracy. Typically, the low coherence technique is used for sub-millimeter resolution measurements with very high sensitivity but only over limited range (< 5 m). OTDR is used for longer range (several kilometers), low-resolution system-level applications. OFDR with millimeter-range resolution is based on swept wavelength[44, 45] .

3.3-1 Principle of the Coherent OFDR

The coherent OFDR technique consists of analyzing the beat signal produced by the optical interference between a fixed reference reflection called local oscillator reflection and different reflections coming from the component under test. The interference signal is obtained with a Michelson interferometer for which the reflection at the end of one of the arms gives the reference signal, or local oscillator (LO)[46].

The device under test is connected to the other arm. Figure(3-4) presents the basic experimental set-up for OFDR measurements. The optical frequency of a laser source is swept linearly and the light is launched at the input arm of a Michelson interferometer. Because of the linearity of the optical frequency sweep, the beat frequency is proportional to the distance between the LO and the reflection point while the reflection intensity is given by the squared amplitude of the beat signal.

The latter, in the present coherent detection scheme, is in turn proportional to the electric field of the reflected light. This is the basic reason of the great improvement in sensitivity with respect to the direct detection technique. A polarization controller is placed in the reference arm in order to match the polarization states of the test and reference arms reflected optical fields.

This is a fundamental problem in coherent detection, The Fourier analysis of the beat signal, which is done by a fast Fourier transform (FFT) spectrum analyzer, allows the visualization of multiple reflections, similarly to an OTDR trace. A Blackman–Harris window is used in the FFT process in order to minimize the scalloping loss and side lobe effects[3].

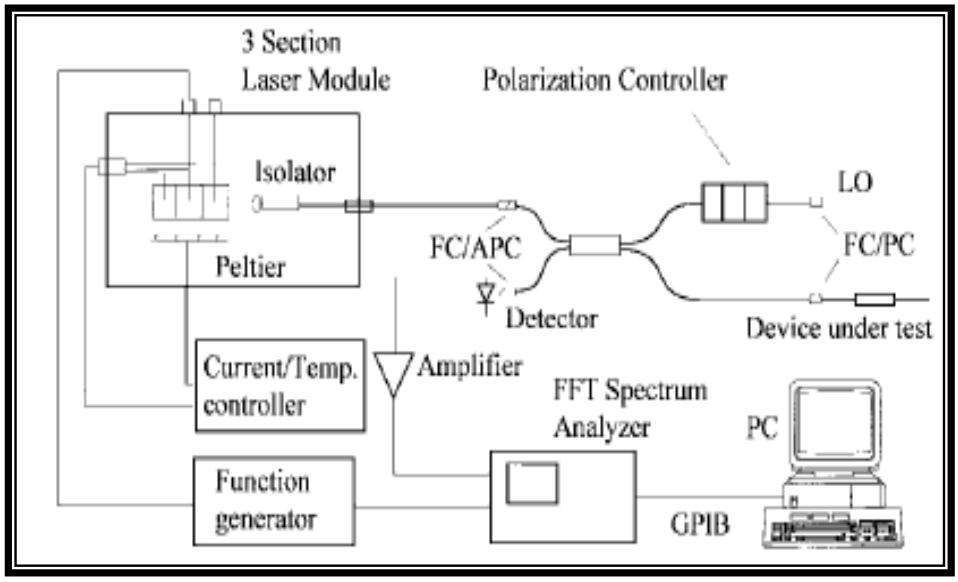

Figure (3-4) Block diagram for OFDR measurements[3]

3.3-2 Coherence Range

Since the signal is obtained from an interference between the DUT and the LO, the range is limited by the coherence of the laser. If the DFB laser has a line width of about 1MHz over the whole tuning range, which gives a spatial range of about 80 m (depending on the strength of the reflections).

Increasing the range is possible, but would require a tunable laser with smaller line width[46]. The coherence length (I_C) is given by[15]:

$$I_C = \frac{c}{2 n_1 \Delta f} \qquad \text{..... (3.9)}$$

Δf : is the line width of the laser .
c : is the light speed
n_1 : is the refractive index of the SMF core[15]

3.3-3 Sensitivity

Due to the coherent detection (interference between a fixed LO and the reflection from the DUT), the sensitivity is very high, above 100 dB in principle . However, strong reflections, even when they are from far away (i.e. further than the coherence length of the laser) generate a large background noise, which limits the sensitivity. The OFDR is thus better suited to the measurement of optical networks and devices with low back reflection levels, below –30 dB. This is not a major limitation anymore, since all recent systems have such a low back reflection[47].

3.3-4 Spatial Resolution

Spatial resolution is a key feature in reflectometry. For an ideal optical source with zero line width, the spacing between the FFT frequencies gives the resolution limit[3] :

$$\Delta \ell = \frac{c}{2 n_1 \Delta \upsilon} \qquad \text{..... (3.10)}$$

$\Delta \ell$: Spatial Resolution
$\Delta \nu$: total optical frequency sweep

The round-trip time of flight of the light in the test arm of the interferometer is given[3] :

$$\tau = 2 n_1 Z / C \qquad \text{..... (3.11)}$$

τ : is the round-trip time of flight

Z : distance of any point in the (DUT)

The coherence time of the laser is given by [3] :

$$t_c = 1 / \pi . \Delta f \qquad \text{..... (3.12)}$$

t_c : is the coherence time of the laser.

Nonlinearities in the optical frequency sweep, will impose further limits on the resolution, because the beat frequency corresponding to a given reflection peak varies during the data acquisition. The nonlinearity arises because of the thermal response of the laser. Adding a second order term (γ) to the optical frequency sweep the angular frequency of the light $\omega(t)$ can be written as[3] :

$$\omega(t) = \omega_o + \beta t + \gamma t^2 \qquad \text{..... (3.13)}$$

where (ω_o) is the start frequency and (β) is the sweep rate. Neglecting the laser phase noise, the optical beat signal $I(t, \tau)$ corresponding to a single reflection in the test arm, at a distance (Z) from the local oscillator will be given by[3] :

$$I(t,\tau) = (e^{-t/t_c}) \frac{E_o^2}{2} \sqrt{R_{LO} R_{DUT}} \cos[\ \omega_o \tau - \frac{\beta \tau^2}{2} + \frac{\gamma \tau^3}{3} + (\beta\tau - \gamma\tau^2)t + \gamma\tau t^2\ ] \qquad \text{..... (3.14)}$$

E_0^2 : laser optical power .
R_{LO} : reflectivities of the local oscillator .
R_{DUT} : reflectivities of single mode fiber (DUT).

The beat frequency (f_b)corresponding to this reflection will be given by[3]

$$2\pi f_b = (\beta - \gamma\tau)\tau + 2\gamma\tau t \qquad \text{..... (3.15)}$$

which means that the beat frequency changes linearly along the sweep, no more being constant. In the case of a small nonlinearity ($2.\gamma.t << \beta$) the reflection will be characterized by a peak in the frequency spectrum whose width is proportional to the round-trip time (τ) , i.e., to the distance between the reflection and the local oscillator[3]. so that the sweep rate is given by[15]:

$$\beta = \frac{\Delta v}{\Delta T} \qquad \text{..... (3.16)}$$

ΔT : the period of the triangular waveform .

So from equation (3.17) the beat frequency (f_b) is given by [3][15] :

$$f_b = \frac{\beta \tau}{2\pi} \qquad \text{..... (3.17)}$$

A full sweep of 6 GHz limiting the resolution to 1.6 cm. The choice of the full optical frequency span depends on the actual length of the device under test[15][3] .

The peak power in the frequency spectrum will decrease not only due to the finite coherence time of the laser only but also because of the attenuation along the fiber and non linearity and must be calculated by the Fourier transform of equation (3.16) .This effect is clearly shown in Figure(3-5) where it was measured[3].

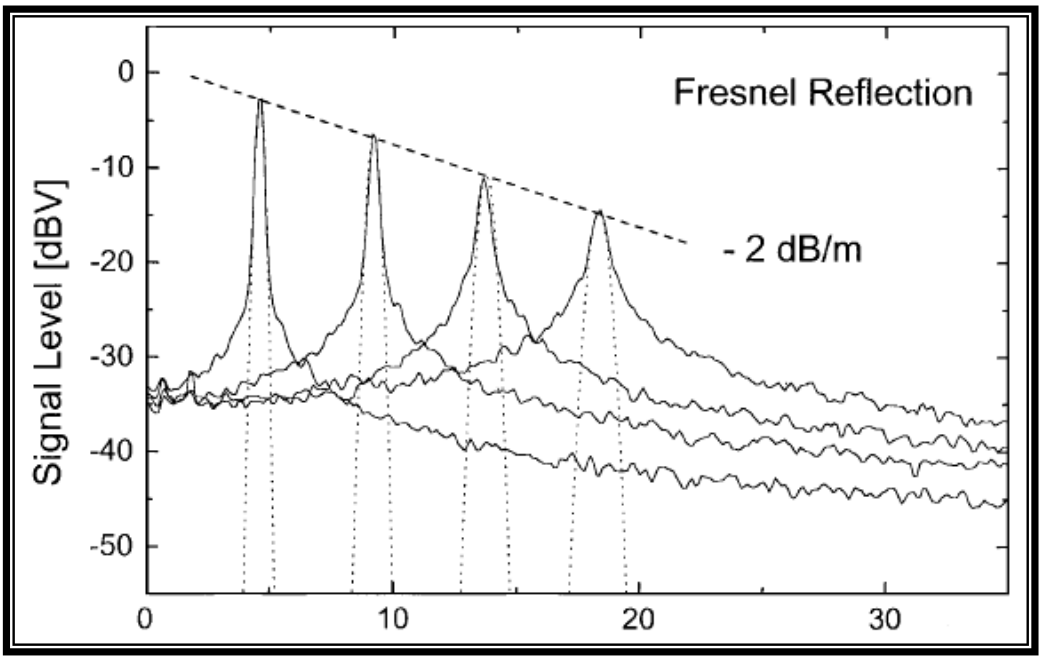

Figure (3-5) Beat Frequency (kHz)[3]

The Fresnel reflection signal coming from the end of an 11- m fiber end, so that the input conditions were kept unchanged. The peak intensity decays exponentially at a rate of 2 dB/m, and the spatial resolution degrades, meaning that the attenuation and coherence time and sweep nonlinearities are present in the measurement.

The dashed line in Figure(3-5) shows the theoretical prediction from equation (3.16) by using a Blackman–Harris window in the FFT calculation. From equation (3.16) the root mean square (rms) beat signal power level will be[3] :

$$\bar{P} = \frac{1}{\sqrt{2}}\left(e^{-\tau / t_c}\right)\frac{E_o^2}{2}\sqrt{R_{LO}\,R_{DUT}} \qquad \text{..... (3.18)}$$

In many detection systems, a highly coherent laser source is necessary to perform sensitive interferometric or coherent measurements. A compact laser system that provides a stable laser frequency with a very narrow line width using a 60mW DFB semiconductor laser was built, the laser line width was tuned from 570 kHz down to an equivalent of 1.8 kHz. Similarly, the coherence length was increased from 145m up to 45km[48] DFB laser diodes have recently become available tuning within a wavelength range between (730 and 2800) nm[49]

3.3-5 Applications of the OFDR

The initial applications were essentially in the detection of discrete reflections, such as the ones created by splices, connections or defects in the fibers, see Figure (3-6)[46]

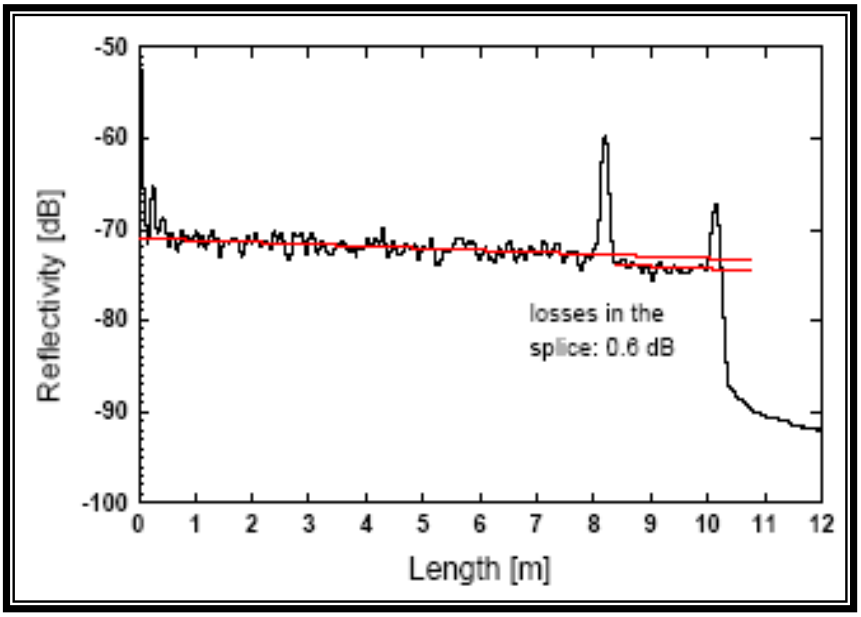

Figure (3-6)Measurement of a mechanical splice[46] .

The OFDR can also measure the reflections from optical elements. We present here, as an example, a wavelength division multiplexed (WDM) filter, see Figure(3-7) [50].

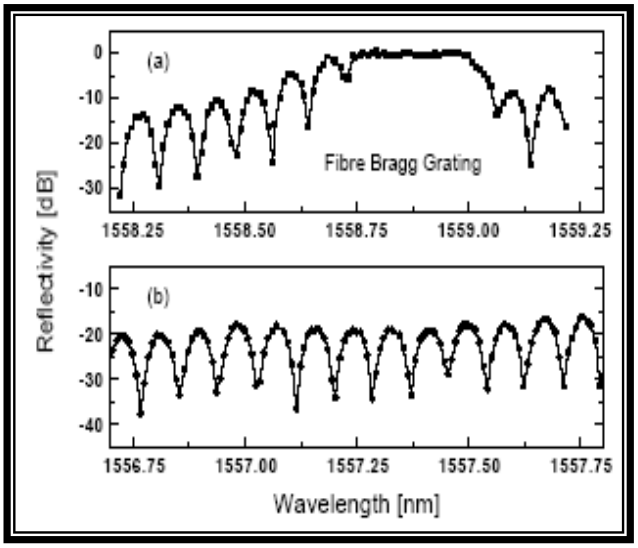

Figure (3-7) Characterization of a WDM filter[50]

In addition, the instrument is also very good at detecting distributed reflections. For example, the distributed loss and gain in Erbium-doped fibers, see Figure(3-8)[51].

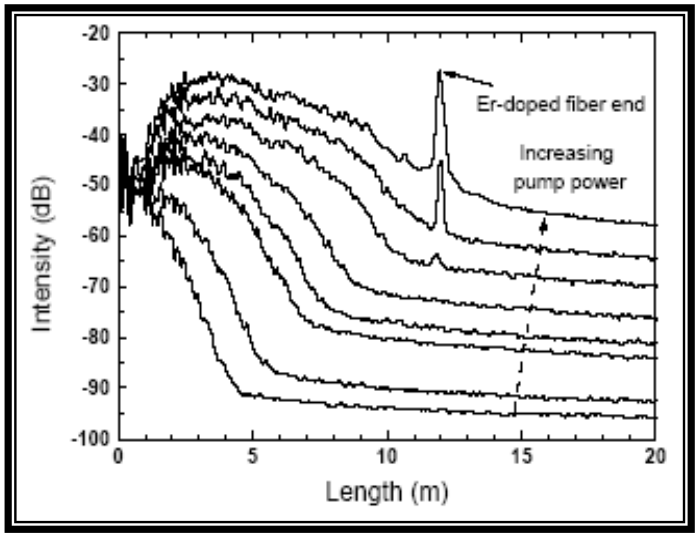

Figure (3-8) Distributed gain of an Erbium-doped fiber[51]

3.4 Artificial Neural Networks(ANNS)

Scientists and engineers often need to know if a particular object or condition is present. For instance, geophysicists explore the earth for oil, physicians examine patients for disease, astronomers search the universe for extraterrestrial intelligence, and optical communication engineers for detect, localize, identification faults in the optical fiber, etc. These problems usually involve comparing the acquired data against a threshold. If the threshold is exceeded, the target (the object or condition being sought) is deemed present .

3.4-1 Neural Network Architecture

Humans and other animals process information with neural networks. These are formed from trillions of neurons (nerve cells) exchanging brief electrical pulses called action potentials. Computer algorithms that mimic these biological structures are formally called (artificial neural networks ANNS) to distinguish them from the squishy things inside of animals.

Neural network research is motivated by two desires: to obtain a better understanding of the human brain, and to develop computers that can deal with abstract and poorly defined problems.

For example, conventional computers have trouble understanding speech and recognizing people's faces. In comparison, humans do extremely well at these tasks. Many different neural network structures have been tried [52] .

The most commonly used structure is shown in Figure(3.9) .This neural network is formed in three layers, called the input layer, hidden layer, and output layer.

Each layer consists of one or more nodes, represented in this diagram by the small circles. The lines between the nodes indicate the flow of information from one node to the next. In this particular type of neural network, the information flows only from the input to the output (that is, from left-to-right). Other types of neural networks have more complicated connections, such as feedback paths.

The nodes of the input layer are passive, meaning they do not modify the data. They receive a single value on their input, and duplicate the value to their multiple outputs.

In comparison, the nodes of the hidden and output layer are active. This means they modify the data as shown in Figure (3-10). The variables: ($X1_1$,$X1_2$,$X1_{15}$) hold the data to be evaluated, see Figure(3-9). For example, they may be pixel values from an image[53], or they may also be the output of some other algorithm, such as the classifiers in our research faults detection of optical fiber, like the amplitude of connector or splice , etc.

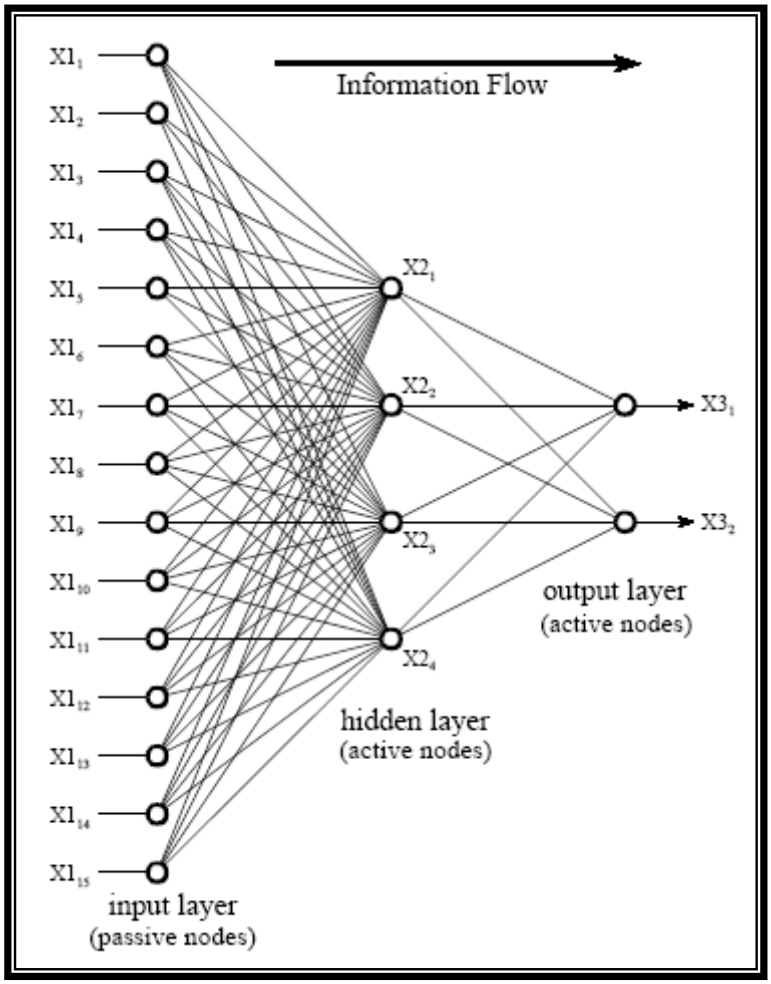

Figure (3-9) Neural network architecture[53] .

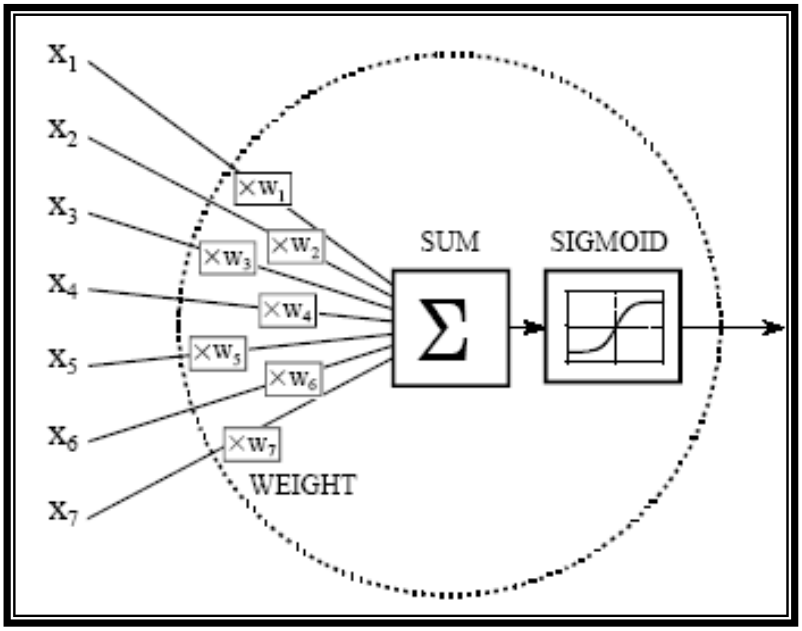

Figure (3-10) Neural network active node[53]

3.4-2 Multilayer Layer Perception (MLP)

The most useful neural networks in function approximation are Multilayer Layer Perceptron (MLP) and Radial Basis Function (RBF) networks. Here we concentrate on MLP networks. A MLP consists of an input layer, several hidden layers, and an output layer. Node(i), also called a neuron, MLP network is shown in Figure(3-11). It includes a summer and a nonlinear activation function (g).

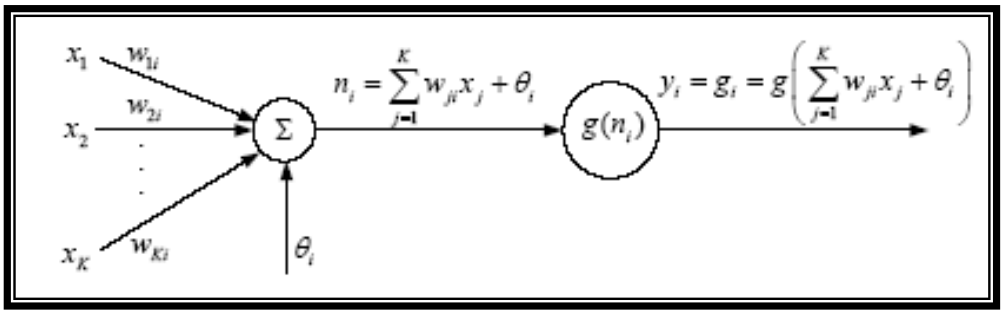

Figure(3-11) Single node in a MLP network[54]

The activation function was originally chosen to be a relay function, but for mathematical convenience a hyperbolic tangent (tanh) or a sigmoid function are most commonly used. Hyberbolic tangent is defined as[54]:

$$\tanh(x) = \frac{1 - e^{-x}}{1 + e^{-x}} \qquad \text{..... (3.19)}$$

The output of node *i* becomes[54] :

$$y_i = g_i = g\left(\sum_{j-1}^{k} w_{ji}x_j + \theta_i\right) \qquad \text{..... (3.20)}$$

Connecting several nodes in parallel and series, a MLP network is formed. A typical network is shown in Figure (3.12).

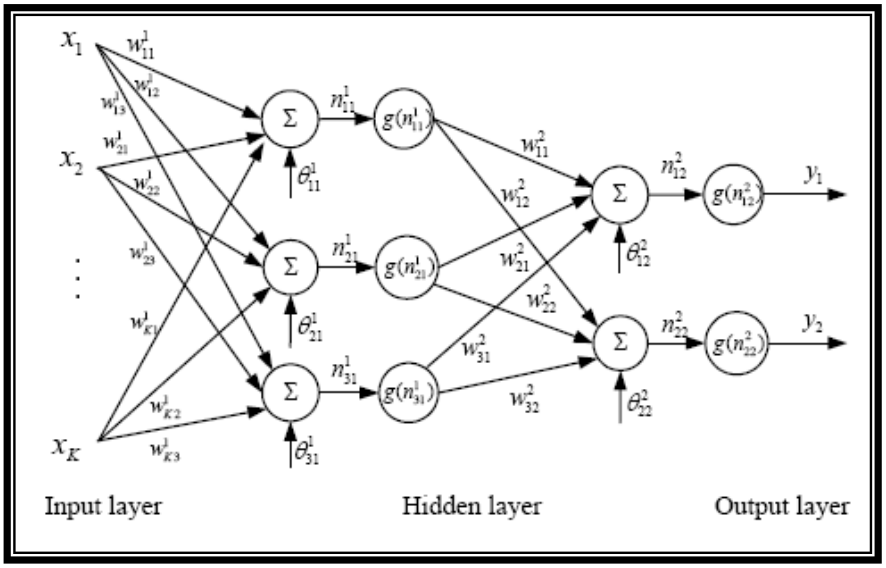

Figure (3-12) A multilayer perceptron network with one hidden layer. Here the same activation function *g* is used in both layers[54]

The output (y_i) , i = 1, 2 , of the MLP network becomes[54] :

$$y_i = g\left(\sum_{j-1}^{3} w_{ji}^2 g(n_{j1}^2) + \theta_{j2}^2\right) = g\left(\sum_{j-1}^{3} w_{ji}^2 g\left(\sum_{j-1}^{k} w_{kj}^2 x_k + \theta_{j1}^2\right) + \theta_{j2}^2\right) \quad \text{..... (3.21)}$$

Many algorithms exist for determining the network parameters. In neural network literature the algorithms are called learning or teaching algorithms, in system identification they belong to parameter estimation algorithms.

The most well-known are back-propagation and Levenberg-Marquardt algorithms. Back-propagation is a gradient based algorithm, which has many variants. Levenberg-Marquardt is usually more efficient, but needs more computer memory.

Here we will concentrate only on using the algorithms. Summarizing the procedure of teaching algorithms for multilayer perceptron networks:

a. The structure of the network is first defined. In the network, activation functions are chosen and the network parameters, weights and biases, are initialized.

b. The parameters associated with the training algorithm like error goal, maximum number of epochs (iterations), etc, are defined.

c. The training algorithm is called.

d. After the neural network has been determined, the result is first tested by simulating the output of the neural network with the measured input data. This is compared with the measured outputs. Final validation must be carried out with independent data[54].

3.4-3 Neural Network Applications

Today, neural networks can solve problems of economic importance that could not be approached previously in any practical way. Today the neural networks can solve problems for any field. these fields are :

1) Aerospace

High performance aircraft autopilot, flight path simulation, aircraft control systems, autopilot enhancements, aircraft component simulation, aircraft component fault detection .

2) Automotive: Automobile automatic guidance system .

3) Defence

Weapon steering, target tracking, object discrimination, facial recognition, new kinds of sensors, sonar, radar and image signal processing including data compression, feature extraction and noise suppression, signal/image identification .

4) Electronics

Code sequence prediction, integrated circuit chip layout, process control, chip failure analysis, machine vision, voice synthesis, nonlinear modeling .

5) Manufacturing

Manufacturing process control, product design and analysis, process and machine diagnosis, real-time particle identification, visual quality inspection systems, beer testing, welding quality analysis, paper quality prediction, computer-chip quality analysis, analysis of grinding operations, chemical product design analysis, machine maintenance analysis, project bidding, planning and management, dynamic modeling of chemical process system .

6)Medical

Breast cancer cell analysis, EEG and ECG analysis, prosthesis design, optimization of transplant times, hospital expense reduction, hospital quality improvement, emergency-room test advisement .

7) Telecommunications

Image and data compression, automated information services, real-time translation of spoken language, customer payment processing systems[55] .

Chapter Two

Theoretical Analysis of Fiber Optic Cable Parameters

2.1 Introduction

This chapter focuses on the Single Mode Fiber Optic Attenuation, Windows, Rayleigh scattering, Normalized frequency, and Losses of Fiber Optics in Connector, Splices, Bending and Coupler. Optical fiber use for communication purposes was considered impractical because of high losses (~ 1000 dB/km)[17].The losses of optical fiber was reduced to 0.2dB/km near the 1.55μm spectral region[18] .

2.2 Fiber Attenuation and Windows

The attenuation of the optical fiber is a result of two factors-absorption and scattering Figure (2-1). Absorption is caused by the absorption of the light and conversion to heat by molecules in the glass. Primary absorbers are residual OH^+ and dopants used to modify the refractive index of the glass. This absorption occurs at discrete wavelengths, determined by the elements absorbing the light. The OH^+ absorption is predominant, and occurs most strongly around 1000nm, 1400nm, and above 1600nm[5]. To reduce absorption, the optical fiber must be free of impurities that have electronic or atomic resonance near the transmission wavelength. Much of the work devoted to reducing the amount of absorption in optical fibers has been directed toward the development of ultra pure silica glass.

The impurities of most concern are water vapor and the first row of transition metals (vanadium, chromium, magnesium, iron, cobalt, and nickel).As a general rule, concentrations of these impurities must be kept below about one part in 10^9, or their contribution to absorption exceeds 1dB/km at wavelengths near 1μm [19].

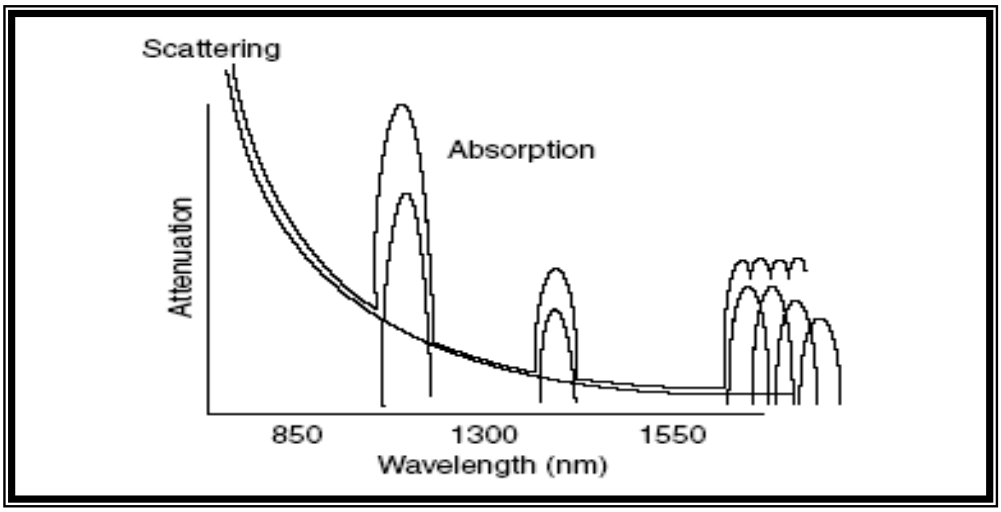

Figure (2-1) Fiber loss mechanisms[5].

The largest cause of attenuation is scattering. Scattering occurs when light collides with individual atoms in the glass and is anisotropic. Light that is scattered at angles outside the critical angle of the fiber will be absorbed into the cladding or scattered in all directions, even transmitted back toward the source. Scattering is also a function of wavelength, proportional to the inverse fourth power of the wavelength of the light. Thus, if the wavelength of the light is double, The scattering losses will be reduce by 2^4 or 16 times. Therefore, for long distance transmission, it is advantageous to use the longest practical wavelength for minimal attenuation and maximum distance between repeaters. Together, absorption and scattering produce the attenuation curve for a typical glass optical fiber shown in Figure (2-1).

Fiber optic systems transmit in the windows created between the absorption bands at 850nm, 1300nm, and 1550nm, where physics also allows one to fabricate lasers and detectors easily. Plastic fiber has a more limited wavelength band that limits practical use to 660nm LED sources. As the optical signal propagates over a long stretch of fiber, it becomes attenuated because of scattering, absorption by material impurities, and other effects[5]. Silica glass has two low loss windows, one around the wavelength λ=1.3μm and one around λ=1.55μm, which both are used for optical fiber communication. The popular single-mode fiber has a loss of about 0.2dB/km at the 1.55μm. A third wavelength window around λ=0.85μm, where the loss is about 2.5dB/km, is used for short-reach (data) communication applications, mostly because low-cost optical sources and detectors are available for this wavelength. The loss of modem silica-glass fiber is phenomenally low compared with that of an RF coaxial cable at high frequencies. A high-performance RF coaxial cable operating at 10GHz has an attenuation of about 500dB/km.

Compare this with 0.25dB/km for a fiber On a historical note, it is interesting to know that low loss fiber was not easy to produce. In 1965, the best glass fiber had a loss of around l,000dB/km. It was estimated that for a fiber to be useful for optical communication, its loss must be reduced to 20dB/km or less, that is, an improvement by 98 orders of magnitude was required[20]. Some wavelengths are not desirable, 1380nm for example. The losses at this wavelength are very high due to water within the glass. It is a real surprise to find that glass is not totally waterproof. Water in the form of hydroxyl ions is absorbed within the molecular structure and absorbs energy with a wavelength of 1380nm.

During manufacture it is therefore of great importance to keep the glass as dry as possible with water content as low as 1 part in 10^9. It makes commercial sense to agree on standard wavelengths to ensure that equipment from different manufacturers is compatible[19]. These standard wavelengths are called window and the performance of fibers and light sources are optimized that performed at their best within one of these windows Figure (2-2)[21].

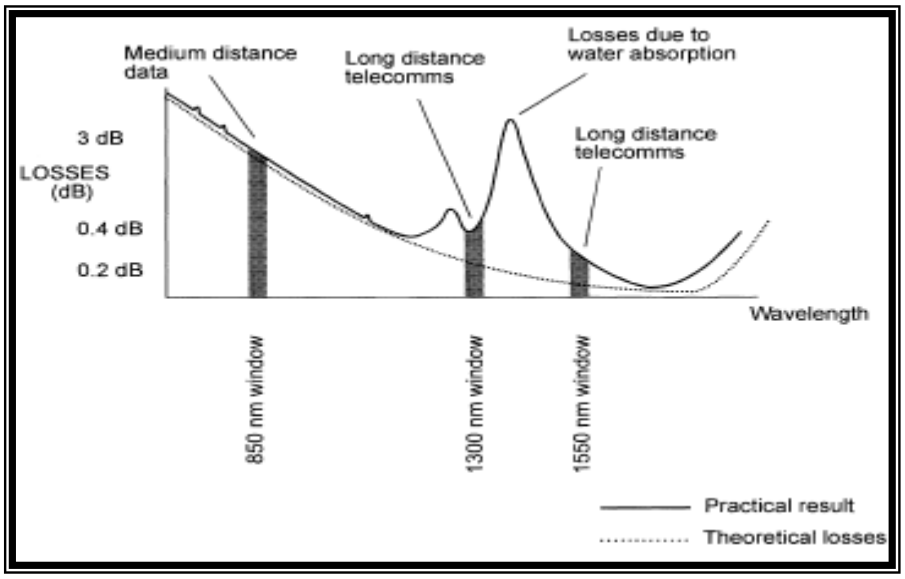

Figure (2-2) The infrared windows used in optical fiber[21].

The 1310 nm and 1550nm windows have much lower losses and are used for long distance communications. The shorter wavelength window centered around 850nm has higher losses and is used for shorter range data transmissions and local area networks (LANs), perhaps up to 10 km or so. The 850 nm window remains in use because the system is less expensive and easier to install[21]. Signal attenuation is defined as the ratio of optical input power (P_i) to the optical output power (P_o). Optical input power is the power injected into the fiber from an optical source.

Optical output power is the power received at the fiber end or optical detector. The following equation defines signal attenuation as a unit of length[22]:

$$\text{Attenuation } \alpha\left(dB/km\right) = \frac{10}{Z(km)}\log_{10}\left(\frac{P_i}{P_o}\right) \qquad \text{..... (2.1)}$$

2.3 Rayleigh Scattering

When light is scattered from objects much smaller than the wavelength of light, as it is in optical fiber called Rayleigh scattering. In modern telecommunications fiber, Rayleigh scattering is the primary source of attenuation. Fiber manufacturers try to minimize the amount of light lost to Rayleigh scattering by reducing the size of the microscopic discontinuities. One way to do this is to cool the fiber slowly and in a carefully controlled manner[19]. Light traveling through the fiber interacts with the density areas as shown in figure (2.3). Light is then partially scattered in all directions [22].

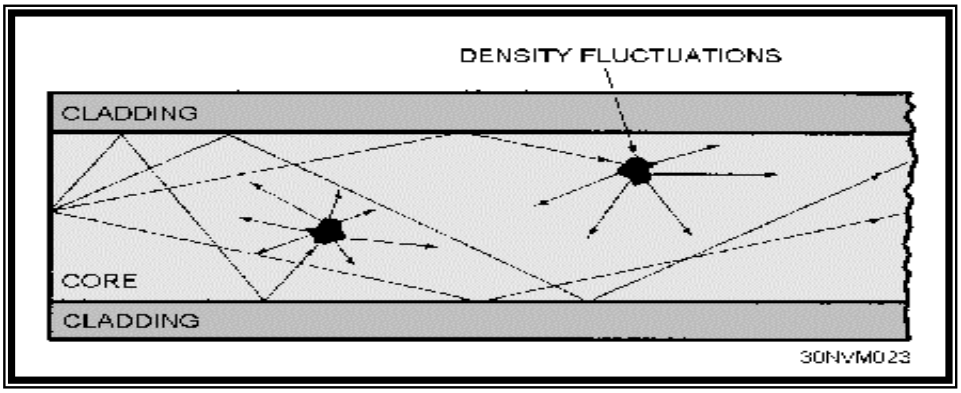

Figure (2.3) light scattering [22]

Today, modern single-mode telecommunications fibers have total attenuation due to scattering and absorption about 0.34dB/km at 1310 nm and about 0.2dB/km at 1550 nm[19]

2.4 Fiber Performance

Purity of the medium is very important for best transmission of an optical signal inside the fiber. Perfect vacuum is the purest medium to transmit light. Since all optical fibers are made of solid, not hollow, cores, It must settled for second best in terms of purity. Technology makes it possible for us to make glass very pure, however. Impurities are the unwanted things that can get into the fiber and become a part of its structure. Dirt and impurities are two different things. Dirt comes to the fiber from dirty hands and a dirty work environment. This can be cleaned off with alcohol wipes. Impurities, on the other hand, are built into the fiber at the time of manufacture; they cannot be cleaned off. These impurities will cause parts of optical signal to be lost due to scattering or absorption causing attenuation of the signal[5].

2.5 Optical Confinement

Optical fibers work by confining the light within a long strand of glass. In their simplest form, they are cylindrical dielectric waveguides made up of central cylinder of glass with one index of refraction, surrounded by an annulus with a slightly different index of refraction. One confinement process that traps the light inside the fiber and allows it to propagate down the length of the fiber is based on the principle of total internal reflection at the interface of two dielectric media. Consider an optical-plane-wave incident on an infinite planar interface between two dielectric media[22]. The propagation direction of the plane wave make sun angle of incidence(θ_1) with the normal to the interface as shown in the figure(2-4)[23].

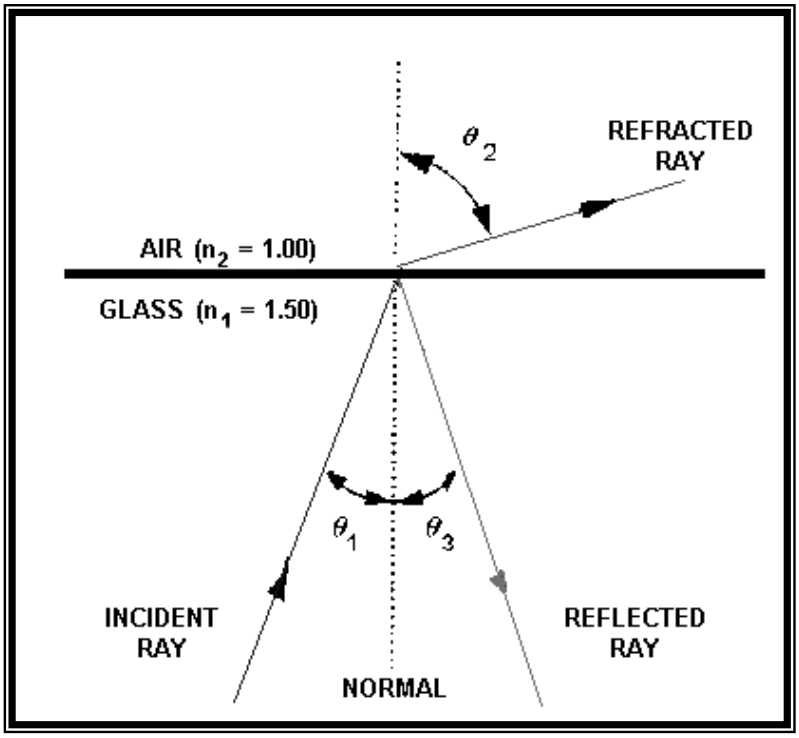

Figure (2-4) Light reflection and refraction at a glass-air boundary[23].

2.6 Single Mode Fiber (SMF)

Consider the geometry of Fig. (2.5), where a ray making an angle θ_i with the fiber axis is incident at the core center. Because of refraction at the fiber-air interface, the ray bends toward the normal.

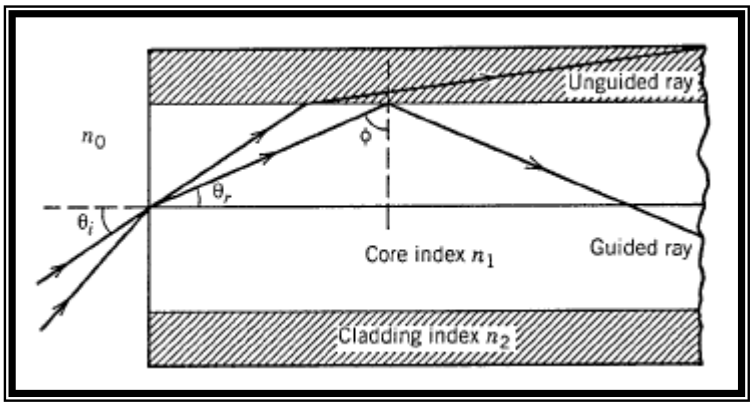

Figure (2-5) Light confinement through total internal reflection in single mode fibers[24].

The angle θ_r of the refracted ray is given by[24]:

$$n_o \sin\theta_i = n_1 \sin\theta_r \qquad \text{..... (2.2)}$$

Where:

n_1 and n_o are the refractive indices of the fiber core and air, respectively

The refracted ray hits the core–cladding interface and is refracted again. However, refraction is possible only for an angle of incidence ϕ such that sin $\phi < n_2/n_1$. For angles larger than a critical angle ϕ_c, defined by[24]:

$$\sin\phi_c = n_2/n_1 \qquad \text{..... (2.3)}$$

Where: n_2 is the cladding index

The ray experiences total internal reflection at the core-cladding interface. Since such reflections occur throughout the fiber length, all rays with $\phi > \phi_c$ remain confined to the fiber core. This is the basic mechanism behind light confinement in optical fibers.

Rays for which $\phi < \phi_c$ are refracted out of the core. So from Eqs. (2-2) and (2-3) numerical aperture defined by[24]:

$$n_o \sin\theta_i = n_1 \cos\phi_c = \left(n_1^2 - n_2^2\right)^{1/2} \qquad \text{..... (2.4)}$$

$[n_o \sin(\theta_i)]$ is known as the numerical aperture (NA) of the fiber. It represents the light-gathering capacity of an optical fiber. For $n_1 \cong n_2$ the NA can be approximated by[24]:

$$NA \approx n_1 \left(2\Delta\right)^{1/2}, \Delta \approx \left(n_1 - n_2\right)/n_1 \qquad \text{..... (2.5)}$$

Where: Δ is the fractional index change at the core-cladding interface.

Clearly, Δ should be made as large as possible in order to couple maximum light into the fiber[24]. The approximation Δ was used (good for Δ<< 1, called a weakly guided waveguide Typical values of Δ can range between 0.001 and 0.02 (i.e., 0.1% to 2%). Typically, the cladding is also surrounded by a plastic protective jacket for handling purposes and to protect the fiber surface. Table (2.1) summarizes some of the typical parameters associated with standard fibers, While the sizes are standardized[22].

Table (2-1) Representative parameters for standard fibers[22]

Type	Core diameter (μm)	Cladding diameter (μm)	Δ	Application
8/125 single-mode	8	125	0.1% to 2%	Long distance, high data rate
50/125 multimode	50	125	1% to 2%	Short distance, moderate data rate
62.5/125 multimode	62.5	125	1% to 2%	Local area networks
100/140	100	140	1% to 2%	Local area networks, short distance

2.7 Normalized Frequency (V) in Single Mode Fiber (SMF)

The simplest modes are those with an electric field transverse to the propagation direction, called TE (transverse electric) modes, with radial symmetry and those with a magnetic field transverse to the propagation direction, called TM (transverse magnetic) modes. These modes also exist in metallic waveguides.

In addition, hybrid modes (i.e., combinations of TE and TM modes) also exist and are called HE, and EH, modes. (These modes have electric and magnetic fields along the propagation direction.) Some modes are linearly polarized and are called LP modes.

Each mode not only has its own geometric electric and magnetic fields, but also will have a unique value of propagation coefficient. Much of the electromagnetic analyses of optical fibers is the description of these modes and their propagation coefficients. The results of these analyses are extracted selectively. A key parameter that describes the mode structure is the V-parameter (normalized frequency), V defined by[22]:

$$V = \frac{2\pi a}{\lambda}\sqrt{n_1^2 - n_2^2} = \frac{2\pi a}{\lambda} n_1 \sqrt{2\Delta} \qquad \text{..... (2.6)}$$

Where:

a is the radius of the core of the fiber

λ is the nominal free-space wavelength of the light

The V-parameter is important because it determines the number of electromagnetic modes in the fiber [22] . Figure (2-6) shows a plot of b as a function of V for a few low-order fiber modes obtained . A fiber with a large value of V supports many modes. the number of modes decreases rapidly as V is reduced. As seen in Figure (2-6), a fiber with V=5 supports seven modes. Below a certain value of V all modes except the HE_{11} mode reach cutoff. Such fibers support a single mode and are called single-mode fibers(SMF). The properties of single-mode fibers are described in Figure(2.6). Single-mode fibers support only the HE_{11} mode, also known as the fundamental mode of the fiber. The fiber is designed such that all higher-order modes are cut off at the operating wavelength.

As seen in Figure(2.6), the V parameter determines the number of modes supported by a fiber. The cutoff condition of various modes is also determined by V. The fundamental mode has no cutoff and is always supported by a fiber. A fiber designed such that V≤2.405 supports only the fundamental HE_{11} mode. This is the single-mode condition [24].

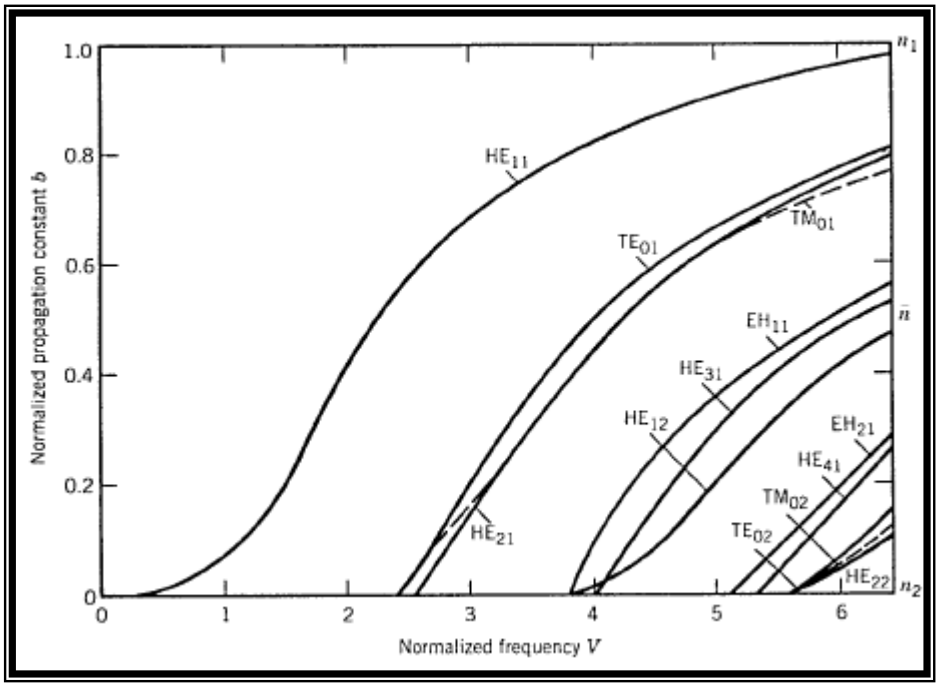

Figure (2-6) Normalized propagation constant b as a function of normalized frequency V for a few low-order fiber modes. The right scale shows the mode index n[24].

2.8 Cutoff Wavelength

For a fiber to start supporting only a single mode at a wavelength λ cutoff, the following condition (derived from solutions to Maxwell's equations for a circular waveguide) needs to be satisfied [25] :

$$\lambda_{cutoff} = \frac{2\pi a}{2.405}\left(n_1^2 - n_2^2\right)^{1/2} \qquad \text{..... (2.7)}$$

The fundamental mode ,HE_{11} , is always guided, i.e. for all values of V and all wavelengths. In this sense, It can be compared to the fundamental mode of a coaxial (electric) cable.

The next-order mode, TE_{11} and LP_{11} is only guided if V is larger than 2.405, i.e. if the wavelength is shorter. From this concept, The cutoff wavelength is the minimum wavelength which guarantees the propagation of one mode only. therefore, the condition for single-mode operation is [26]:

$$V < \mathrm{V}_{\min} = 2.405 \qquad \text{..... (2.8)}$$

$$\lambda > \lambda_{cutoff} = 3.7a\ n_1\sqrt{\Delta} \qquad \text{..... (2.9)}$$

2.9 Index of Refraction for glass (SMF)

A good approximation for the index of refraction (n_2) in glass, over the wavelength (λ) range from 365 to 2300nm, is[19]:

$$n_2 = \left(\frac{B_1\lambda^2}{\lambda^2 - C_1} + \frac{B_2\lambda^2}{\lambda^2 - C_2} + \frac{B_3\lambda^2}{\lambda^2 - C_3} + 1 \right)^{0.5} \qquad \text{..... (2.10)}$$

In equation (2-10), λ is the wavelength of light (in nm) and the constants B_1 through C_3 (usually supplied by the manufacturer) depend on the specific glass. Table (2.2) lists these constants for a few common bulk glasses and for fused quartz.

Table(2-2) Constants for some common types of glass[19].

	BK7 Glass	SF11 Glass	F2 Glass	Fused Quartz
B_1	1.03961212	1.73848403	1.34533359	0.6961663
B_2	0.231792344	0.311168974	0.209073176	0.4079426
B_3	1.01046945	1.17490871	0.937357162	0.8974794
C_1	$6.00069867 \cdot 10^{-3}$	$13.6068604 \cdot 10^{-3}$	$9.97743871 \cdot 10^{-3}$	$4.679148 \cdot 10^{-3}$
C_2	$2.00179144 \cdot 10^{-2}$	$6.15960463 \cdot 10^{-2}$	$4.70450767 \cdot 10^{-2}$	$1.351206 \cdot 10^{-2}$
C_3	$1.03560653 \cdot 10^{2}$	$1.21922711 \cdot 10^{2}$	$1.11886764 \cdot 10^{2}$	$9.896161 \cdot 10^{1}$

Figure (2-7) shows how the index of refraction changes with wavelength for fused quartz (silica optical fiber), which is the basic material used to manufacture optical fibers.

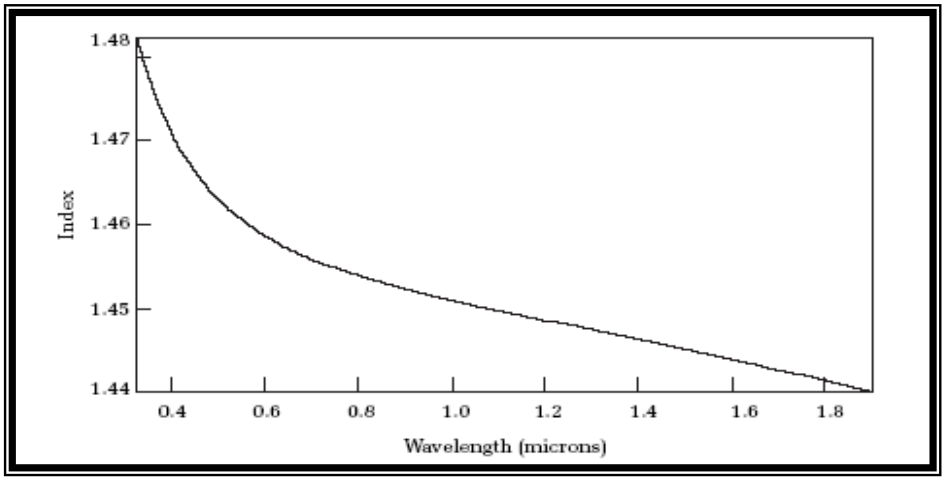

Figure (2-7) Wavelength dependence of the index of refraction of fused Quartz[19].

Optical fiber is manufactured by doping the center, or core region of pure optical silica, with impurities designed to raise the index of refraction. The boundary formed by doped and undoped regions of the glass defines the transition from core to cladding in the optical fiber. Since the cladding is undoped fused silica, The cladding refraction index approximation as[19]:

$$n=\left[1+\lambda^2\left(\frac{0.6961663}{\lambda^2-(0.0684043)^2}+\frac{0.4079426}{\lambda^2-(0.1162414)^2}+\frac{0.874794}{\lambda^2-(9.896161)^2}\right)\right]^{0.5} \qquad \textbf{.....(2.11)}$$

Where, λ is the wavelength in microns n is the index of refraction. Using equation (2-11), The cladding index at (1310) nanometers is(1.4468) and at (1550) nanometers is (1.44402)[19].

2.10 Bandwidth of Optical Fiber

Fiber bandwidth is usually characterized in the time-domain as pulse broadening or more technically as (dispersion). The information-carrying capacity of the fiber is limited by various distortion mechanisms in the fiber, such as signal dispersion effect[27].

There are two different types of dispersion in optical fibers. The types are intramodal and intermodal dispersion. Intramodal, or chromatic, dispersion occurs in all types of fibers. Intermodal, or modal, dispersion occurs only in multimode fibers. Each type of dispersion mechanism leads to pulse spreading. As a pulse spreads, energy is overlapped. This condition is shown in Figure (2-8). The spreading of the optical pulse as it travels along the fiber limits the information capacity of the fiber[23].

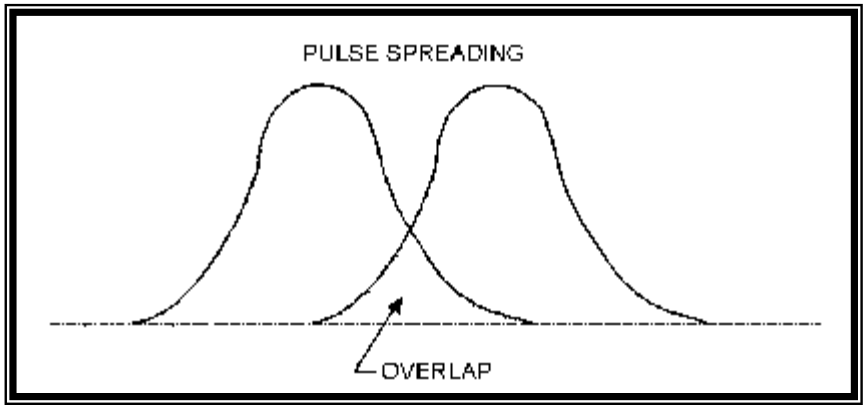

Figure (2-8) Pulse overlap[23].

If optical pulses travel sufficiently far in a fiber, they will eventually overlap with neighboring pulses, thereby creating errors in the output since they become indistinguishable to the receiver[25]. Intramodal Dispersion , or chromatic, dispersion depends primarily on fiber materials. There are two types of intramodal dispersion. The first type is material dispersion.

The second type is waveguide dispersion. Intramodal dispersion occurs because different colors of light travel through different materials and different waveguide structures at different speeds. Material dispersion occurs because the spreading of a light pulse is dependent on the wavelengths' interaction with the refractive index of the fiber core. Different wavelengths travel at different speeds in the fiber material. Different wavelengths of a light pulse that enter a fiber at one time exit the fiber at different times. Material dispersion is a function of the source spectral width.

The spectral width specifies the range of wavelengths that can propagate in the fiber. Material dispersion is less at longer wavelengths. Waveguide dispersion occurs because the mode propagation constant (b) is a function of the size of the fiber's core relative to the wavelength of operation.

Waveguide dispersion also occurs because light propagates differently in the core than in the cladding. In multimode fibers, waveguide dispersion and material dispersion are basically separate properties. Multimode waveguide dispersion is generally small compared to material dispersion. Waveguide dispersion is usually neglected. However, in single mode fibers, material and waveguide dispersion are interrelated. The total dispersion present in single mode fibers may be minimized by trading material and waveguide properties depending on the wavelength of operation. Intermodal dispersion intermodal or modal dispersion causes the input light pulse to spread. The input light pulse is made up of a group of modes. As the modes propagate along the fiber, light energy distributed among the modes is delayed by different amounts. The pulse spreads because each mode propagates along the fiber at different speeds. Since modes travel in different directions, some modes travel longer distances. Modal dispersion occurs because each mode travels a different distance over the same time span, as shown in Figure (2-9).

The modes of a light pulse that enter the fiber at one time exit the fiber a different times. This condition causes the light pulse to spread. As the length of the fiber increases, modal dispersion increases[23].

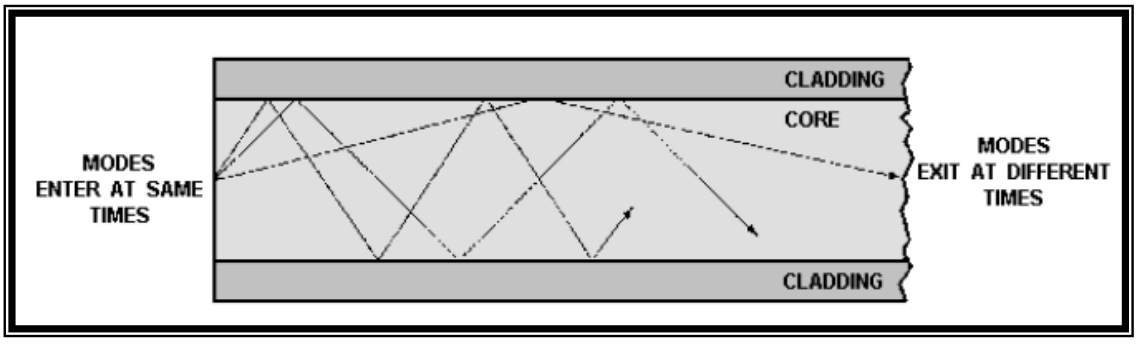

Figure (2-9) Distance traveled by each mode over the same time span.[23]

2.11 Glass Fiber

A glass-based fiber-optic cable has a glass core and glass cladding, with impurities added to obtain the desired indices of refraction necessary to guide light rays through the fiber. This type of cable has the lowest value of attenuation; however, it is also the most expensive of the three types of materials used to create an optical fiber. Concerning utilization, a glass-based fiber-optic cable is by far the most commonly used type of optical cable. Thus, it also represents the type of cable that installers are most familiar working with, which means that functions such as cable splicing and pulling techniques are well known. Because of its low attenuation, a glass fiber is always used for single mode optical cable.

Because single-mode fiber requires a very thin core, Its composition eliminates the potential use of plastic, which requires a thicker core. Another characteristic of glass fiber is its capability to support a relatively high signaling rate. Some types of single-mode step-index optical fiber can support a gigahertz signaling rate[28].

2.12 Birefringence in fiber optics

A birefringent material has a crystal structure. Within this structure there is an “optic axis” (in some materials more than one). When a ray enters the crystal at an angle to the optic axis it is split into two rays. One ray (the ordinary ray) has polarization perpendicular to the optic axis. The other ray (the extraordinary ray) has polarization orthogonal to that of the ordinary ray[26].

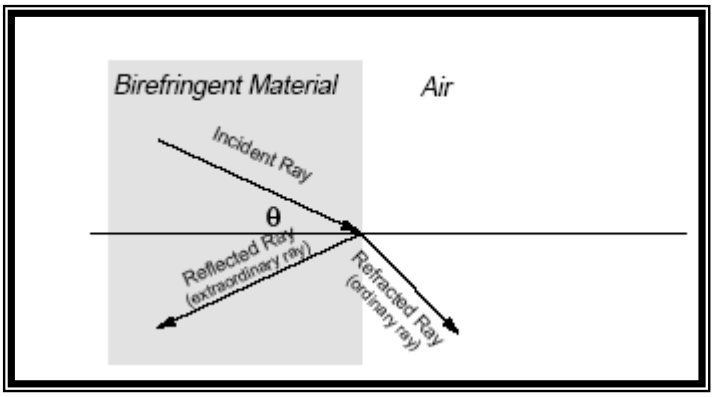

Fig.(2-10) Birefringent Material[26]

Many modern optical components, particularly those used in coherent optical communications, rely on a fixed state of polarization. However, unstable birefringence in standard single-mode fibers cause the state of polarization to change in an unpredictable way.

In all single-mode fibers, there are two perpendicular orientations of the (transverse) electric field which lead to a maximum difference in phase velocity: the fiber exhibits linear birefringence. The name of the above orientations is fast and slow axes. Coupling linear polarized light into one of the axes yields linear-polarized light at the output of the fiber[26].

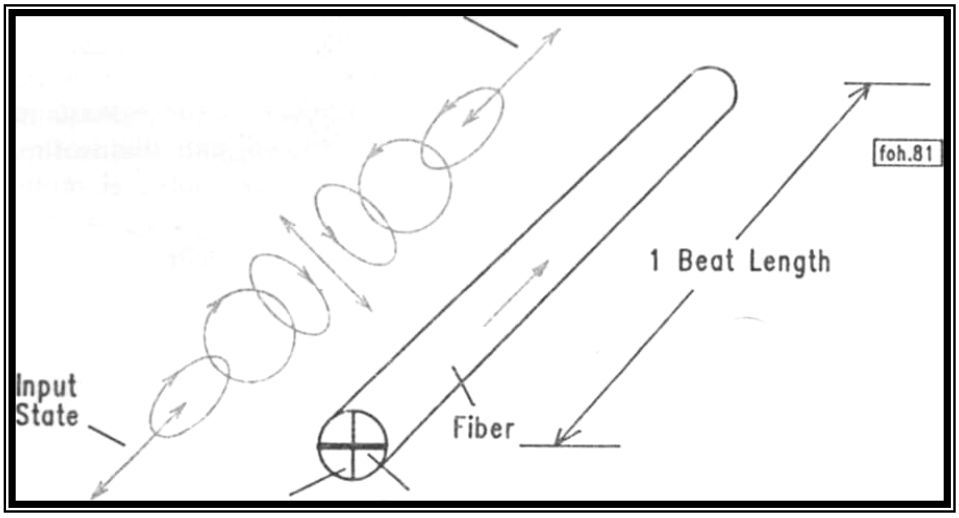

Figure (2-11) Pure linear birefringence in a single-mode fiber (Fiber length = 1 beat length, linear input polarization coupled at 45°:relative to axes)[26].

The electric field vector of an electromagnetic wave propagating in free space vibrates in a specific plane the wave is said to be plane polarized. Any real beam light comprises many individual waves and in general the planes of vibration of their electric fields will be randomly orientated. Such a beam of light is unpolarized and the resultant electric field vector changes orientation randomly in lime. It is possible, however, to have light beams characterized by highly orientated electric fields and such light is referred to as being polarized. The simplest form of polarization is plane polarized light, which is similar to the single wave[29]. The term linear polarization is used when the electric field is oriented in only one direction of the transverse plane. The projection of the field vectors to the plane is a simple line.

Modern laser diodes generate nearly 100 % linear-polarized radiation. The term circular polarization is applied to a wave in which the electric field vector rotates by 360° within one wavelength. In this case, the projected field vectors form a circle. The figure shows the field vectors of both types at a fixed time. In free space, both of the packages of vectors travel at the speed of light[30].

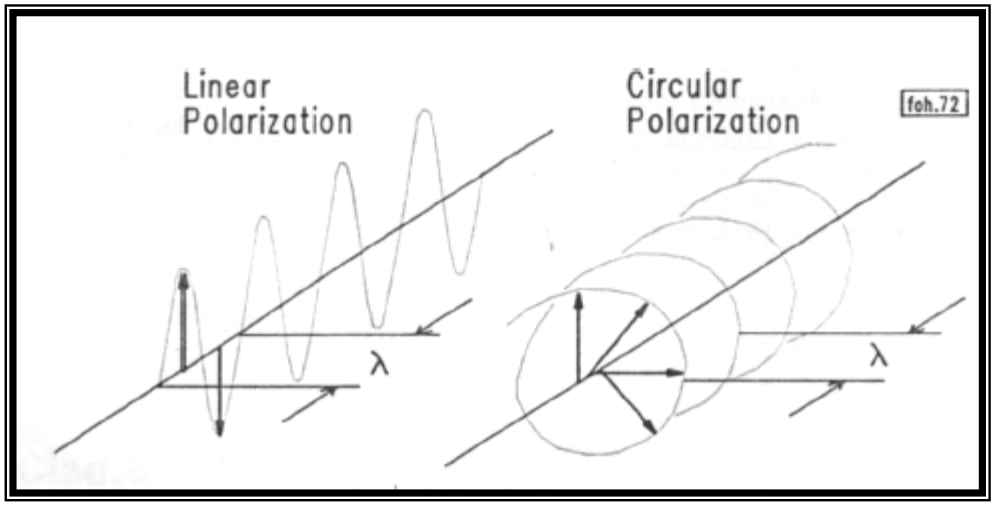

Fig.(2-12) (linear polarization and clockwise rotating circular polarization)[30]

2.13 Polarization Control (PC)

Controlling the state of polarization is important because many modern fiber optic components require a well defined state of polarization. In coherent communications, a polarization controller is one of the key components. Retardation plates can be used for polarization control, More elegant, however, is polarization control which does not require an interruption of the fiber. The basic idea is that a loop of single-mode fiber can replace a retardation plate[26]. One common type of polarization controller is made with a fiber loop.

PC must receives the light in any polarizations state and can convert it without loss into any other polarization. To do this PC must be birefringent but which can have its axes of birefringence rotated. If loop of fiber made with a relatively small diameter as illustrated in Figure (2-13), then the inner part of the fiber is compressed slightly and the outer part put under tension. Although this is a relatively small effect it induces birefringence in the fiber loop as illustrated in Figure (2-14)[31].

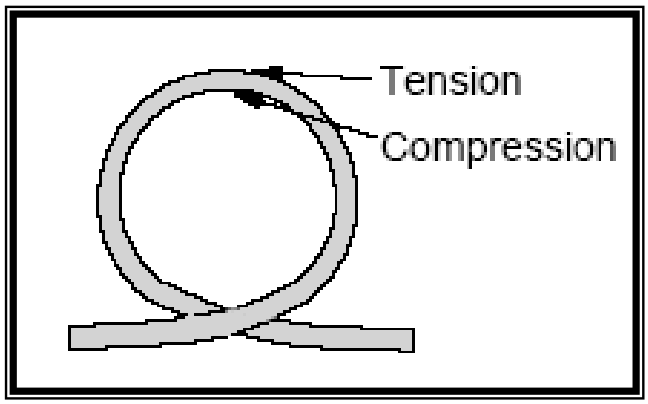

Figure (2-13) Fiber-based polarization control[31]

When light arrives on the input fiber it tends to stay in its original orientation (in terms of its polarizations axes) regardless of twists in the fiber. A slight twist in a symmetric fiber isn't noticed by the signal and the polarization states are not changed in relation to axes in free space regardless of the fiber axes.

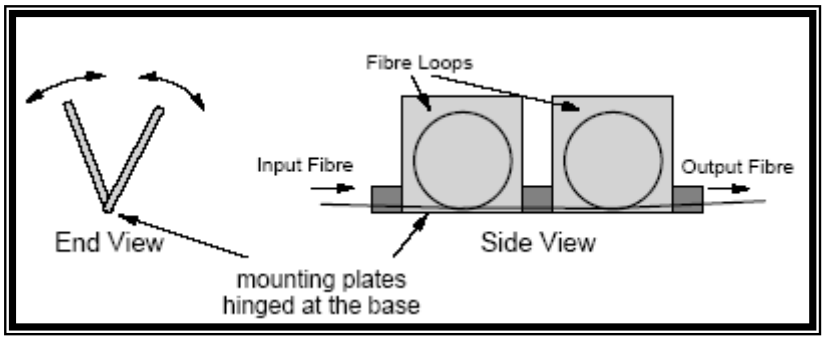

Figure (2-14) Fiber Loop Polarization Controller[31]

Thus when the fiber loop is rotated around the axis of the fiber the fast and slow axes rotate in relation to the signal. This rotation of the birefringent axes has the effect of phase retardation of one component of the signal light in relation to the other. Thus it changes the polarization of the signal. By rotating the fiber loops the device was adjusted to produce light at any desired polarization. The loop radius must be greater than the bend radius of the fiber. If the loop is too tight light will leave the fiber. A typical device might have a loop diameter of about 750mm[31].

2.14 Losses of Fiber Optics

When several fibers are connected to form an installed cable plant, the (OTDR and OFDR) can characterize optical fiber and optical connection properties along the entire length of the cable plant. A fiber optic cable plant consists of optical fiber cables, connectors, splices, mounting panels, jumper cables, and other components.

A cable plant does not include active components such as optical transmitters or receivers. By analyzing the (OTDR and OFDR) plot, or trace, End users can measure fiber attenuation and transmission loss or(FAULTS) between any two points along the cable plant. End users can also measure insertion loss and reflectance of any optical connection. In addition, end users use the (OTDR and OFDR) trace to locate fiber breaks or (faults). A point defect, or fault, can be reflective or non reflective. A point defect normally exhibits a loss of optical power. However, Figure (2-15) shows different types of faults like fresnel reflection (initial input reflection), Splice fault ,connector fault (mechanical misalignment), or differences in the geometrical and waveguide characteristics of any two waveguides being joined ,bending fault, ending fresnel reflection fault. fresnel reflection indicating for starting and ending of optical fiber [31].

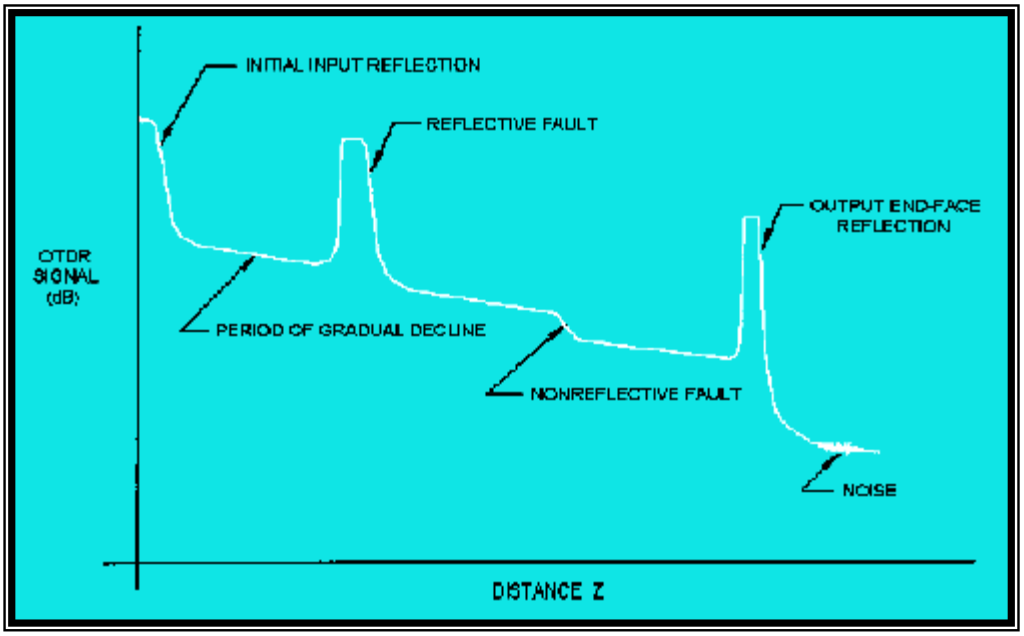

Figure (2-15) Types of faults of optical fiber by (OTDR) [31].

2.15 Fresnel Reflection

A major consideration with all types of fiber-fiber connection is the optical loss encountered at the interface. Even when the two jointed fiber ends are smooth and perpendicular to the fiber axes, and the two fiber axes are perfectly aligned, a small proportion of the light may be reflected back into the transmitting fiber causing attenuation at the joint. This phenomenon, known as Fresnel reflection, is associated with the step changes in refractive index at the jointed interface (i.e. glass-air-glass).

The magnitude of this partial reflection of the light transmitted through the interface may be estimated using the classical Fresnel formula for light of normal incidence and is given by [32]:

$$r = \left(\frac{n_1 - n}{n_1 + n} \right)^2 \qquad \text{..... (2.12)}$$

Where:
r is the fraction of the light reflected at a single interface

n_1 is the refractive index of the fiber core

n is the refractive index of the medium between the two jointed fibers (i.e. for air n=1).

However in order to determine the amount of light reflected at a fiber joint, Fresnel reflection at both fiber interfaces must be taken into account. The loss in decibels due to Fresnel reflection was given by [26]:

$$Loss_{fresnel} = 10 \log_{10}(r) \qquad \text{..... (2.13)}$$

Hence using the relationships given in equation (2.12) and equation (2.13) it is possible to determine the optical attenuation due to Fresnel reflection at a fiber-fiber joint. It is apparent that Fresnel reflection may give a significant loss at a fiber joint even when all other aspects of the connection are ideal[32].

2.16 Extrinsic and Intrinsic losses

a) Extrinsic Losses :

Single-mode fibers have core diameters on the order of 9μm. Owing to this microscopic size, mechanical misalignment is a major challenge in joining two fibers by connector or splice. Power losses result from misalignments because the radiation cone of the emitting fiber does not match the acceptance cone of the receiving fiber. The magnitude of the power loss depends on the degree of misalignment. Figures (2-16),(2-17),(2-18) illustrates the three fundamental types of misalignment(Extrinsic) between two fibers.

1. **Axial displacement** (also called lateral displacement): Results when the axes of the two fibers are offset by a distance (d). The misalignment to which a connection is most sensitive is lateral displacement, shown in Figure(2.16). Mechanical misalignments of the fibers cause losses because of the areas of the fiber core do not overlap sufficiently. In the analysis of misalignments the usual assumptions are that the fibers have equal radii, index profiles, And numerical apertures to isolate the effects of the misalignment .The losses of lateral displacement misalignment for ($d \ll \omega_o$) is[19].

$$L_{Lat}(dB) = -10\log_{10}\left(\exp-\left(\frac{d}{\bar{\omega}_o}\right)^2\right) \qquad \text{..... (2.14)}$$

Where($\bar{\omega}_0$) is the spot size of the fundamental mode. The spot size is usually defined as the width to (1/e) intensity to the (LP_{01}) mode, or in terms of the spot size of an incident Gaussian beam which gives maximum launching efficiency[32]. However, the spot size for the (LP_{01}) mode (corresponding to HE mode) may be obtained from the empirical formula ($\bar{\omega}_0$) given by Marcuse [33][34].

$$\bar{\omega}_o = a\left(0.65 + 1.619V^{-3/2} + 2.879V^{-1}\right) \qquad \text{..... (2.15)}$$

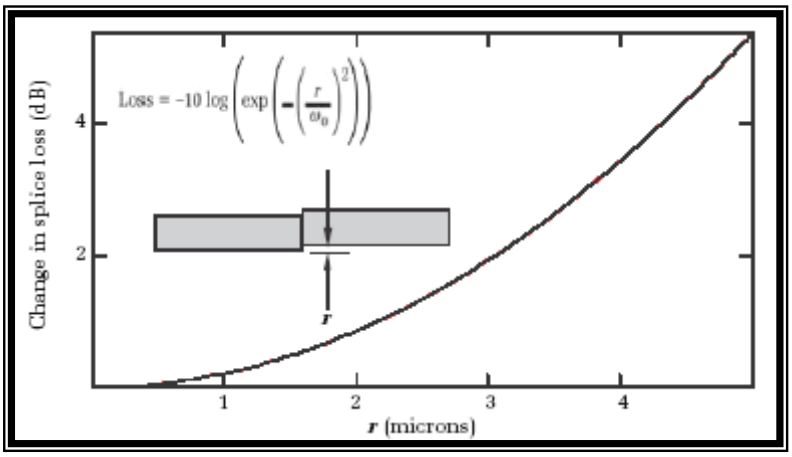

Figure (2-16) Coupling loss in single-mode fiber as a function of lateral misalignment[19].

2. Longitudinal separation

Occurs when the fibers have the same axis but have a gap s between their end faces

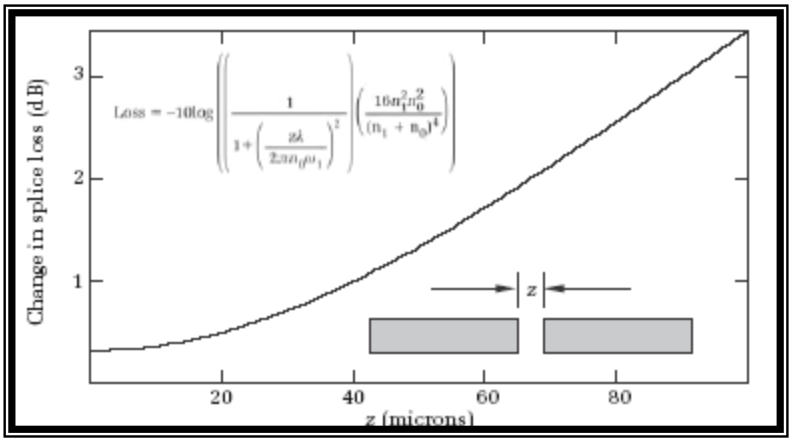

Figure(2-17) Coupling loss in single-mode fiber as a function of longitudinal misalignment[19].

3. Angular misalignment

Results when the two axes form an angle so that the fiber end faces are no longer parallel[19].

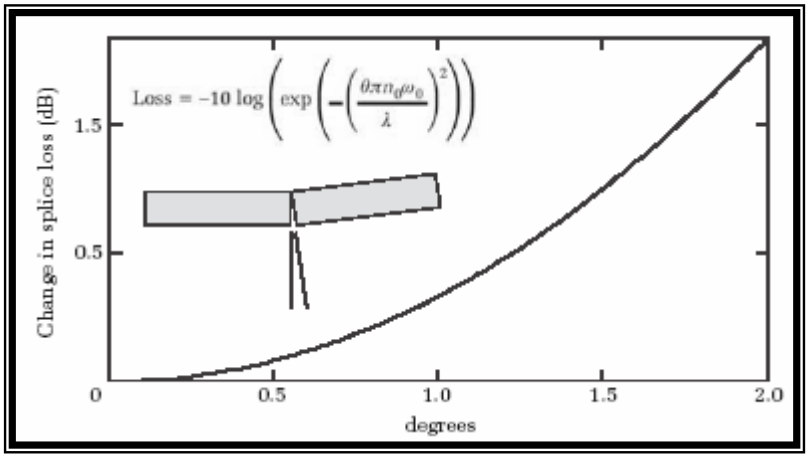

Figure (2-18) Coupling loss in single-mode fiber as a function of angular misalignment.[19]

b) Intrinsic Losses :

In addition to mechanical misalignments, differences in the geometric and waveguide characteristics of any two mated fibers can have a profound effect on the joint loss. The differences include variations in core diameter, core-area ellipticity, numerical aperture, and core-cladding concentricity of each fiber. Since these are manufacturer-related variations, the user has little control over them, except to specify certain tolerances in these parameters when purchasing the fiber. For a given percentage mismatch between fiber parameters, differences in core sizes and numerical apertures have a significantly larger effect on joint losses than mismatches in the refractive-index profile or core ellipticity [25].

1. Core area mismatches :

For simplicity let the subscripts E and R refer to the emitting and receiving fibers, respectively. If the axial numerical apertures and the core index profiles are equal that is:

($NA_E = NA_R$)

($n_E = n_R$)

But the fiber diameters (d_E) and(d_R) are not equal, then the coupling loss is[33]:

$$L_F(d)\begin{cases} -10\log\left(\frac{d_R}{d_E}\right)^2 & for\ d_R < d_E \\ 0 & for\ d_R \geq d_E \end{cases} \qquad \text{..... (2.16)}$$

Core area mismatches can occur when one is trying to connect a 62.5μm fiber to one with a 50-μm core, for example. In this case, going from the larger to the smaller fiber results in a 1.9dB loss, or 36 percent of the power.

A much more serious loss occurs when one inadvertently tries to couple light from a multimode to a single-mode fiber. For example, if one connects a 62.5μm multimode fiber to a 9-μm single-mode fiber, the loss from the area mismatch will be 17 dB, or almost 98 percent of the light.

2. Numerical aperture mismatches

In the case of the diameters and the index profiles of two coupled fibers are identical but their axial numerical apertures are different, then the joint loss from this effect is[33] :

$$L_F(NA)\begin{cases} -10\log\left(\frac{NA_R}{NA_E}\right)^2 & for\ NA_R < NA_E \\ 0 & for\ NA_R \geq NA_E \end{cases} \quad \text{..... (2.17)}$$

3. Core index mismatches

If the fiber diameters and the axial numerical apertures are the same but the core refractive-index profiles differ in the joined fibers, then the joint loss is[33]:

$$L_F(n)\begin{cases} -10\log\frac{n_R(n_E+2)}{n_E(n_R+2)} & for\ n_R < n_E \\ 0 & for\ n_R \geq n_E \end{cases} \quad \text{..... (2.18)}$$

This relationship comes about because for($n_R < n_E$) the number of modes that the receiving fiber can support is less than the number of modes in the emitting fiber. If ($n_E < n_R$) then the receiving fiber captures all modes from the emitting fiber[33][19].

2.17 Single-Mode Connector Return Loss

A connection point in an optical link can be categorized into three different styles called flat finish, physical contact (PC), and angled physical contact (APC). Many of the connectors are offered in different finishing styles so the connector names are shown with a PC or APC added on the end. If nothing is mentioned. A flat finish is simply polished to produce a smooth flat end to the fiber so that the light comes straight out of the connector within the acceptance angle of the other fiber, fig.(2.19).

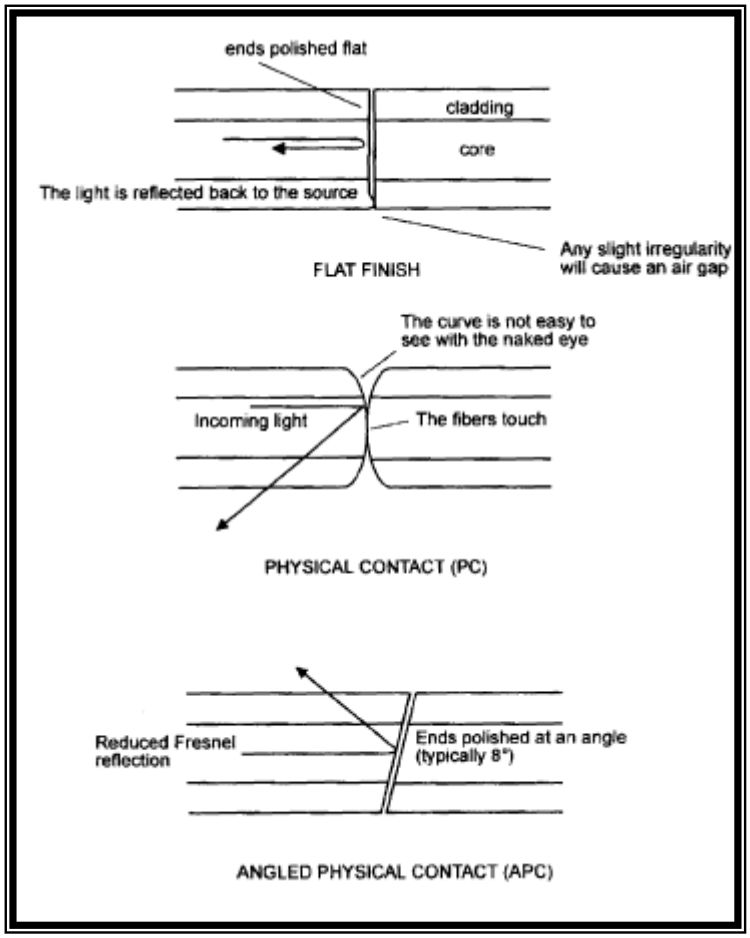

Figure (2-19) The alternative finishes of connector[21]

Type connectors without index-matching material are traditionally used in situations where frequent reconnections are required, such as within a building or on localized premises. Index-matching connectors are standardly employed in outside cable plants where the reconnections are infrequent, but need to have a low loss. Optical reflections provide a source of unwanted feedback into the laser cavity. This can affect the optical frequency response, the line width, and the internal noise of the laser, which results in degradation of system performance[21].

2.18 Reflection from Connector Pair

Figure (2-20) shows a model of an index-matched connection with perpendicular fiber end faces. In this figure and in the following analyses, offsets and angular misalignments are not taken into account. The connection model shows that the fiber end faces have a thin surface layer of thickness (h) having a high refractive index ($\bar{n}_2$) relative to the core index, which is a result of fiber polishing. The fiber core has an index($\bar{n}_0$), and the gap width ($\bar{d}$) between the end faces is filled with index-matching material having a refractive index($\bar{n}_1$). The return loss (RL_{IM}) in decibels for the index-matched gap region is given by[33][35]:

$$RL_{IM} = -10Log_{10}\left\{2R\left[1-\cos\left(\frac{4\pi\,\bar{n}_1\,\bar{d}}{\lambda}\right)\right]\right\} \qquad \text{..... (2.19)}$$

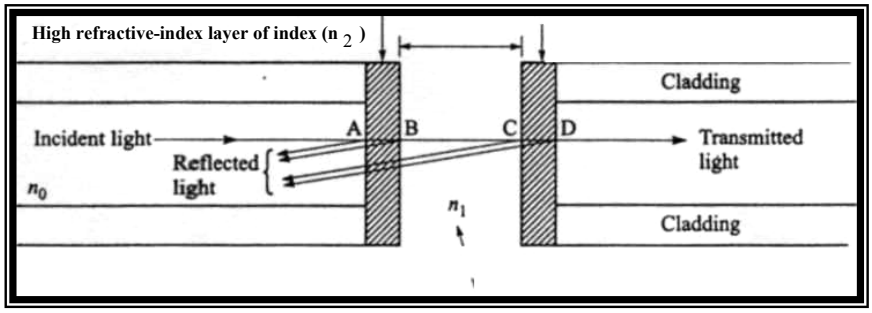

Figure (2-20) model of an index-matched connection with perpendicular fiber end face [33]

$$R = \frac{r_1^{\,2} + r_2^{\,2} + 2r_1 r_2 \cos\,\delta}{1 + r_1^{\,2} r_2^{\,2} + 2r_1 r_2 \cos\,\delta} \qquad \text{..... (2.20)}$$

Where, R is the reflectivity at a single material-coated end face

$$r_1 = \frac{\bar{n}_0 - \bar{n}_2}{\bar{n}_0 + \bar{n}_2}\ ,\ r_2 = \frac{\bar{n}_2 - \bar{n}_1}{\bar{n}_2 + \bar{n}_1} \qquad \text{..... (2.21)}$$

Where, r_1 and r_2 are the reflection coefficients through the core from the high-index layer and through the high-index layer from the core, respectively.

$$\delta = \left(\frac{4\pi}{\lambda}\right) \bar{n}_2 \, h \qquad \text{..... (2.22)}$$

The parameter δ is the phase difference in the high-index layer. The factor 2 in Equation. (2.19) accounts for reflections at both fiber end faces. The value of ($\bar{n}_2$) of the glass surface layer varies from (1.21 to 1.60), and the thickness (h) ranges from (0 to 0.15) μm[33]. The measure of the reflection properties of a fiber join is its return loss, defined by[22]:

$$\alpha = -10 \log_{10}\left(\frac{P_{reflected}}{P_{incident}}\right) \qquad \text{..... (2.23)}$$

2.19 Connector Parameters

a) Insertion Loss

This is the most important measure of the performance of a connector. If an optical fiber is broken and reconnected by two connectors and an in-line adapter. If the loss of the system is measured and found to have increased by 0.4 dB then this is the value of the insertion loss. It is the loss caused by inserting a mated pair of connectors in a fiber.

b) Return Loss

This is a measure of the Fresnel reflection. This power is being reflected off the connector back towards the light source. The lasers and LEDs used for multimode working are not greatly affected by the reflected power and so the return loss is not usually quoted in this instance. In single mode systems the laser is affected and produces a noisy output. The laser suppliers will always be pleased to advise on permitted levels of return loss[36], Appendix A lists some types of connectors and splices .

2.20 Bending Losses in Single Mode Fiber

Bend losses are particularly important in single-mode fiber. In these fibers, the bend losses show a dramatic increase above a critical wavelength when the fiber is bent or perturbed. In particular, it has been observed that the bend losses can be appreciably high at 1550 nm than in fibers designed for operation at 1300 nm [36]. The susceptibility of a fiber to these losses depends on the mode-field diameter and the cutoff wavelength [33,37]. the worst-case condition is in a fiber with a large mode-field diameter and a low cut off wavelength, so Bending losses are minimized in single-mode fibers by avoiding this combination of features[38].

Fibers show increased losses due to bending effects. Large bends of the cable and fiber are macrobends, Small-scale bends in the core cladding interface are microbends. These latter localized bends can develop during deployment of the fiber, or can be due to local mechanical stresses placed on the fiber (e.g., stresses induced by cabling the fiber or wrapping the fiber on a spool or bobbin). These latter losses are called the cabling loss and spooling loss, respectively[22]. The loss coefficient associated with a fiber bend is given by [38]:

$$\frac{P_{out}}{P_{in}} = e^{-\alpha_{bend} \cdot z} \qquad \text{..... (2.24)}$$

and the attenuation coefficient (α_{bend}) is given by:

$$\alpha_{bend} = c_1 e^{-c_2 r_b} \qquad \text{..... (2.25)}$$

where (r_b) is the radius of curvature of the fiber bend and (c_1) and (c_2) are constants. The losses are negligible until the radius reaches a critical size given by[22] :

$$r_{cririca l} \approx \frac{3n_2\lambda}{4\pi(NA)^3} \qquad \text{..... (2.26)}$$

From this relation to minimize these losses, The fiber must be with a large NA and operated at a short wavelength. Fortunately, macrobending does not cause appreciable losses until the radius of curvature of the bend is below (approximately) 1 cm. This requirement does not present much problem in the practical utilization of fiber cables, but does present a minimum curvature to the fiber. Frequently the fiber jacket is stiffened to prevent an attempt to loop the fiber into too small a curvature[22] . the pure bending loss in a single-mode fiber is[27]:

$$\alpha_b = \frac{1}{2}\left(\frac{\pi}{4\alpha R W^3}\right)^{0.5}\left(\frac{u}{VK_1(W)}\right)^2 \exp\left(-\frac{1}{6\pi^2}\frac{W^3\lambda^2 R}{a^3 n_2^2}\right) \qquad \text{..... (2.27)}$$

Where

(α_b) = is the bend's attenuation in Nepers/km.

R = radius of the bend fiber

V^2(Normalized frequency) = $U^2 + W^2$

$K_1(\omega)$ = modified Hankel function

λ = wavelength in (um)

n_2 = refractive index of cladding

To convert from Nepers/km to dB/km, multiply by 8.686. From equation (2.27) Figure(2.21) was plotted. it shows how the bending attenuation in a single-mode fiber changes with different bend radii at 1310 nm and 1550 nm. Observe the same general trend at both wavelengths[27].

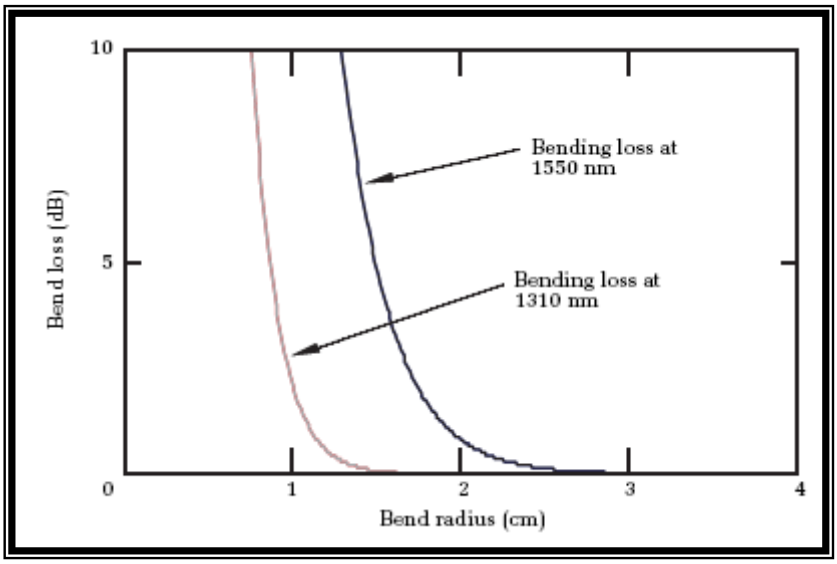

Figure (2-21) Bending loss as a function of bend radius using equation [2-30] loss at 1550 nm is considerably greater than it is at 1310 nm[27]

There is essentially no bending loss until a certain critical radius is reached, whereupon the bending loss increases dramatically. Notice also that the critical bend radius is dramatically different for the two wavelengths. At 1310nm, the critical bend radius is about 1.5 cm; and the bending losses is (0.2) db at bending radius of (1.35cm). At 1550nm the critical bend radius is about 2.5cm (these critical bend radius change, depending on the fiber's numerical aperture and core radius) , so the bending loses is (8.3)dB at bending radius of(1.35)cm [19].

2.21 Couplers

If an optic fiber carrying an input signal that needs to be connected to two different destinations. The signal needs to be split into two. This is easily achieved by a coupler. When used for this purpose, it is often referred to as a splitter. Couplers are bi-directional, they can carry light in either direction. Therefore the coupler described above could equally well be used to combine the signals from two transmitters onto a single optic fiber. In this case, it is called a combiner. It is exactly the same device, it is just used differently[21] .

2.21-1 Basic 2×2 Coupler

The 2×2 coupler is a simple fundamental device that used here to demonstrate the operational principles of optical couplers. These are known as directional couplers. A common construction is the fused-fiber coupler illustrated in Figure (2.22). This is fabricated by twisting together, melting, and pulling two single-mode fibers so they get fused together over a uniform section of length W.

Each input and output fiber has a long tapered section of length L, since the transverse dimensions are reduced gradually down to that of the coupling region when the fibers are pulled during the fusion process. This device is known as a fused biconical tapered coupler. As shown in Figure (2-22), P_o is the input power on the top fiber (that takes as the primary fiber in a link), P_1 is the throughput power, and P_2 is the power coupled into the second fiber. Parameters P_3 is extremely low optical signal levels below the input power level. These result from backward reflections and scattering due to packaging effects and bending in the device. The amount of optical power coupled from one fiber to another can be varied by changing the coupling length W or the distance between the two fiber cores[25].

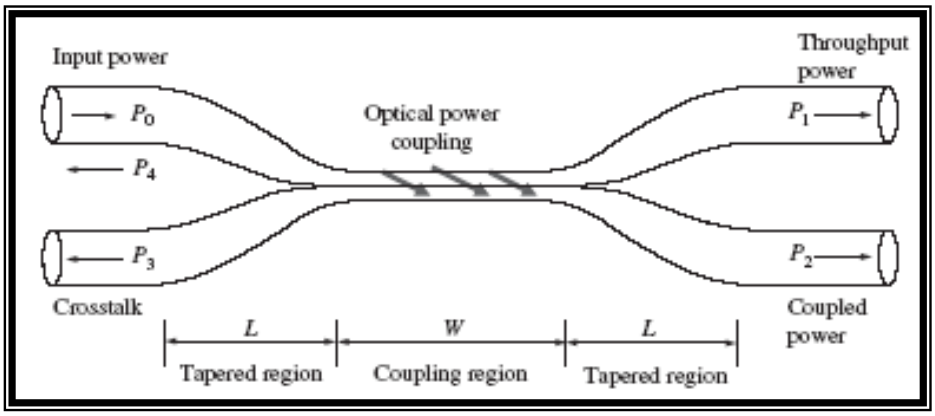

Figure (2-22) Cross-sectional view of a fused-fiber coupler having a coupling region W and two tapered regions of length L. The total span (2L + W) is the coupler draw length[25] .

2.21-2 Coupler Performance

In specifying the performance of an optical coupler, one usually indicates the percentage division of optical power between the output ports by means of the splitting ratio or coupling ratio. Referring to Figure. (2.29), with (P_o) being the input power and (P_1) and (P_2) the output powers, the splitting ratio is[33]:

$$Splitting\ ratio = \left(\frac{P_2}{P_1 + P_2} \right) \times 100\% \qquad \text{..... (2.28)}$$

By adjusting the parameters so that power is divided evenly, with one-half of the input power going to each output, one creates a 3-dB coupler. in any practical coupler there is always some light that is lost when a signal goes through it. The two basic losses are excess loss and insertion loss.

The excess loss is defined as the ratio of the input power to the total output power. Thus, in decibels, the excess loss for a 2×2 coupler is[33]:

$$Excess\ loss = 10 \log \left(\frac{P_0}{P_1 + P_2} \right) \qquad \text{..... (2.29)}$$

The excess loss is often less than (0.5db) in modern couplers for silica fiber[26]. The insertion loss refers to the loss for a particular port-to-port path. For example, for the path from input port i to output port j, in Decibels is[33]:

$$Insertion\ \ loss = 10\log\left(\frac{P_i}{P_j}\right) \qquad \textbf{..... (2.30)}$$

Another performance parameter is crosstalk, which measures the degree of isolation between the input at one port and the optical power scattered or reflected back into the other input port. That is, it is a measure of the optical power level (P_3) shown in Figure (2-22)[33] :

$$Crosstalk = 10\log\left(\frac{P_3}{P_0}\right) \qquad \textbf{..... (2.31)}$$

Appendix-B lists some typical power-splitting ratios for a fiber optic coupler operating at either 1310 nm or 1550 nm. The first number in the designation PP/SP is for the throughput channel (primary power), and the second number is for the coupled channel (secondary power).

List of Contents

Chapter Five ***Results and Discussion***

Chapter Six ***Conclusion & Future Work***

1. List of alphabetic

Symbol	***Meaning***
a	*Radius of the Core*
c	*Velocity of the light in vacuum*
d	*Lateral Displacement*
d_R	*Core Diameter of Receiving Fiber*
d_E	*Core Diameter of Emitting Fiber*
E_0^2	*Laser Optical Power*
f_b	*Beat Frequency*
I_C	*Coherence Range*
K	*Index Over Frequency*
$L_F(d)$	*Coupling Losses Core Area Mismatches*
$L_F(NA)$	*Coupling Losses Numerical Aperture Mismatches*
$L_F(n)$	*Coupling Losses of Core Index Mismatches*
N	*Number of Samples*
n	*Refractive Index of one Medium*
n_o	*Refractive index in free space*
n_1	*Core Refractive Index*
n_{gr}	*Group Index*
NA	*Numerical Aperture*
P_0	*Power Launched into the Fiber*
P	*Average Photoelastic Coefficient*
$\bar{P}$	*(rms) beat signal power*
RL_{IM}	*Return loss of connector*
R	*Reflectivity at Single material/coated end face*
R_{LO}	*Reflectivities of the Local Oscillator .*
R_{DUT}	*Reflectivities of Single Mode Fiber (DUT).*
$\bar{R}$	*Gain Responsivity*
r	*Fractional of light reflected at single interface*
r_b	*Radius of curvature of the fiber bend*
$r_{critical}$	*Critical Raduis*
S	*Backscattering Factor*
T	*Spacing of Samples*
T_s	*Round-Trip transmission rate of the beam splitter in (OTDR)*
t	*Round Trip time from fiber input to location z*
t_c	*coherence time of the laser.*
T_F	*Fictive temperature*
v	*Velocity of the light in vacuum in the medium*
V	*Normalized Frequency*
V_{min}	*Minimum Normalized Frequency*
v_{gr}	*Group Velocity*
$\overline{\omega_o}$	*Spot Size of Fundamental Mode*
w	*Pulse Duration*
Z	*Distance of any Point in the (DUT)*

2. Greek Symbols

Symbol	*Meaning*
α	*Total Attenuation of Optical Fiber*
α_{bend}	*Attenuation Coefficient due to Bending*
α_b	*Bending Losses*
$\bar{\alpha}$	*Attenuation Coefficient*
α_a	*Absorption Attenuation*
λ	*Wavelength*
α_s	*Scattering Coefficient*
λ_{cutoff}	*Cutoff Wavelength*
Δ	*Fractional Index change at the core/cladding interface*
Δf	*Line Width of the Laser*
Δz	*pulse length on the fiber*
$\Delta \ell$	*Spatial Resolution*
$\Delta \nu$	*Total Optical Frequency Sweep*
ΔT	*period of the triangular waveform*
ϕ_c	*Critical Angle*
β_c	*Isothermal compressibility*
β	*Sweep Rate*
γ	*Nonlineartiy of Source Laser*
δ	*Phase Difference*
Ω	*Angular Frequency*
τ	*round-trip time of flight*

3. List of abbreviations symbols

Symbol	***Meaning***
OTDR	*Optical Time Domain Reflectometer*
OFDR	*Optical Frequency Domain Reflectometer*
SMF	*Single Mode Fiber*
DFB	*Distributed feedback Laser*
SPAD	*Single-photon avalanche diode*
OLCR	*Optical Low Coherence Reflectometer*
ANNS	*Artificial Neural Networks*
FFT	*Fast Fourier Transform*
WDM	*Wavelength-Division Multiplexed*
DUT	*Device Under Test*
FMCW	*Frequency-Modulated Continuous-Wave*
LANs	*Local Area Networks*
TE	*Transverse Electric*
TM	*Transverse Magnetic*
HE	*Hybrid Modes*
LP	*Linearly Polarized*
HE_{11}	*Fundamental Mode*
PC	*Physical Contact Connector*
APC	*Angled Physical Contact Connector*
APD	*Avalanch Photo Diode*
PIN	*P-Type Intrinsic N-Type*
MLP	*Multiplayer Layer Perceptron*
RBF	*Radial Basic Function*
GUI	*Graphical User Interface*
DFT	*Discrete Fourier Transform*

References

[1] Woodward W. R. "Optical Time Domain Reflectometer-Basic Theory and Application",W.R.system,Ltd.,www.ecpi.edu., 2002.

[2] Sorin W. and D. Baney,"Measurement of Rayleigh backscatter at 1.55 µm with 32 µm spatial resolution" IEEE Photonics.vol.4,pp. 374-376 Apr. 1992.

[3] Von der J. P., Weid, Rogiero Passy, and G.Mussi,"On the characterization of optical fiber network components with optical frequency domain reflectometry"J.Lightwave,vol.15,pp.1131-1141,Jul.1997.

[4] Oberson P.,Huttner and Gisin"Optical frequency domain reflectometry with a narrow linewidth fiber laser"IEEE Photon,vol.12,pp.867-869,Apr.2000.

[5] Jim.Hayes,"Fiber Optics Technician's Manual"2nd Edition,pp.24-25, Technician's Mannal,2003.

[6] Barnoski M.K.and Jensen,"Fiber waveguides A novel technique for investigating attenuation characteristics"Appl.Opt.,vol.15,pp.2112-2115,1976.

[7] Barnoski and S.D. personick, "Measurements in Fiber optics" Proceed.IEEE,Vol.66,pp.429-441,Apr.1978.

[8] Gilgen H.H. and Novak, "Submillimeter Optical Reflectometry" J. Light wave Technology,Vol.7,pp.1225-1227,Aug.1989.

[9] Ripamonti G. "No Dead-Space Optical Time-Domain Reflectometer", J. light wave technology,vol.8,PP.1278-1280, Sep.1990.

[10] Glombitza U. and Brinkmegner "Coherent Frequency-Domain Reflectometry for Characterization of Single-Mode Integrated-Optical Waveguides", J. light wave technology,vol.11,pp.1377-1380,Aug.1993.

[11] Passy R., N. Gisin and J.P. von der Weid ,"Experimental and Theoretical Investigations of Coherent OFDR with Semiconductor Laser Sources" Journal of Lightwave Technology,Vol.12,pp.1622-1630,Sep.1994.

[12] Mussi G., P. Stamp, and N. Gisin,"Polarization Effects in Coherent Optical Frequency-Domain Reflectometry" IEEE Photonics T.,Vol.8, pp.1513-1515,Nov.1996.

[13] Von der Weid J.P. and R. Passy , " Return Loss Measurements of WDM Filters with Tunable Coherent Optical Frequency-Domain Reflectometry "IEEE Photonics,Vol.9,pp.1508-1510,Nov.1997

[14] Huttner B.,J. Reecht and N. Gisin, "Polarization OFDR for measurements of Birefringence and Polarization Mode Coupling Lengths In Optical Fibers"Group of appl.Physics,1997.

[15] Yoshihkot and Y. Sampei , "Optical Fiber Inspection Device" Yokogawa Electric Corporation,PP.1-14, Japan, 1999.

[16] Jihong Geng and Christine Spiegelberg ," Narrow Linewidth Fiber Laser for 100-km Optical Frequency Domain Reflectometry " IEEE Photonics T.,Vol.17,pp.1827-1829,Sep.2005.

[17] Kao K. C. and Hockhman "An Introduction to Optical Waveguides" Proc. IEE 113,1966.

[18] Buck J. A.," Fundamentals of Optical Fibers" Wiley, New York, 1995.

[19] Duwayne R. and Jonson "Troubleshooting Optical-Fiber Networks" Second Edition, Copyright, pp.21-33-273, 2004.

[20] Sackinger E. "Broadband Circuits for Optical Fiber Communication",pp.11-12,Copyright by John Wiley & Sons ,2005.

[21] Crisp J.," Introduction to Fiber Optics",2nd Edition,pp.18-20,2001.

[22] power J., "An Introduction To Fiber Optics Systems "McGraw-Hill, 1986.

[23] Jones D., "Introduction to Fiber Optics" Naval Education A. T. Sep.1998.

[24] Agrawal G. p, "Fiber-Optic Communication Systems Third Edition, Wiley & Sons, 2002.

[25] Abdullah A.Z. " Optical Communications Essentials"@ McGraw-Hill, 2004.

[26] Hentschel C. "Fiber Optics Handbook" second Edition, Hewlett-Packard,PP.126,1988.

[27] Gower J. "Optical Communications Systems" Prentice Hall,PP.50 1984.

[28] Held G. "Deploying Optical Networking Components "McGraw-Hill, 2001

[29] Wilson J. "Optoelectronics An Introduction"Prentic-Hall, 1983

[30] Walker N. G. "Polarisation Control For Coherent Optical Fiber System "British Telecom.vol.5,Apr.1987.

[31] Kelley P. L. and Kaminon "Nonlinear Fiber Optics "Third Edition, Copyright by Academic Press, 2001.

[32] John M. Senior "Optical Fiber Communications"Prentic-Hiall,PP.69-154,1985.

[33] Keiser Gerd ,"Optical Fiber Communications",3rd Edition, McGraw-Hill,PP.230-385,2000.

[34] Marcuse D. "Loss analysis of single-mode fiber splices",Tech.J., V.56,pp.703-718,Jun. 1977.

[35] Kihara M. "Return loss characteristic of optical fiber connectors", J.Lightwave Tech.,Vol.14,pp.1986-1991,Sep.1996 .

[36] Kaiser P. and Keck" Fiber types and their status,"pp. 29-54, New York Academic Press, 1988.

[37] Artiglia M. "Simple and accurate rnicrobending loss evaluation in generic single mode fibers," Proc. 12th ECOC,vol. 1, pp. 341-344, 1986.

[38] Charles H. "Optical fiber cables,", pp. 217-261, New York: Academic Press, 1988.

[39] TIA / EIA FOTP-59,"Measurement of fiber point defects using on OTDR",Nov.1989.

[40] Danielson D. "Backscatter Measurements on Optical Fibers", us Department of commerce 1981.

[41] Lucas G. "An Optical Time Domain Reflectometey Set-up for Laboratory Work at E'cole Supe'rieure d'Optique",France,2005

[42] YU L. and K. Li. "Optical sources for fibers,"pp. 5.1-5.61, New York McGraw-Hill, 1990.

[43] Shumate P. "Lightwave transmitters in optical fiber", pp. 723-757, New York: Academic Press, 1988.

[44] Soller B. J. and Mark "High resolution optical frequency domain reflectometery for characterization of components and assemblies" optics Exp.,Vol.13,Jan. 2005.

[45] Von der J. P. and Nicolas "On the characteristics of optical fiber network components with optical frequency domain reflectometry" Light wave Tech.,pp.1131,1997.

[46] Huttner B. and Gisin "Optical Frequency Domain Reflectometry For characterization of optical Networks And Devices" University of Geneva,1999.

[47] Mussi G and Vonder Weid,"–152.5dB sensitivity high dynamic range optical frequency domain reflectometry" Electronics Letter 32,pp.926,1996.

[48] Francois J. and Allard" High-power and ultra narrow DFB Laser ,The effect of Line width reduction systems on coherence length and interferometer noise"Spie,Vol.6216,May. 2006.

[49] Wegmuller and L. Gminnard "Overview of coherent reflecometry techniques, characterization of components and small systems" Group of Applied Physics,Geneva,2001.

[50] Vonder Weid and Forno "Return loss measurements of WDM filters with tunable coherent optical frequency domain reflectometry",IEEE photonics Tech.,V.9,NO.11PP.1508,1997.

[51] Gisin N. "Coherent reflectometry of optical fiber amplifiers",IEEE Photonics Tech.,V.9,pp.1253,1997.

[52] David J. "An Exploration And Development of Current Artificial Neural Network Theory And Applications With Emphasis On Artificial life", May 6,1997.

[53] Steven W. "Digital Signal Processing"2nd Edition, California Tech.,pp.225-415,1999.

[54] Heikki N. " Neural Networks Basics using Matlab Neural Network Toolbox", 2006.

[55] Demuth H. and Beale, "Neural Network Tools", MathWorks, p.1-3, By The Mathworks.Inc.2000 .

[56] "Simulink Dynamic System Simulation for MATLAB", from Internet www.mathworks.com, by the Mathworks.Inc . 1999 .

[57] "MatlabR2008a", from Internet www.mathworks.com, by the Mathworks.Inc February 2008 .

[58] Burak K., "Practical Usage Of Fast Fourier Transform(FFT)", By AMSC document Information,V1.0,Apr.2004 .

Republic of Iraq
Ministry of Higher Education and Scientific Research
University of Technology
Laser and Optoelectronics Engineering Department

Computer Simulation of Reflectometer for Optical Fiber Fault Detection

A Thesis Submitted to the
Laser and Optoelectronics Engineering Department,
University of Technology in a Partial Fulfillment of the
Requirements for the Degree of Doctor of Philosophy of
Science in Optoelectronics Engineering

By

Salah A. Adnan Taha

M. Sc. Optoelectronics Engineering 2002

Supervisor

Asst. Prof. Dr. Hussain Joma Abbas

2009 A.D 1430 A.H

نرّفعُ دَرَجَاتٍ مَنْ نَشَاءُ وَفَوْقَ
كُلِّ ذِي عِلْمٍ عَلِيمٌ

سورة يوسف
الآية 76